A high-throughput procedure for the identification of genes contributing to plant defence mechanisms

Inaugural-Dissertation

zur

Erlangung des Doktorgrades

der Mathematisch-Naturwissenschaftlichen Fakultät

der Universität zu Köln

vorgelegt von

Marco Miklis

aus Duisburg-Rheinhausen

Köln, Dezember 2004

Berichterstatter:	Prof. Dr. Paul Schulze-Lefert
	Prof. Dr. Martin Hülskamp
Prüfungsvorsitzender:	Prof. Dr. Ulf-Ingo Flügge
Tag der mündlichen Prüfung:	03. Februar 2005

Meiner Familie Steffi, Anna, Maria
und für Rafael

Abbreviations

(v/v)	volume per volume
(w/v)	weight per volume
$[Ca^{2+}]_{CYT}$	free cytosolic calcium
µ	micro
ABP	actin-binding protein
ADF	actin depolymerising factor
AGT	appressorial germ tube
AIP	appressorial infection peg
Amp	Ampicillin
APP	appressorium
Arp	actin-related protein
At	*Arabidopsis thaliana*
ATP	adenosine 5-triphosphate
avr	avirulence
Bgh	*Blumeria graminis* f.sp. *hordei*
Bgt	*Blumeria graminis* f.sp. *tritici*
bp	base pair(s)
C	carboxy
c	centi
CaM	calmodulin
CaMBD	calmodulin-binding domain
CC	coiled-coil
Cdc	cell division cycle
cDNA	copy DNA
CDPK	calmodulin-like domain protein kinase
CLSM	confocal laser scanning microscopy
cofilin	co-sediments with filamentous actin
CT	carboxy-terminal
cv.	cultivar
CWA	cell wall apposition
d	deoxy
dATP	deoxyadenosinetriphosphate

dCTP	deoxycytidinetriphosphate
dd	dideoxy
ddH$_2$O	deionised and distilled water
DEPC	diethylpolycarbonate
dGTP	deoxyguanosinetriphosphate
dicot	dicotyledonous
DMSO	dimythysulfoxide
DNA	deoxyribonucleic acid
DNase	deoxyribonuclease
dNTP	deoxynucleosidetriphosphate
dsRNAi	double-stranded RNA interference
DTT	dithiothreitol
dTTP	dioxythimydinetriphosphate
EDTA	ethylenediaminetetraacetic acid
ER	endoplasmic reticulum
ESH	elongating secondary hyphae
EST	expressed sequence tag
EtBr	ethidium bromide
EtOH	ethanol
f.sp.	*forma specialis*
F-actin	filamentous actin
FRET	Fluorescence Resonance Energy Transfer
g	gram
g	gravity constant
G-actin	globular actin
GFP	green fluorescent protein
GPCR	G-protein-coupled receptor
gsl	glucan synthase-like
GUS	β-glucuronidase
h	hour
H$^+$	hydrogen proton
hpi	hours post inoculation
hpRNA	hairpin RNA
HR	hypersensitive response

Hv	*Hordeum vulgare*
ihpRNA	intron-containing hairpin RNA
Kan	Kanamycin
kb	kilobase(s)
kDa	kiloDalton(s)
l	litre
LRR	leucine-rich repeats
m	milli
M	Molar
MAPK	mitogen-activated protein kinase
min	Minute(s)
Mla	Mildew-resistance locus-a
Mlg	Mildew resistance locus-g
Mlo	Mildew resistance locus-o
mmol	millimolar
monocot	monocotyledonous
mRNA	messenger ribonucleic acid
N	amino
NBS	nucleotide binding site
ng	nanogram
Nt	*Nicotiana tabacum*
ORF	open reading frame
Os	*Oryza sativa*
p	pico
PAMP	pathogen-associated molecular pattern
PCR	polymerase chain reaction
PEG	polyethylene glycol
pen	penetration
pg	picogram
PGT	primary germ tube
pH	negative decimal logarithm of the H^+ concentration
phox	phagocyte oxidase
PIP_2	phosphatidyl-inositol 4,5-bisphosphat
pmol	picomolar

pmr	powdery mildew resistance
PR	pathogenesis related
PTGS	post-transcriptional gene silencing
pv.	pathovar
R	resistance
rar	required for *Mla* resistance
ras	rat sarcoma
RFP	red fluorescent protein
Rho	ras homolog
RLK	receptor like kinases
RNA	ribonucleic acid
Rop	Rho of plants
ror	required for *mlo* resistance
ROS	reactive oxygen species
rpm	rounds per minute
RT	room temperature
RT-PCR	reverse transcription-polymerase chain reaction
SDS	sodium dodecyl sulphate
sec	second(s)
SNARE	soluble N-ethylmaleimide-sensitive fusion protein attachment protein receptor
ssp.	species
Ta	*Triticum aestivum*
T-DNA	transfer DNA
TESK	testicular protein kinase
TIR	*Drosophila* Toll and human interleukin-1 receptor
TLR	Toll-like receptor
TM	transmembrane
TRIS	Tris-(hydroxymethyl)-aminomethane
TRS	two fluorescent protein reporter system
U	unit
UTR	untranslated region
UV	ultraviolet
V	Volt

VIGS	virus induced gene silencing
vir	virulence
WT	wild-type
X-Gal	5-bromo-4-chloro-3-indolyl-β-D-galactopyranoside
X-Gluc	5-bromo-4-chloro-3-indolyl-β-D-glucuronic acid
Zm	*Zea mays*

Table of contents

3   Establishment of a dsRNAi-based high-throughput screen for genes implicated in barley powdery mildew resistance   48

1   General Introduction

Since the first appearance of land plants in the mid-Ordovician (~476 million years ago) and their subsequent still ongoing evolution and diversification, plants became important components of the terrestrial ecosystems (Kenrick and Crane, 1997). Autotrophic plants represent 96-99% of the total available biomass on earth being the most efficient reducer of atmospheric CO_2 concentrations. Therefore, green plants and algae, as primary producers, represent the first link in the food chain.

This fact also entails that plants have to protect themselves from a vast majority of predators trying to feed and/or live on them. These predators are not exclusively vertebrates (that are predominantly fend off by spikes, taste, or toxins) but additionally comprise species from invertebrates, fungi, bacteria, and viruses that menace plants. To react to these pathogens, plants had to evolve sophisticated molecular defence mechanisms in order to survive.

Vertebrates possess a somatically generated, adaptive immune system in which defence-associated components like macrophages, leukocytes and antibodies survey the organism and on demand are shuttled to sites of infection. As plants do not have a circulatory system like vertebrates, they had to develop a cell-autonomous immune response to pathogens that confers each single cell a repertoire of defence options.

The innate immunity of plants is based on the ability to discriminate between self and nonself to activate defence responses against potential microbial invaders. In general, most plants can resist challenges of most pathogen species. This kind of resistance is termed as non-host resistance and relies on concerted action of constitutive and inducible barriers (Heath, 2000; Thordal-Christensen, 2003; Mysore and Ryu, 2004). Pathogens that were able to overcome constitutive defence mechanisms induce a plant defence response that is triggered by highly conserved general elicitors, the so-called pathogen-associated molecular patterns (PAMPs). PAMPs are unique to microbes and not generated by potential host plants (Nürnberger *et al.*, 2004). Recognition of PAMPs in the mammalian system occurs by means of extracellular leucine-rich repeats (LRR) of the Toll-like receptor (TLR) family, which transduce the signals through a cytoplasmic TIR domain (*Drosophila* Toll and human IL-1 receptor) (Underhill and Ozinsky, 2002). In *Arabidopsis,* a range

of receptors has been identified showing structural similarities to the mammalian TLR family. One of these LRR-receptor like kinases (RLK), encoded by *FLS2*, is essential for flagellin perception in plants (Gómez-Gómez and Boller, 2002). A mitogen-activated protein kinase (MAPK) cascade, which activates gene expression under the control of a WRKY transcription factor (Eulgem *et al.*, 2000), subsequently transduces signals that are perceived by the flagellin receptor (Asai *et al.*, 2002).

In contrast to the animal kingdom, plants possess a further recognition potential, which renders individual plant cultivars of an otherwise susceptible plant species resistant to attack by particular pathogen variants. This race-specific resistance is mediated by the specific recognition of pathogen factors and allows the plant to resist infection by this particular pathogen strain/race (Nürnberger *et al.*, 2004). Following Flor's gene-for-gene concept (Flor, 1971), cultivar-specific perception of microbial effectors is governed by specific interactions between microbial *Avirulence* (*Avr*) gene loci and alleles of corresponding plant disease *Resistance* (*R*) loci. Interaction leads to an onset of signal transduction cascades resulting in disease resistance, which is often accompanied by hypersensitive cell death (Dangl and Jones, 2001). Many *Avr* genes encode specific virulence effectors, and lack of perception by *R* gene products ultimately results in disease (Jones and Takemoto, 2004).

However, an emerging picture is that the boundaries between "basal defence", "non-host", and "race-specific resistance" are not clear-cut and that there appears to be a substantial mechanistic overlap between these types of resistance. For example, the LRR-RLK Xa21 from rice confers cultivar-specific resistance to *Xanthomonas oryzae* pv. *oryzae* strains expressing AvrXa21 (Song *et al.*, 1995). Interestingly, *Xa21* encodes a protein with similar structure and sequence as the flagellin receptor FLS2 from *Arabidopsis*. This suggests that plants exploit similar molecular modules for PAMP and pathogen race-specific Avr factor perception. Indeed, recent findings suggest that race-specific resistance and non-host resistance may overlap by utilising at least some common genes, e.g. *SGT1* (*SUPPRESSOR OF G2 ALLELE OF SKP1*), *RAR1* (*REQUIRED FOR MLA RESISTANCE*), *NOH1* (*NON HOST1*), *HSP90* (*HEAT SHOCK PROTEIN 90*) and *EDS1* (*ENHANCED DISEASE SUSCEPTIBILITY1*) (Parker *et al.*, 1996; Falk *et al.*, 1999; Lu *et al.*, 2001; Austin *et*

al., 2002; Azevedo *et al.*, 2002; Peart *et al.*, 2002; Kang *et al.*, 2003; Kanzaki *et al.*, 2003).

1.1   Plant defence mechanisms

Since non-host resistance is commonly associated with a similar subset of molecular events as basal defence and race-specific resistance, this defence variant was chosen to illustrate some of the mechanistic possibilities that plants employ to react to pathogen attack. Moreover, non-host resistance can be considered as the first layer of defence that enables all members of a plant species to protect themselves against all genetic variants of particular pathogen species (Mysore and Ryu, 2004). A major contributor to resistance is the plant unique cell wall as the primary interface of a plant-pathogen interaction. However, this preformed physical barrier, consisting of crosslinked high molecular weight polysaccharides and preformed antimicrobial compounds (Vorwerk *et al.*, 2004), is only one of many constituents contributing to plant defence.

1.1.1   Phytoalexins and secondary metabolites

An early defence mechanism induced by pathogens is the accumulation of *de novo* synthesised phytoalexins and secondary metabolites associated with the plant cell wall. These substances often possess antimicrobial properties and therefore are highly capable in preventing microbial ingress (Darvill and Albersheim, 1984; Thomma *et al.*, 2002). Several *Arabidopsis thaliana* (*At*) genes have been identified that are required for the biosynthesis of an indole phytoalexin, camalexin. Inoculation experiments of *Arabidopsis* phytoalexin-deficient (*pad*) mutants with the filamentous, necrotrophic fungus *Alternaria brassicicola* revealed that plants harbouring the *pad1*, *pad2*, *pad3*, and *pad5* mutations were more susceptible to the inappropriate pathogen (van Wees *et al.*, 2003).

Besides the transcriptional induction of genes encoding proteins of the camalexin biosynthetic pathway, the *Pdf1.2* gene is also upregulated in non-host *Arabidopsis* leaf tissue upon pathogen challenge with *Alternaria brassicicola* and *Pseudomonas*

infestans. The gene encodes a plant defensin, a small peptide with antimicrobial properties, that accumulates upon pathogenic challenge (Penninckx *et al.*, 1996; Huitema *et al.*, 2003) and can partially contribute to plant resistance (Thomma *et al.*, 2002).

Interestingly, elemental sulphur (S^0), an ancient fungicide of mankind, is also produced *in planta* and there is evidence that, besides constitutive levels, S^0 acts as a constituent of induced defence (Williams and Cooper, 2004).

1.1.2   Reactive oxygen species

Another presumed plant defence mechanism is the generation of reactive oxygen species (ROS). Although there is no direct evidence that ROS generation determines resistance, functional properties of ROS argue for their involvement in defence processes. A likely direct role of extracellular hydrogen peroxide (H_2O_2) generation upon attempted and subsequently restricted fungal penetration could be demonstrated in three diverse types of plant/pathogen interactions. Non-host interactions of the plantain powdery mildew fungus (*Erysiphe cichoracearum*) on cowpea plants and the cowpea rust fungus (*Uromyces vignae*) on pea plants were investigated as well as the compatible interaction involving the tomato anthracnose fungus (*Colletotrichum coccodes*) and cotyledons of young tomato plants. H_2O_2 generation was detectable in all interactions as a response that spatially and temporally coincided with fungal penetration failures. Additionally, enzymatic removal of H_2O_2 contributed to an enhanced penetration frequency in all three plant/pathogen interactions (Mellersh *et al.*, 2002).

In the non-host interaction of barley (*Hordeum vulgare*) with the inappropriate *forma specialis* pathogen, the wheat powdery mildew fungus *Blumeria graminis* f.sp. *tritici* (*Bgt*), spatially confined H_2O_2 accumulation preceded the onset of a hypersensitive response (HR)-like cell death. H_2O_2 co-localised with cell wall appositions (CWAs *syn.* papillae) that were deposited in close proximity to invading pathogenic infection structures (Hückelhoven *et al.*, 2001). These findings are consistent with the assumption that generation of ROS, besides its proposed antimicrobial function, might also be involved in fortification of the cell wall and CWAs via oxidative

crosslinking of distinct components at sites of microbial penetration attempts (Brisson *et al.*, 1994; Thordal-Christensen *et al.*, 1997). Additionally, the findings substantiate the notion that ROS accumulation might be involved in triggering a localised cell death/HR (Levine *et al.*, 1994; Van Breusegem *et al.*, 2001). On the other hand, it has been recently shown that *Arabidopsis* cells depleted of the majority of total ROS exhibited enhanced cell death upon inoculation with a virulent pathogen. However, these results in general do not exclude a role for ROS in triggering cell death/HR. It was assumed that ROS rather act as regulatory components in cell death signalling (Torres *et al.*, 2002).

Despite the frequent association of HR-like cell death with race-specific-resistance and non-host resistance, the pathogen-triggered cell death is likely a non-specific defence reaction (Schulze-Lefert, 2004). To date, convincing evidence is lacking that the HR-like cell death contributes to disease resistance in any plant-pathogen interaction (Yu *et al.*, 1998; Lu *et al.*, 2003).

1.1.3   Cell wall appositions

The formation of CWAs, a further presumptive mechanism in plant disease resistance, is often associated with non-host resistance. In fact, papilla formation is particularly evident in non-host resistance. CWAs consist mainly of callose, a (1→3)-β-D-glucan (Jacobs *et al.*, 2003). Additionally, also glycoproteins and phenolic compounds are rapidly deposited and oxidatively crosslinked in papillae upon microbial attack (Brown *et al.*, 1998). Recently, the general assumption of crosslinked callose serving as a physical barrier to pathogenic invasion and therefore contributing to resistance was challenged. *Arabidopsis* mutants, defective in a specific isoform of the glucan synthase-like gene family (*GSL5*/*POWDERY MILDEW RESISTANCE4* (*PMR4*)) were largely depleted of callose in CWAs deposited in response to pathogenic challenge. Interestingly, these mutants were fully resistant to two different virulent powdery mildew fungi (*Sphaerotheca fusca* and *Golovinomyces orontii*) and an oomycete (*Peronospora parasitica*), but exhibited no altered susceptibility to a bacterial pathogen (Jacobs *et al.*, 2003; Nishimura *et al.*, 2003). Despite the lack of callose in CWAs, papillae-like subcellular structures were microscopically visible in

proximity to microbial penetration attempts (Jacobs *et al.*, 2003; Nishimura *et al.*, 2003). This argues for an involvement of other CWA components like phenolic compounds in developing physical barriers (von Röpenack *et al.*, 1998; Mellersh *et al.*, 2002). Alternatively, papilla deposition may not contribute to efficient defence in this patho-system.

1.1.4   Vesicle trafficking

Papilla-related vesicle trafficking to the plasma membrane is suggested to be associated with various types of resistance. In barley, basal defence, broad-spectrum and also *forma specialis* resistance are accompanied by deposition of H_2O_2-containing vesicles adjacent to "effective" (non-penetrated) papillae (Hückelhoven *et al.*, 1999; Hückelhoven *et al.*, 2001). Broad-spectrum powdery mildew resistant barley mutants (*mlo*) (see chapter 1.2.1), harbouring additional mutations in a gene designated as *ror2* (<u>r</u>equired for *ml<u>o</u>* <u>r</u>esistance2), showed a reduced amount of H_2O_2-containing vesicles at failed fungal penetration sites in comparison to the *mlo* mutant phenotype. This variation in *mlo/ror2* double mutant plants might be responsible for the partially compromised *mlo*-mediated broad-spectrum resistance to all known isolates of the barley powdery mildew fungus <u>Blumeria graminis</u> (DC Speer) f.sp. <u>hordei</u> (Marchal) (*Bgh*) (Freialdenhoven *et al.*, 1996). *Ror2* does also contribute to basal defence, a resistance response that is mounted even in a compatible plant/pathogen interaction to limit pathogenic growth to a certain extent (Glazebrook *et al.*, 1996). Mutations in barley *ror2* compromise basal defence and account for an enhanced susceptibility of *Mlo* wild-type plants to its natural pathogen *Bgh*. (Peterhänsel *et al.*, 1997; Collins *et al.*, 2003). Map-based cloning of *Ror2* in barley revealed a mutation in a gene encoding a plasma-membrane resident syntaxin (Collins *et al.*, 2003). Syntaxins belong to the protein superfamily of SNAREs (<u>s</u>oluble <u>N</u>-ethylmaleimide-sensitive fusion protein <u>at</u>tachment protein <u>re</u>ceptors) that form complexes with other SNARE proteins and are implicated in vesicle trafficking in yeast and animals. For this function, the SNARE members interact to attract and attach vesicles to target membranes and promote the fusion of the bilayers to different extents (Pratelli *et al.*, 2004). In fact, the reduced appearance of H_2O_2-containing vesicles at fungal penetration structures is not fully consistent with a

model favouring ROR2-facilitated vesicle fusion and exocytosis. Therefore, Collins and co-workers (2003) suggested an alternative function of ROR2 in homotypic vesicle fusion (Lauber *et al.*, 1997). The fusion of small vesicles may lead to larger vesicular structures that can be microscopically recognised. However, there is also evidence for an involvement of SNARE proteins in signalling events which might contribute to pathogen responses (Pratelli *et al.*, 2004).

It is possible to mechanistically link barley basal defence, involving SNARE complex-mediated vesicle trafficking, to *Arabidopsis* non-host resistance. *Arabidopsis Pen1* (<u>pen</u>etration1), the closest homolog of *Ror2* from monocotyledonous barley, was identified in a mutant screen for impaired non-host resistance of dicotyledonous *Arabidopsis* to the barley powdery mildew fungus (*Bgh*). *Bgh* conidiospores germinating on *Arabidopsis pen1* mutant leaf epidermal cells showed an enhanced penetration success, recognisable by the presence of more fungal digit-like feeding structures (haustoria). Although most of the haustoria were subsequently encapsulated by callose, in rare cases growth of short secondary hyphae occurred, indicative of some fungal nutrient uptake. Nevertheless, penetrated non-host cells ultimately underwent a HR-like cell death (Collins *et al.*, 2003).

Reduced H_2O_2 accumulation in barley *mlo/ror2* plants as well as a lowered incidence of H_2O_2-containing vesicles in barley *Mlo/ror2* plants at fungal penetration sites correlate with the compromised basal defence and broad-spectrum resistance (Hückelhoven *et al.*, 2000; Collins *et al.*, 2003). Altered H_2O_2 accumulation, possibly perturbed by impaired vesicle fusion events, could also account for the delayed inhibition of fungal growth in *Arabidopsis pen1* plants, either due to compromised H_2O_2-dependent antimicrobial activities and/or due to insufficient crosslinking of distinct papilla components.

1.2 Broad-spectrum resistance in barley

In rare cases, dominantly acting host genes or recessively inherited loss-of-function mutations confer resistance to a range of or even all genetic variants of a normally virulent pathogen species. This type of resistance is frequently termed as "broad-spectrum resistance". Examples comprise loss-of function alleles such as barley *mlo* (see below), *Arabidopsis edr1* (Frye and Innes, 1998) or *pmr6* (Vogel *et al.*, 2002)

and dominantly acting genes (*RPW8.1* and *RPW8.2*) of the *Arabidopsis* RESISTANCE TO POWDERY MILDEW (RPW) locus (Xiao *et al.*, 2001). This chapter focuses on *mlo*-mediated resistance, because of its relevance for this thesis.

1.2.1   Enhanced basal resistance mediated by mutations at the *Mlo* locus

Barley wild-type *Mlo* plants defend themselves against the barley powdery mildew fungus (*Bgh*) by basal defence mechanisms and in a race-specific manner (see chapter 1.3.1) according to the gene-for-gene concept (Flor, 1971; Jørgensen, 1994). Freisleben and Lein (1942) were the first who identified a broad-spectrum *Bgh* resistant plant generated by X-ray irradiation of a susceptible summer barley. The mutated gene confers resistance against all known *Bgh* isolates and was later designated as Mildew resistance locus-o (*Mlo*). Further recessively inherited homozygous loss-of-function alleles (*mlo*) residing at the *Mlo* locus on chromosome 4H were obtained by radiation- or chemical-induced mutagenesis (Jørgensen, 1992). Ethiopian landraces of barley, collected in 1937-38, harbour the so far only known *mlo* allele of natural origin, designated as *mlo*-11 (Nover and Schwarzbach, 1971; Jørgensen, 1976). Interestingly, recent haplotype analyses strongly suggest that the *mlo*-11 allele potentially arose during cultivation of primitive barley landraces. A low selection pressure for *mlo* mutants due to sufficiently diversified *R* gene-mediated resistance against *Bgh* and/or the below described pleiotropic effects of *Mlo* mutant alleles probably suppressed inheritance of spontaneous *Mlo* mutations in wild barley, *Hordeum spontaneum* (Piffanelli *et al.*, 2004).

Despite the advantageous powdery mildew resistance trait [Fig. 1], barley *mlo* plants were a long time neglected by breeders, because of negative pleiotropic effects associated with *mlo* genotypes. Barley plants harbouring mutations in *Mlo* show premature leaf chlorosis and/or necrosis, possibly as a consequence of spontaneously occurring mesophyll cell death (Wolter *et al.*, 1993; Peterhänsel *et al.*, 1997; Piffanelli *et al.*, 2002). This premature senescence results in a lower grain yield due to a reduction of the effective photosynthetic leaf area. However, sophisticated breeding strategies diminished these pleiotropic effects. Nowadays, broad-spectrum powdery mildew resistant barley varieties predominantly containing either the natural

mlo-11 or the induced *mlo*-9 mutant allele are extensively used in European agriculture (Jørgensen, 1992).
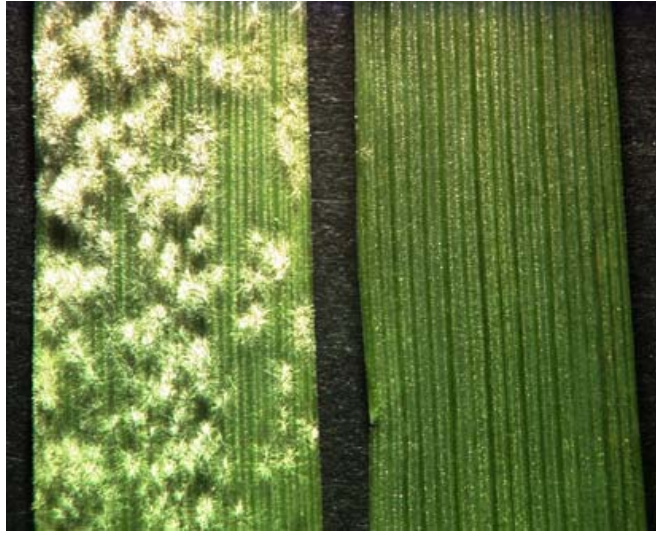
Figure 1. Powdery mildew infection phenotypes of barley *Mlo* wild-type and *mlo* mutant plants.
Leaves of either genotype (*Mlo*, left; *mlo*, right) were inoculated with a high density of *Bgh* conidiospores. While *Mlo* wild-type plants support the growth of sporulating mildew colonies on the leaf surface, *mlo* mutant plants are immune to fungal attack. The photograph was taken 6 days post spore inoculation. (from Panstruga and Schulze-Lefert, 2003)

1.2.1.1   Molecular characteristics of MLO

The barley *Mlo* gene, encoding a 60 kD protein, was isolated by positional cloning (Büschges *et al.*, 1997). Barley *Mlo* homologues sharing an average overall amino acid identity of 45% and similarity of 70% are confined to higher plants and bryophytes (Büschges *et al.*, 1997; Devoto *et al.*, 2003) A topological study of wild-type MLO deduced a seven-transmembrane (TM) domain organisation of the protein, with an intracellular, cytosolic C-terminus and an extracellular N-terminus [Fig. 2] (Devoto *et al.*, 1999). Comparison of available sequence-related *Mlo* genes from monocot species as well as the dicot *Arabidopsis* revealed that all MLO proteins presumably maintain the 7-TM topology (Devoto *et al.*, 1999; Devoto *et al.*, 2003). Subcellular fractionation further disclosed that barley MLO and a rice homolog (OsMLO1) reside in the plasma membrane (Devoto *et al.*, 1999; Kim *et al.*, 2002b).
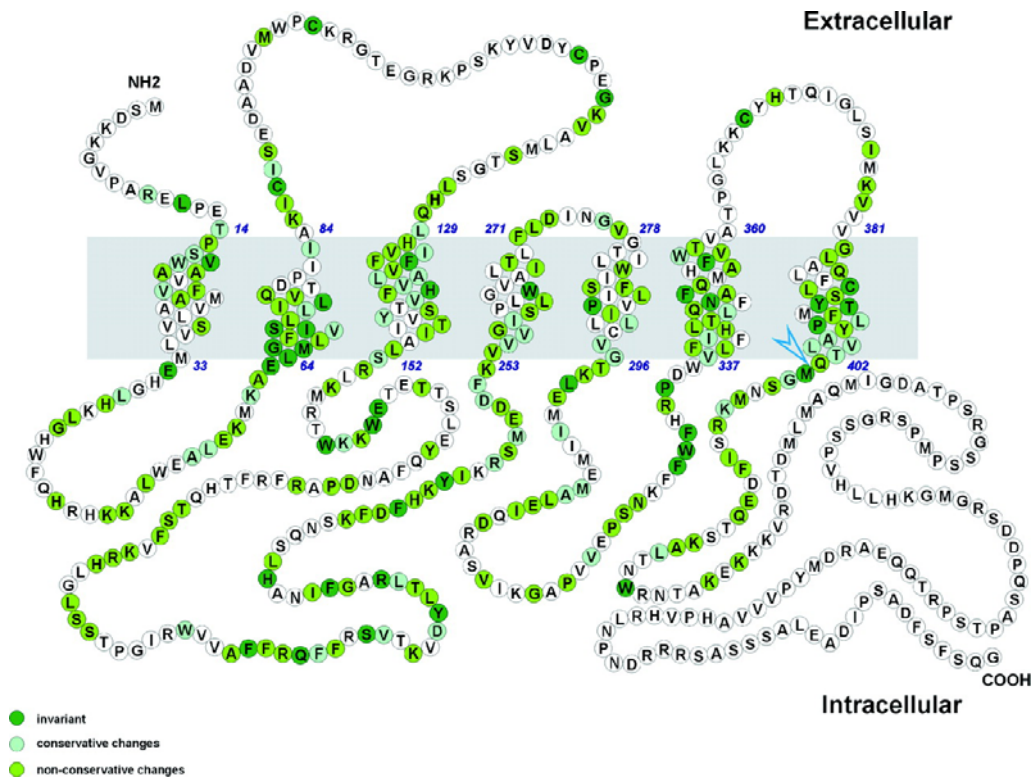
Figure 2. The common scaffold topology of the MLO family.
Graphic representation of the deduced 7-TM topology of barley MLO. The grey horizontal bar represents the plasma membrane lipid bilayer. Circles with letters represent amino acids identified by the single-letter amino acid code. Alignment of protein sequences from 20 full-length MLO family members revealed highly variable and conserved residues (colour-coded). Invariant residues, dark green; conservative changes in positions with at least 50% identical residues, light green; non-conservative changes in positions with at least 50% identical residues, green. Numbers indicate amino acid positions. (from Devoto *et al.*, 1999)

Regarding the heptahelical topology, the sequence diversification of family members and the plasma membrane localisation, MLO is reminiscent of 7-TM domain G-protein-coupled receptors (GPCRs) (Devoto *et al.*, 1999). Comprising more than 800 highly diverse genes in metazoans, the 7-TM domain GPCRs are classified in three distinct families, with versatile functions including drug-, hormone-, neurotransmitter-, chemokine-, odorant- and even light-perception. 7-TM domain GPCRs mainly transduce perceived signals through regulatory heterotrimeric guanine-nucleotide protein (G-protein) complexes composed of Gα, Gβ and Gγ subunits (Pierce *et al.*, 2002; Daly and McGrath, 2003). In *Arabidopsis*, a single gene (*GCR1*) was identified encoding a 7-TM protein with weak amino acid identity (max. 23%) to members of the three GPCR families (Plakidou-Dymock *et al.*, 1998). Although GCR1 has been

shown to directly interact with the sole *Arabidopsis* canonical Gα subunit *in vitro*, *in vivo* and *in planta*, to date no clear evidence for the involvement of this interaction in prototypical GPCR-signalling could be provided (Chen *et al.*, 2004b; Pandey and Assmann, 2004). Investigations of the potential involvement of barley MLO in heterotrimeric G-protein-mediated signalling revealed that MLO acts independently of the single copy barley Gα subunit (*HvGα*) in regard to MLO-dependent defence modulation (Kim *et al.*, 2002a). However, this finding does not exclude MLO-coupled G-protein-mediated signalling in other biological processes.

In a gel overlay assay, calmodulin (CaM) from soybean (SCaM1) was found to physically bind to a chimerical MLO protein composed of rice OsMLO1 and OsMLO2. The α-helical amphiphilic <u>ca</u>l<u>m</u>odulin <u>b</u>inding <u>d</u>omain (CaMBD) of the chimera could be located in the cytoplasmic C-terminal domain (Kim *et al.*, 2002b). Sequence conservation of the region harbouring the *OsMlo1/OsMlo2* CaMBD throughout the MLO protein family suggested that CaM is a common interactor of MLO proteins. Mutational studies of the *HvMlo* CaMBD revealed an enhanced MLO activity in *Bgh*-mediated defence suppression upon Ca^{2+}-dependent CaM binding. These findings are controversial to studies in which increased levels of free cytosolic Ca^{2+} ($[Ca^{2+}]_{CYT}$) were reported to trigger early defence processes in response to pathogenic challenge in plants (Grant *et al.*, 2000; Reddy *et al.*, 2003; Ludwig *et al.*, 2004). A possible explanation for this discrepancy is that *Bgh* might utilise increased $[Ca^{2+}]_{CYT}$ to manipulate *Mlo*-mediated defence to gain access to barley epidermal cells. This strategy was also be observed in various mammalian pathogens exploiting $[Ca^{2+}]_{CYT}$ for bacterial toxin-mediated effects or triggering of cytoskeletal rearrangements required for host cell binding or internalisation (Nhieu *et al.*, 2004).

1.2.1.2   The function of *Mlo*

In transient gene expression experiments, based on the ballistic transfection of single barley leaf epidermal cells, overexpression of barley wild-type *Mlo* has been shown to render cells of resistant barley *mlo* genotypes (*mlo*-4 and *mlo*-6) susceptible to *Bgh* (Shirasu et al., 1999a). These experiments suggested that MLO might act in a cell-autonomous manner, since fungal sporelings which successfully colonised *Mlo*-

transfected cells were not able to enter neighbouring untransfected epidermal barley epidermal cells of a *mlo* genotype (Shirasu *et al.*, 1999a; Schweizer *et al.*, 1999b; Panstruga, 2004). Moreover, transient overexpression of *Mlo* upon bombardment in barley wild-type *Mlo* leaves resulted in enhanced susceptibility (super-susceptibility) to *Bgh* (Kim *et al.*, 2002a). This phenotype suggests a role for the native promoter-driven MLO as an inefficient suppressor of basal defence.

Supporting the hypothesis of a potential negative regulatory MLO function in disease resistance, *mlo* genotypes are more susceptible to the hemibiotrophic rice blast fungus, *Magnaporthe grisea*, and the necrotrophic pathogen *Bipolaris sorokiniana* (Jarosch *et al.*, 1999; Kumar *et al.*, 2001; Jarosch *et al.*, 2003), respectively. It has been documented in *Arabidopsis* that different defence pathways can be mutually inhibitory (Glazebrook, 2001). Elevated *Bgh* resistance conferred by *mlo* mutations in barley could thus suppress resistance processes to other pathogens such as *Magnaporthe grisea*. Therefore, MLO additionally might be considered as a balancing component between mutually inhibitory defence pathways.

In accordance with a proposed incomplete suppression of basal defence by MLO, mutations in the genes *Ror1* and *Ror2* (Freialdenhoven *et al.*, 1996) mediated elevated susceptibility to *Bgh* in barley *Mlo* wild-type plants (Collins *et al.*, 2003). In case of the *Ror2*-encoded syntaxin, $\underline{F}$luorescence $\underline{R}$esonance $\underline{E}$nergy $\underline{T}$ransfer (FRET) (Jares-Erijman and Jovin, 2003) analysis indicated interaction with MLO *in planta* (Ryiaz Bhat, personal communication). Additionally, *Arabidopsis* isoforms of MLO were found to physically interact with the ROR2 ortholog from the dicot *Arabidopsis* (PEN1) in a yeast split-ubiquitin system (Chiara Connsoni, personal communication; Stagljar *et al.*, 1998). Thus, it is conceivable that MLO modulates ROR2 function during vesicle fusion processes.

The latter findings and the rapid increase of $[Ca^{2+}]_{CYT}$ of epidermal cells in response to barley mildew, presumably triggering the resistance-suppressing activity of MLO (Kim *et al.*, 2002a), support the notion that *Bgh* potentially modulates MLO to gain access to barley epidermal cells.

1.2.1.3 A potential role for papillae in *mlo*-mediated broad-spectrum resistance

A critical step during pathogenesis of powdery mildew fungi is the penetration of the cell wall of epidermal host cells. The penetration step in both barley genotypes (*Mlo* and *mlo*) is accompanied by an reinforcement of the plant cell wall and the formation of ring-shaped CWAs beneath sites of penetration attempts by the fungal appressorium (Skou, 1982). Although papillae appear in both barley genotypes, the abortion of fungal penetration attempts in *mlo* plants is temporally and spatially tightly linked to the presence of CWAs. In *Mlo* genotypes, CWAs are generally smaller, appear later after pathogen challenge and are more often penetrated (70%) compared to near-isogenic *mlo* lines (0.5%) (Skou *et al.*, 1984; Stolzenburg *et al.*, 1984; Freialdenhoven *et al.*, 1996). In addition, spontaneous papilla formation occurs in *mlo* plants only, even when grown aseptically, suggesting a perturbation of CWA-associated processes by lack of *Mlo* (Wolter *et al.*, 1993).

Moreover, earlier appearance and higher levels of H_2O_2 were observed at developing papillae in *mlo* resistant lines compared to *Mlo* susceptible lines (Hückelhoven *et al.*, 1999; Piffanelli *et al.*, 2002). These findings about temporal aspects of papilla formation correlate with results obtained from the investigation of papilla composition. Phenolic compounds of the papillae become resistant to extraction by saponification approximately two hours earlier in *Bgh* challenged *mlo* than in *Mlo* plants (von Röpenack *et al.*, 1998). As a conclusion from these results, it is conceivable that temporally shifts in the onset of papilla formation and/or structurally differences of CWAs contribute to *mlo*-mediated resistance. This assumption would be compatible with the finding that in both barley genotypes (*mlo* and *Mlo*) no difference in the expression profiles of <u>p</u>athogenesis-<u>r</u>elated (PR) genes during the early stages of *Bgh* attack (up to 24 hours) was observed (Gregersen *et al.*, 1997). Moreover, *mlo* resistance is apparently not mediated by constitutively expressed defence responses (Jørgensen, 1992; Peterhänsel *et al.*, 1997). Enhanced H_2O_2-mediated crosslinking of cell wall components like phenolic compounds might result in papillae that are more resistant to penetration by the fungal pathogen. Barley *mlo/ror1* double mutants show partial susceptibility to *Bgh*, but accumulate similar levels of H_2O_2 as barley *Mlo /Ror1* wild-type plants (Piffanelli *et al.*, 2002). This finding makes it unlikely that *mlo*-mediated resistance is solely dependent on enhanced H_2O_2 accumulation.

1.3   Race-specific resistance in barley

As already mentioned above (see Chapter 1), effective race-specific resistance requires the presence of a matching pair of a host R protein and a pathogen-derived AVR protein. The interaction of a host R protein and the cognate AVR effector was originally proposed to be direct. However, only two examples were reported that support this "receptor-ligand model" (Hammond-Kosack and Jones, 1997; Jia *et al.*, 2000; Deslandes *et al.*, 2003). Due to lacking evidence for direct interaction from other patho-systems, a further model, the "guard hypothesis", has been proposed. In this model, the pathogen-derived AVR protein applies its effector function to a host target molecule or macromolecule (proteins or protein complexes) to accomplish susceptibility of the host. The target host molecule, referred to as "guardee", in turn is surveyed by R protein(s), the "guards", for such AVR-mediated guardee interference. Recognition of the altered status of the guardee consequently initiates signal cascades leading to the resistance response (van der Biezen and Jones, 1998).

Recently, many *R* genes have been isolated from both dicot and monocot plants. Most of these show striking structural similarities (Hammond-Kosack and Parker, 2003). This makes it possible to classify different groups of R proteins. The most prevalent group consists of intracellular <u>n</u>ucleotide-<u>b</u>inding-<u>s</u>ite-LRR (NBS-LRR) proteins with variable N-terminal domains of either the TIR or <u>c</u>oiled-<u>c</u>oil (CC) motif (Jones and Takemoto, 2004), to which also the barley *Mla*-encoded R proteins belong.

1.3.1   Barley race-specific resistance mediated by either the *Mla* or *Mlg* locus

Twenty-eight specificities of the <u>*Mildew* *r*esistance locus-*a*</u> (*Mla*) implicated in race-specific resistance to *Bgh* reside on chromosome 1H of barley (Jørgensen, 1994). So far, all isolated *Mla* alleles (*Mla1*, *Mla6*, *Mla12*, *Mla13*) belong to the group of CC-NBS-LRR R proteins with an additional <u>C</u>-<u>t</u>erminal region (CT) (Halterman *et al.*, 2001; Zhou *et al.*, 2001; Halterman *et al.*, 2003; Shen *et al.*, 2003). All deduced MLA proteins share high sequence similarities of approximately 97% in the CC-NBS region and approximately 87% in the LRR-CT region (Halterman *et al.*, 2003; Shen *et*

al., 2003). *Mla*-mediated resistance is generally accompanied by hypersensitive cell death of host cells, but interestingly, despite the high sequence similarity of MLA proteins, the spatially extent and temporally onset of the HR varies among individual *Mla* alleles. For example, *Mla1* and *Mla6*-induced HR upon challenge with the avirulent barley powdery mildew isolate CC1 generally is confined to the attacked epidermal barley cell. In contrast, in *Mla3-* and *Mla7*-containing plants the HR spreads to the underlying mesophyll cells upon attack by the same avirulent fungal race and results in a cessation of pathogenic growth at a later stage (Boyd *et al.*, 1995). *Mla1*, *Mla6* and *Mla13* represent *Mla* alleles capable of a rapid arrest of pathogenic growth at early stages. Contrary, *Mla3*, *Mla7*, *Mla10*, *Mla12* and *Mla14* terminate pathogenic expansion at formation of secondary hyphae (Jørgensen, 1994; Boyd *et al.*, 1995; Wei *et al.*, 1999).

Temporally shifts in the onset and/or speed of resistance responses were shown to be dependent on the dosage of *Mla12* and *Mlg* (Görg *et al.*, 1993; Shen *et al.*, 2003). However, also different requirements for *Rar1* and *Sgt1* could determine differences in timing and spatial extent of defence mechanisms (Shirasu *et al.*, 1999b; Azevedo *et al.*, 2002; Shen *et al.*, 2003; Halterman and Wise, 2004). *Mla12* plants harbouring mutations in *rar1* are susceptible when challenged with a normaly avirulent powdery mildew isolate (*AvrMla12*). In these interactions, reduced PR protein accumulation and cell death progression likely account for susceptibility (Freialdenhoven *et al.*, 1996).

Race-specific resistance mediated by the <u>*M*</u>*ildew* <u>*r*</u>*esistance* <u>*locus-g*</u> (*Mlg*), residing on chromosome 4H, terminates *Bgh* fungal growth before the onset of an HR. Interestingly, the fungus fails to penetrate the cell wall at sites of CWAs, which is reminiscent of the *mlo*-mediated broad-spectrum resistance to *Bgh* (Görg *et al.*, 1993) (see chapter 1.2.1.3). However, mutations in the *Ror1* gene, identified by compromising *mlo*-mediated resistance, do not affect *Mlg*-specified resistance (Freialdenhoven *et al.*, 1996; Peterhänsel *et al.*, 1997). This argues for distinct pathways conferring broad-spectrum *mlo* resistance and race-specific *Mlg* resistance. Moreover, in *Mlg* resistance, loss of *Rar1* does not lead to compatibility or loss of the HR but was reported to slightly increase the frequency of cell wall penetration by the fungus (Peterhänsel *et al.*, 1997).

1.4 The role of the actin cytoskeleton in plant defence processes

Though non-host, broad-spectrum and race-specific resistance appear to differ in the signalling pathways and/or effector components rapid polarised rearrangement of the plant cytoskeleton towards sites of pathogen penetration attempts is apparently common to all types of resistance (Takemoto *et al.*, 2003). Furthermore, it is thought that the cytoplasmic aggregation that frequently occurs upon pathogen attack is dependent on the actin cytoskeleton (Schmelzer, 2002). The translocation of organelles is reported from various interactions including potato or parsley and *Phytophthora infestans* (Gross *et al.*, 1993; Freytag *et al.*, 1994), cowpea and *Uromyces vignae* (Heath and Heath, 1978), onion and *Botrytis cinerea* or *Magnaporthe grisea* (Xu *et al.*, 1998; McLusky *et al.*, 1999), flax and *Melampsora lini* (Kobayashi *et al.*, 1994), barley and *Erysiphe pisi* (Kunoh *et al.*, 1985) Arabidopsis and *Phytophthora sojae* or *Peronospora parasitica* (Takemoto *et al.*, 2003). Occurrence of similar cellular responses by a range of plant host species to a variety of pathogens suggests a conserved role for the actin cytoskeleton in an evolutionarily conserved basal defence program.

Several pharmacological studies with polymerisation inhibitors of filamentous actin (F-actin) corroborate a role for actin cytoskeleton polarisation in plant defence. Application of inhibitors delayed or inhibited the hypersensitive cell death in barley coleoptiles (Hazen and Bushnell, 1983), in cowpea (Skalamera and Heath, 1998), potato (Takemoto *et al.*, 1999) and *Arabidopsis* (Yun *et al.*, 2003) upon fungal attack. Furthermore, inhibitor application interfered with callose deposition in barley (Kobayashi *et al.*, 1997b; Kobayashi *et al.*, 1997a), cowpea (Skalamera and Heath, 1996; Skalamera and Heath, 1998), and Arabidopsis (Yun *et al.*, 2003).

Direct evidence for the impact of actin cytoskeleton dynamics on the expression of defence responses is provided by investigations of the pea powdery mildew fungus, *Erysiphe pisi*, interacting with the non-host plant barley, and from *Arabidopsis* challenged with the wheat powdery mildew fungus, *Bgt*. In these experiments, the non-host pathogen *Erysiphe pisi* was able to penetrate barley coleoptile cells treated with actin polymerisation inhibitors (cytochalasins). In contrast to untreated control leaves, the biotrophic fungus succeeded in cytochalasin-treated samples in formation

of its digitate, bilateral feeding organ (haustorium). Partially compromised non-host resistance in barley coleoptiles by cytochalasin treatment was also observed upon challenge with the hemibiotrophic and necrotrophic filamentous fungi *Colletotrichum lagenarium* and *Alternaria alternata*, respectively (Kobayashi *et al.*, 1997b). Despite successful penetration, formation of haustoria and onset of secondary hyphal growth of the fungus, it has never been reported whether the inappropriate powdery mildew pathogen was able to generate conidiophores on the non-host barley. Development of conidiophores would be indicative of successful completion of the asexual fungal life cycle on the non-host plant.

In another non-host interaction, the inappropriate pathogen *Bgt* was found to penetrate epidermal cells of cytochalasin-treated *Arabidopsis* wild-type plants, to form haustoria and to establish secondary hyphae before growth is halted. However, in an *Arabidopsis eds1* mutant, occasional generation of conidiophores with chains of fully developed fungal spores (conidia) was observed (Yun *et al.*, 2003), demonstrating that the plant became susceptible due to synchronous interference with actin dynamics and downstream defence processes. Interestingly, partial susceptibility of a dicot non-host plant (*Arabidopsis*) to a monocot pathogen (*Bgt*), caused by the synergistic effect of loss of actin cytoskeleton polarisation and *EDS1* function supports the hypothesis that in principle all plants physiologically meet the requirements for susceptibility to most pathogens, but became non-hosts by superimposed defence mechanisms during evolutionary diversification (Heath, 1981).

Pharmacological inhibitors of actin dynamics do not specifically interfere with defence-related processes. Different subsets of actin filaments generated by different actin-binding proteins (ABPs) or by multiple isoforms of actin, which coexist in plant tissue (Janßen *et al.*, 1996), might confer specificity of actin dynamics in plant disease resistance. Thus, it can currently not be excluded that observed effects are due to interference with other pivotal functions of the actin cytoskeleton, e.g. cell maintenance (Takemoto *et al.*, 2003).

To date, apart from inhibitor studies, only circumstantial evidence is available linking polarised rearrangement of the actin cytoskeleton to functions in plant defence responses.

One example is the suggested partial contribution of a membrane-associated NADPH oxidase complex for generation of ROS in response to pathogen attack (Thordal-Christensen *et al.*, 1997). Movement of cytosolic proteins (p67-<u>ph</u>agocyte <u>ox</u>idase (*phox*), p47-*phox* and rac2) to the membrane is necessary to activate the NADPH complex. Application of fungal intercellular fluids, derived from an incompatible *Cladosporium fulvum* strain, was sufficient to elicit the movement and subsequent accumulation of respective proteins at the plasma membrane of tomato leaf cells. Interestingly, the NADPH protein complex was proposed to be plasma membrane-associated cytoskeleton and treatment by DNAse I, known to bind to <u>g</u>lobular actin (G-actin) and depolymerise F-actin, released p67-phox, p47-phox and rac2 from the membrane-connected cytoskeleton (Xing *et al.*, 1997). This makes it tempting to speculate that ROS generation at sites of pathogen penetration attempts (Thordal-Christensen *et al.*, 1997; Hückelhoven *et al.*, 1999) is locally restricted by focal rearrangement of the actin cytoskeleton functioning in the recruitment of the NADPH oxidase-activating phox proteins to the plasma membrane. This hypothesis is further supported by the fact that a small GTP-binding protein, HvRACB, implicated in barley defence against *Bgh* (Schultheiss *et al.*, 2002), presumably plays a role in NADPH activation in linking pathogen-elicited signals (e.g. Ca^{2+} influx) to changes in actin organisation or membrane transport (Hückelhoven and Kogel, 2003).

1.4.1 Are actin-binding proteins involved in defence-related actin-dynamising processes?

Besides indirect evidence suggesting an involvement of the actin cytoskeleton in defence response to pathogens *in planta* to date no ABP has been identified required for pathogen attack-triggered actin dynamising processes. Guinea pig as well as human neutrophils, however, supposedly require an ABP to fulfil their antimicrobial activities. An <u>a</u>ctin <u>d</u>epolymerising <u>f</u>actor (ADF) seems to participate in the polymerisation and depolymerisation of F-actin, giving rise to oscillatory patterns of ROS production linked to the NADPH oxidase in neutrophilic membrane ruffles, the major sites of H_2O_2 production (Heyworth *et al.*, 1997).

In metazoans, phosphorylation of the ABPs ADF and cofilin is mediated by kinases that in turn are downstream targets of the ras (<u>ra</u>t <u>s</u>arcoma oncogene product) <u>ho</u>molog (Rho) GTPases (Gungabissoon and Bamburg, 2003). With respect to microbial pathogenicity, human bacterial pathogens like *Yersinia* interfere with Rho GTPases to transiently perturb host actin dynamics for attenuation of the host immune response (Grosdent *et al.*, 2002). Likewise, *Salmonella* and *Pseudomonas* interfere with Rho GTPases to gain access to their respective host cells (Barbieri *et al.*, 2002). Interestingly, the enteropathogen *Salmonella enterica* serovar *Typhimurium* modulates actin cytoskeleton dynamics in attacked vertebrate cells by interfering with ADF for efficient bacterial entry (Dai *et al.*, 2004; McGhie *et al.*, 2004). *In planta*, NtRAC1 from *Nicotiana tabacum* belonging to the plant ras-related C3 botulinum toxin substrate (Rac)/<u>R</u>ho <u>of</u> <u>p</u>lants (Rop) family of GTPase is suggested to modulate NtADF1 activity via phosphorylation processes to regulate actin dynamics in pollen tube growth (Chen *et al.*, 2003). Remarkably, *NtRac1* is a homologous gene of barley *HvRacB*, which is implicated in plant defence (Schultheiss *et al.*, 2002).

1.4.1.1   The ADF/cofilin group

Based on the evidence outlined above it is conceivable that ADF/cofilin (<u>co</u>-sediments with <u>fil</u>amentous act<u>in</u>) proteins may contribute to actin cytoskeleton dynamising processes upon pathogen attack.

Cofilins, which do not exist in plants, have similar qualitative properties as ADFs by interacting with actin (Maciver and Hussey, 2002), but show quantitative differences *in vivo* (Chen *et al.*, 2004a). Therefore, ADFs and cofilins are collectively referred to as the ADF/cofilin group (Staiger, 2000; Maciver and Hussey, 2002). Members of the ADF/cofilin family are relatively small proteins (15-19 kDa) that are expressed in virtually all eukaryotic cells. They bind G-actin as well as F-actin and modulate actin filament dynamics. In concert with other ABPs, ADF/cofilins are responsible for the depolymerisation of actin filaments. In addition, ADF/cofilins might nucleate the assembly of new actin filaments (Dos Remedios *et al.*, 2003).

Multiple isoforms of ADF exist in plants and differences in structure and biochemical activities between pollen and vegetative ADFs have been described (Maciver and

Hussey, 2002). This might indicate that selection pressure has resulted in the evolution of specific ADF isotypes that perform subtly different roles in different tissues and organs of plants (Smertenko *et al.*, 2001). ADF isoforms have been found to be implicated in many cytological processes, like root hair growth (Braun *et al.*, 2004), pollen tube growth (Chen *et al.*, 2002), flowering time, trichome growth, cell expansion (Dong *et al.*, 2001), cold acclimation (Ouellet *et al.*, 2001) and gravity-oriented polarised growth in rhizoids (Braun *et al.*, 2004). However, a direct contribution of ADFs in disease resistance processes in plants has not been reported to date.

2 Material and Methods

2.1 Materials

2.1.1 Antibiotics

Ampicillin (Amp): 100 mg/ml in H_2O
Kanamycin (Kan): 50 mg/ml in H_2O
Stock solutions (1000 x) stored at -20°C.

2.1.2 *Escherichia coli* strains

DH5α:

Genotype: *supE*44*, *Δ(*lacZYA-argF*)U169*, (*Θ80d*lacZ*ΔM15)*,   Hanahan,1983
*hsdR*17*, recA*1*, endA*1*, gyrA*96*, thi*-1*, relA*1*, deoR*

DB3.1:

Genotype: F⁻ *gyrA*462 *endA*1 Δ(*sr*1-*rec*A) *mcr*B *mrr*   Invitrogen™
*hsd*S20(rB⁻, mB⁻) *sup*E44 *ara*14 *gal*K2 *lac*Y1
*pro*A2 *rps*L20(Smʳ) *xyl*5 Δ*leu mtl*1

2.1.3 Powdery mildew fungus strains

2.1.3.1 Barley powdery mildew fungus

The known avirulence/virulence gene profiles of the two *Blumeria graminis* f.sp. *hordei* isolates (James Brown, personal communication) is listed below (*Avr*-Avirulence, *vir*-virulence):

Isolate K1:

> *Avr:*   *AvrMla1, AvrMla3, AvrMla7, AvrMla22, AvrMlLa, AvrMl(Ab)*
>
> *vir:*   *virMla6, virMla9, virMla10, virMla11, virMla12, virMlg, virMl(CP),*
> *virMlH, virM1K, virMlra*

Isolate A6:

> *Avr:*   *AvrMla3, AvrMla6, AvrMla9, AvrMla10, AvrMla12, AvrMla13,*
> *AvrMlg, AvrMl(CP), AvrMlH, AvrMlK1, AvrMlLa, AvrMl(Ab)*
>
> *vir:*   *virMla1, virMla22*

Bgh strains were maintained on living barley plants or detached leaves.
K1 was maintained on I10, a near-isogenic line of cv. Ingrid containing *Mla12*;
A6 was maintained on P01, a near-isogenic line from cv. Pallas containing *Mla1*.

2.1.3.2   Wheat powdery mildew fungus

The known avirulence/virulence gene profile of the *Blumeria graminis* f.sp. *tritici*
isolate (Elliott *et al.*, 2002) is listed below (*Avr*-Avirulence, *vir*-virulence):

Isolate JIW2:

> *Avr:*   *AvrPm1, AvrPm2, AvrPm3a, AvrPm3b, AvrPm4a, AvrPm4b, AvrPm5,*
> *AvrPm6, AvrPm8*
>
> *vir:*   *virPm3c, virPm3d, virPm3f, virPm7*

The *Bgt* strain was maintained on living wheat plants or detached leaves of cv. Star.

All barley plants or detached leaves were kept at 18°C, 60% relative humidity, and 16
h light / 8 h darkness after inoculation with *Bgh* or *Bgt* conidiospores.

2.1.3.3   Pea powdery mildew fungus

The pea powdery mildew fungal isolate was assigned as *Erysiphe pisi* by ribosomal spacer DNA analysis.

The *Erysiphe pisi* strain was maintained on living pea plants.

Pea plants were kept at 22°C, 70% relative humidity, and 12 h light/12 h darkness after inoculation with *Erysiphe pisi* conidiospores.

2.1.4   Plant materials

All barley seedlings were grown at 20°C, 80% relative humidity, and 16 h light / 8 h darkness in a protected environment.

Golden Promise:
  barley cv. containing *Mlo* but no *Mla* specificity

Ingrid:
  barley cv. containing *Mlo*

I10:
  near-isogenic line in Ingrid background containing *Mla12*

P01:
  near-isogenic line in Pallas background containing *Mla1*

P03:
  near-isogenic line in Pallas background containing *Mla6* and *Mla14*

P10:
  near-isogenic line in Pallas background containing *Mla12*

BC$_7$Ingrid *mlo*-3:	J. McKey,
generated by seven backcrosses with cv. Ingrid	Uppsala, Sweden
BC$_7$Ingrid *mlo*-5:	J. McKey,
generated by seven backcrosses with cv. Ingrid	Uppsala, Sweden
A39/1a (*ror1*-1, *mlo*-5):	Freialdenhoven *et al.*,
generated by EMS mutagenesis of BC$_7$Ingrid *mlo*-5	1996

A89/1a (*ror1*-2, *mlo*-5):   Freialdenhoven *et al.*,

    generated by EMS mutagenesis of BC$_7$Ingrid *mlo*-5   1996

C36/1b (*ror1*-3, *mlo*-5):   Freialdenhoven *et al.*,

    generated by EMS mutagenesis of BC$_7$Ingrid *mlo*-5   1996

C69/1 (*ror1*-4, *mlo*-5):   Freialdenhoven *et al.*,

    generated by EMS mutagenesis of BC$_7$Ingrid *mlo*-5   1996

C88/1b (*ror1*-5, *mlo*-5)   Freialdenhoven *et al.*,

    generated by EMS mutagenesis of BC$_7$Ingrid *mlo*-5   1996

2.1.5   Barley epidermal cDNA library

Tissue: Leaf epidermis tissue of seven-day-old barley (*Hordeum vulgare*) seedlings (BC$_7$Ingrid *mlo*-5) was adaxially stripped 6 and 24 hours post inoculation with *Blumeria graminis* f.sp. *hordei* or *Blumeria graminis* f.sp. *tritici*.

Vector: pBluescript (S/K)+

Restriction site 1:   *Eco*RI   (5'-end of cDNA)

Restriction site 2:   *Xho*I   (3'-end of cDNA)

Selective antibiotic: Ampicillin

Description: Approximately 5% of the clones correspond to cDNA from the fungi *Bgh* and *Bgt*, respectively. The average insert size is 1.2 kb.

The library was kindly provided by U. Zierold and P. Schweizer, Gatersleben, Germany

2.1.6   Vectors

pASSASSIN: Maize-ubiquitin1-promoter::*att*B-cassette (sense)::*Mla1*(3rd intron)::*att*B-cassette (antisense)::nos-polyA signal, GATEWAY$^{®}$ compatible ihpRNA vector; present study

pBluescript$^{™}$(S/K)+: Stratagene, Heidelberg

pcDNA3.1-SipA:	*SipA* containing mammalian cell transfection vector; R. Hayward, Cambridge, U.K.
pDEST™14:	Destination vector, GATEWAY® compatible; Invitrogen, Heidelberg
pDONR™201:	Donor vector GATEWAY® compatible; Invitrogen, Heidelberg
pGEX2T-Δ78SopE:	*sopE* sequence encoding residues 79-240 in eukaryotic expression pGEX2T; A. Wittinghofer, Dortmund, Germany
pGEX2T-Δ96ExoS:	*exoS* sequence encoding residues 97-234 in eukaryotic expression vector pGEX2T; A. Wittinghofer, Dortmund, Germany
pIM157:	*yopT* containing propagation vector; Iriarte and Cornelis, 1998
pTaMlo-dsRNAi:	Wheat *Mlo* ihpRNA vector; R. Panstruga, Cologne, Germany
pUAMBN:	Maize-ubiquitin1-promoter::*att*R-cassette (sense)::*Mla1* (3rd intron)::*att*R-cassette (antisense)::nos-polyA signal, GATEWAY® compatible ihpRNA vector; present study
pUAMBN-i:	Maize-ubiquitin1-promoter::*att*R-cassette (antisense)::*Mla1* (3rd intron)::*att*R-cassette (sense)::nos-polyA signal, GATEWAY® compatible ihpRNA vector; present study
pUAMBN-35S:	Cauliflower-mosaic-virus-35S-promoter::*att*R-cassette (sense)::*Mla1* (3rd intron)::*att*R-cassette (antisense)::nos-polyA signal, GATEWAY® compatible ihpRNA vector; present study
pUbiGATE:	Maize-ubiquitin1-promoter::*att*R-cassette::nos-polyA signal, GATEWAY® compatible overexpression vector; present study
pUbi-Mlo-nos NEW:	Maize-ubiquitin1-promoter::*Mlo*::nos-polyA signal, *Mlo* overexpression vector; R. Panstruga, Cologne, Germany
pUbi-GUS-nos:	Maize-ubiquitin1-promoter::*β-glucuronidase* (GUS)::nos-polyA signal, GATEWAY® compatible ihpRNA vector; Nielsen *et al.*, 1999
pUbi-YFP-GW-nos:	Maize-ubiquitin1-promoter::YFP-*att*R-cassette::nos-polyA signal, GATEWAY® compatible YFP-fusion vector; R. Bhat, Cologne, Germany

2.1.7   Oligonucleotides

Primer	Characteristics	5' → 3' sequence
Gate-attB1	anneals before *Eco*RI restriction site in pBluescript™ SK(+); additionally has *att*B1 sequence for GATEWAY® cloning	**GGG GAC AAG TTT GTA CAA AAA AGC AGG CTG** TGG ATC CCC GGG GCT GCA GG
Gate-attB2	anneals before *Xho*I restriction site in pBluescript™ SK(+); additionally has *att*B2 sequence for GATEWAY® cloning	**GGG GAC CAC TTT GTA CAA GAA AGC TGG GTT** AGG GCG AAT TGG GTA CCG GG
MLO-attB1	anneals inside *Mlo* gene; additionally has *att*B1 **sequence** for GATEWAY® cloning	**GGG GAC AAG TTT GTA CAA AAA AGC AGG CTA** GCC CAG CAA GTA CGT TGA C
MLO-attB2	anneals inside *Mlo* gene; additionally has *att*B2 **sequence** for GATEWAY® cloning	**GGG GAC CAC TTT GTA CAA GAA AGC TGG GTA** TGT CCG TGT CTC GGA
nos-term-Rev	sequencing primer, anneals inside nos-termination sequence	GCA AGA CCG GCA ACA GGA TT
HvADF3-For	anneals at start codon *HvADF3*; additionally has Kozak sequence and *Hin*dIII restriction site	TTT AAG CTT GCC ACC ATG GCA AAC GCT TCA TCA GGT GCT GGG
HvADF3-S6D	anneals at start codon of *HvADF3*; additionally has Kozak sequence, *Hin*dIII restriction site, and mutation of serine 6 to aspartate	TTT AAG CTT GCC ACC ATG GCA AAC GCT TCA GAC GGT GCT GGG
HvADF3-S6A	anneals at start codon of *HvADF3*; additionally has Kozak sequence, *Hin*dIII restriction site, and mutation of serine 6 to alanine	TTT AAG CTT GCC ACC ATG GCA AAC GCT TCA GCA GGT GCT GGG
HvADF3-Rev	anneals at stop codon of *HvADF3*; additionally has *Mlu*I restriction site	GTT ACG CGT CTA GTG TGC GCG CTC CTT GA
HvADF3-Gate-For	anneals at start codon of *HvADF3*; additionally has Kozak sequence and *att*B1 **sequence** for GATEWAY® cloning	**GGG GAC AAG TTT GTA CAA AAA AGC AGG CTT** CGC CAC CAT GGC AAA CGC TTC ATC AGG
HvADF3-Gate-Rev	anneals at stop codon of *HvADF3*; additionally has *att*B2 **sequence** for GATEWAY® cloning	**GGG GAC CAC TTT GTA CAA GAA AGC TGG GTC** TAG TGT GCG CGC TCC TTG A
GFP-For	anneals at start codon of *GFP*; additionally has Kozak sequence and *Hin*dIII restriction site	GCG AAG CTT GCC ACC ATG GTG AGC AAG GGC GAG
GFP-PTS-Rev	anneals before stop codon of *GFP*; additionally has *Mlu*I restriction site and encodes peroxisome targeting signal **(PTS)**	AAG ACG CGT TTA **GAG GCG GGA** CTT GTA CAG CTC

RFP-For	anneals at start codon of *RFP;* additionally has Kozak sequence and *Hin*dIII restriction site	GCG AAG CTT GCC ACC ATG GGG TCT TCC AAG AAT
RFP-PTS-Rev	anneals before stop codon of *RFP;* additionally has *Mlu*I restriction site and encodes peroxisome targeting signal **(PTS)**	GCG ACG CGT CTA **GAG GCG GGA** AAG GAA CAG ATG G
At1g01750-FOR	anneals at start codon of *AthADF;* additionally has Kozak sequence and ***att*B1 sequence** for GATEWAY® cloning	**GGG GAC AAG TTT GTA CAA AAA AGC AGG CTG** CCA CCA TGG CTA ATT CAG CGT CTG G
At1g01750-REV	anneals at stop codon of *AthADF;* additionally has ***att*B2 sequence** for GATEWAY® cloning	**GGG GAC CAC TTT GTA CAA GAA AGC TGG GTT** CAG AGA TTG ACT CGT CCC T
At2g16700-FOR	anneals at start codon of *AthADF;* additionally has Kozak sequence and ***att*B1 sequence** for GATEWAY® cloning	**GGG GAC AAG TTT GTA CAA AAA AGC AGG CTG** CCA CCA TGC GTG TGA CGG ATG AGT G
At2g16700-REV	anneals at stop codon of *AthADF;* additionally has ***att*B2 sequence** for GATEWAY® cloning	**GGG GAC CAC TTT GTA CAA GAA AGC TGG GTC** TAT TTG GCA CGG TCT TGG A
At2g31200-FOR	anneals at start codon of *AthADF;* additionally has Kozak sequence and ***att*B1 sequence** for GATEWAY® cloning	**GGG GAC AAG TTT GTA CAA AAA AGC AGG CTG** CCA CCA TGT CTT TCA GAG GAC TTA G
At2g31200-REV	anneals at stop codon of *AthADF;* additionally has ***att*B2 sequence** for GATEWAY® cloning	**GGG GAC CAC TTT GTA CAA GAA AGC TGG GTT** CAG TTC GCT CGT TCG CGT A
At3g45990-FOR	anneals at start codon of *AthADF;* additionally has Kozak sequence and ***att*B1 sequence** for GATEWAY® cloning	**GGG GAC AAG TTT GTA CAA AAA AGC AGG CTG** CCA CCA TGG TTT TGC ATG ATG ACT G
At3g45990-REV	anneals at stop codon of *AthADF;* additionally has ***att*B2 sequence** for GATEWAY® cloning	**GGG GAC CAC TTT GTA CAA GAA AGC TGG GTT** TAG TTG ATG CGG CGT CTG A
At3g46000-FOR	anneals at start codon of *AthADF*; additionally has Kozak sequence and ***att*B1 sequence** for GATEWAY® cloning	**GGG GAC AAG TTT GTA CAA AAA AGC AGG CTG** CCA CCA TGG CTG TGC ATG ATG ATT G
At3g46000-REV	anneals at stop codon of *AthADF*; additionally has ***att*B2 sequence** for GATEWAY® cloning	**GGG GAC CAC TTT GTA CAA GAA AGC TGG GTT** TAG TTG GTG CGG CTT TTG A
At3g46010-FOR	anneals at start codon of *AthADF*; additionally has Kozak sequence and ***att*B1 sequence** for GATEWAY® cloning	**GGG GAC AAG TTT GTA CAA AAA AGC AGG CTG** CCA CCA TGG CGA ACG CGG CAT CTG G
At3g46010-REV	anneals at stop codon of *AthADF*; additionally has ***att*B2 sequence** for GATEWAY® cloning	**GGG GAC CAC TTT GTA CAA GAA AGC TGG GTT** TAG TTG GCA CGG CTC CTG A
At4g00680-FOR	anneals at start codon of *AthADF*; additionally has	**GGG GAC AAG TTT GTA CAA AAA AGC AGG**

	Kozak sequence and ***att*B1 sequence** for GATEWAY® cloning	**CT**G CCA CCA TGC ATG TGA ATG ATG AAT G
At4g00680-REV	anneals at stop codon of *AthADF*; additionally has ***att*B2 sequence** for GATEWAY® cloning	**GGG GAC CAC TTT GTA CAA GAA AGC TGG GT**T CAG AGA TTG AGT CGT CCT T
At4g25590-FOR	anneals at start codon of *AthADF*; additionally has Kozak sequence and ***att*B1 sequence** for GATEWAY® cloning	**GGG GAC AAG TTT GTA CAA AAA AGC AGG CT**G CCA CCA TGG CAG TGG AGG ACG AGT G
At4g25590-REV	anneals at stop codon of *AthADF*; additionally has ***att*B2 sequence** for GATEWAY® cloning	**GGG GAC CAC TTT GTA CAA GAA AGC TGG GT**C TAG AGA GCT CGG CTT TTG A
At4g34970-FOR	anneals at start codon of *AthADF*; additionally has Kozak sequence and ***att*B1 sequence** for GATEWAY® cloning	**GGG GAC AAG TTT GTA CAA AAA AGC AGG CT**G CCA CCA TGA CGG ATG ATT GCA AGA A
At4g34970-REV	anneals at stop codon of *AthADF*; additionally has ***att*B2 sequence** for GATEWAY® cloning	**GGG GAC CAC TTT GTA CAA GAA AGC TGG GT**T CAT TTG GCC CGG TCC TGG A
At5g52360-FOR	anneals at start codon of *AthADF*; additionally has Kozak sequence and ***att*B1 sequence** for GATEWAY® cloning	**GGG GAC AAG TTT GTA CAA AAA AGC AGG CT**G CCA CCA TGG CGG TGG AGG ACG AGT G
At5g52360-REV	anneals at stop codon of *AthADF*; additionally has ***att*B2 sequence** for GATEWAY® cloning	**GGG GAC CAC TTT GTA CAA GAA AGC TGG GT**C TAG AGA GCT CGA CTT TTG A
At5g59880-FOR	anneals at start codon of *AthADF*; additionally has Kozak sequence and ***att*B1 sequence** for GATEWAY® cloning	**GGG GAC AAG TTT GTA CAA AAA AGC AGG CT**G CCA CCA TGG CAG TCC ATG ATG ACT G
At5g59880-REV	anneals at stop codon of *AthADF*; additionally has ***att*B2 sequence** for GATEWAY® cloning	**GGG GAC CAC TTT GTA CAA GAA AGC TGG GT**T CAA TTG GCT CGG CTT TTG A
At5g59890-REV	anneals at stop codon of *AthADF*; additionally has ***att*B2 sequence** for GATEWAY® cloning	**GGG GAC CAC TTT GTA CAA GAA AGC TGG GT**T TAG TTG ACG CGG CTT TTC A
HvADF6-Gate-For	anneals at start codon of *HvADF6*; additionally has Kozak sequence and ***att*B1 sequence** for GATEWAY® cloning	**GGG GAC AAG TTT GTA CAA AAA AGC AGG CT**G CCA CCA TGG CCT TCA TGC GCA CC
HvADF6-Gate-Rev	anneals at stop codon of *HvADF6*; additionally has ***att*B2 sequence** for GATEWAY® cloning	**GGG GAC CAC TTT GTA CAA GAA AGC TGG GT**C TAG TGC GCC CGG TCA CG
Actin-F	anneals at start codon of *HvActin2/7*; additionally has Kozak sequence and ***att*B1 sequence** for GATEWAY® cloning	**GGG GAC AAG TTT GTA CAA AAA AGC AGG CT**T CGC CAC CAT GGC TGA CGG TGA GGA CAT
Actin-R	anneals at stop codon of *HvActin2/7*; additionally has Kozak sequence and ***att*B2 sequence** for GATEWAY® cloning	**GGG GAC CAC TTT GTA CAA GAA AGC TGG GT**T CAG AAG CAC TTC CTG TGG A

Actin-intron-For	anneals inside barley *HvActin2/7*; overstretches 2nd intron	TGG CAC CCG AGG AGC ACC
Actin-intron-Rev	anneals inside barley *HvActin2/7*; overstretches 2nd intron	GTA ACC TCT CTC GGT GAG
ExoS-For	anneals at start codon of *ExoS*; additionally has Kozak sequence and ***att*B1 sequence** for GATEWAY® cloning	**GGG GAC AAG TTT GTA CAA AAA AGC AGG CT**G CCA CCA TGT CCT CGG CCG TCG TGT TCA A
ExoS-Rev	anneals at stop codon of *ExoS*; additionally has ***att*B2 sequence** for GATEWAY® cloning	**GGG GAC CAC TTT GTA CAA GAA AGC TGG GT**C TAG TCG GCC GAT ACT CTG CT
SopE-For	anneals at start codon of *SopE*; additionally has Kozak sequence and ***att*B1 sequence** for GATEWAY® cloning	**GGG GAC AAG TTT GTA CAA AAA AGC AGG CT**G CCA CCA TGT TGA CAA ATA AAG TC
SopE-Rev	anneals at stop codon of *SopE*; additionally has ***att*B2 sequence** for GATEWAY® cloning	**GGG GAC CAC TTT GTA CAA GAA AGC TGG GT**T CAG GGA GTG TTT TGT AT
YopT-For	anneals at start codon of *YopT*; additionally has Kozak sequence and ***att*B1 sequence** for GATEWAY® cloning	**GGG GAC AAG TTT GTA CAA AAA AGC AGG CT**G CCA CCA TGG ACA GTA TTC ACG GA
YopT-Rev	anneals at stop codon of *YopT*; additionally has ***att*B2 sequence** for GATEWAY® cloning	**GGG GAC CAC TTT GTA CAA GAA AGC TGG GT**T TAA ACC TCC TTG GAG TC
SipA-For	anneals at start codon of *SipA*; additionally has Kozak sequence and ***att*B1 sequence** for GATEWAY® cloning	**GGG GAC AAG TTT GTA CAA AAA AGC AGG CT**T CGC CAC CAT GGT TAC AAG TGT AAG G
SipA-Rev	anneals at stop codon of *SipA*; additionally has ***att*B2 sequence** for GATEWAY® cloning	**GGG GAC CAC TTT GTA CAA GAA AGC TGG GT**T TAA CGC TGC ATG TGC AA
At2g16700-N-Fusion	anneals at start codon of *AthADF*; additionally has Kozak sequence and ***att*B1 sequence** for GATEWAY® cloning	**GGG GAC AAG TTT GTA CAA AAA AGC AGG CT**T CAT GCG TGT GAC GGA TGA GTG
At2g31200-N-Fusion	anneals at start codon of *AthADF*; additionally has Kozak sequence and ***att*B1 sequence** for GATEWAY® cloning	**GGG GAC AAG TTT GTA CAA AAA AGC AGG CT**T CAT GTC TTT CAG AGG ACT TAG
At4g34970-N-Fusion	anneals at start codon of *AthADF*; additionally has Kozak sequence and ***att*B1 sequence** for GATEWAY® cloning	**GGG GAC AAG TTT GTA CAA AAA AGC AGG CT**T CAT GAC GGA TGA TTG CAA GAA

2.1.8   Enzymes

2.1.8.1   Restriction enzymes

Restriction enzymes were purchased from New England Biolabs (Schwalbach), Boehringer (Mannheim), GIBCO BRL, Pharmacia Biotech (Braunschweig), and Stratagene (Heidelberg) unless otherwise stated.

10 x buffers for restriction enzymes were companied with the enzymes and supplied by manufacturers.

2.1.8.2   Nucleic acid modifying enzymes

Standard PCR reactions were performed using homemade *Taq* DNA polymerase while for the cloning of the PCR products, *pfu, pfx*, *pwo* polymerase were used. Modifying enzymes were listed below and purchased from various sources:

Taq DNA Polymerase	Homemade
Pfu DNA-Polymerase	Stratagene (Heidelberg)
Pfx DNA-Polymerase	Invitrogen (Heidelberg)
Pwo DNA-Polymerase	Roche (Mannheim)
T4 DNA ligase	Roche (Mannheim)
T4 Polynucleotide kinase	Roche (Mannheim)
DNase I, from bovine pancrease	Sigma (Deisenhofen)
RNase I, from bovine pancrease	Sigma (Deisenhofen)
Superscript II RT	Invitrogen (Heidelberg)
Shrimp alkaline phosphatase	Roche (Mannheim)
GATEWAY®-Technology	
BP-Clonase	Invitrogen (Heidelberg)
LR-Clonase	Invitrogen (Heidelberg)
Lysozyme	Roche (Mannheim)

2.1.9   Chemicals

Laboratory grade chemicals and reagents were purchased from Roth (Karlsruhe), Serva (Heidelberg), Boehringer (Mannheim), Merck (Darmstadt), Beckman (München), GIBCO BRL (Neu Isenburg) and Sigma (Deisenhofen) unless otherwise stated.

2.1.10   Media

Unless otherwise indicated all media were sterilized by autoclaving at 121°C for 20 minutes. Heat labile solutions were sterilized using filter sterilisation units prior to addition of autoclaved components.
For the addition of antibiotics and other heat liable components the solution or media were cooled down to 55°C.

LB-medium (Lauria-Bertani Broth, Sambrook et al. 1989)

Tryptone	10.0	g/l
Yeast extract	5.0	g/l
NaCl	5.0	g/l

For agar plates 1.5-2% agar was added to the above broth.

SOC-Medium

Tryptone	20.0	g/l
Yeast extract	5.0	g/l
NaCl	10.0	mM
KCl	2.5	mM
$MgCl_2$	10.0	mM
$MgSO_4$	10.0	mM
Glucose	20.0	mM

2.1.11   Buffers and solutions

2.1.11.1   General buffers and solutions

Ethylenediaminetetraacetic acid (EDTA) stock solution (0.5 M)

Na_2EDTA	186.1	g
H_2O	ad 1000.0	ml

Dissolve Na_2EDTA in 700 ml water, adjust pH to 8.0 with 10 M NaOH (~ 50 ml; add slowly), add water up to 1000 ml. Filter-sterilize. Store at room temperature.

IPTG stock solution (0.1 M)

IPTG	1.2	g
ddH_20	ad 50	ml

Filter-sterilize. Store at 4°C.

piperazine-*N*, *N*-bis (2-ethanesulfonic acid) (PIPES) buffer (2x)

PIPES	50.0	mM
$MgCl_2$	2.0	mM
EGTA	2.0	mM
Tween 20	0.05	% (w/v)

Phosphate buffered saline (PBS) solution (2x)

$Na_2HPO_4 \cdot 2H_2O$	1.4	g
KH_2PO4	0.2	g
NaCl	8.0	g
KCl	0.2	g
ddH_2O	ad 1000.0	ml

Adjust pH to 6.8 or 7.4. Store at room temperature.

Sodium phosphate buffer (0.1 M)

    Solution A:

$NaH_2PO_4 \cdot H_2O$	0.2	M

    Solution B:

$Na_2HPO_4 \cdot 7H_2O$	0.2	M

Mix the different volumes of solutions A and B to 100 ml for desired pH, then dilute with water to 200 ml. Filter-sterilize if necessary. Store at room temperature.

TE (Tris/EDTA) buffer

Tris/HCl	10.0	mM
EDTA	1.0	mM

Adjust to pH 7.4, 7.5, or 8.0.

<u>T</u>ris/<u>a</u>cetate/<u>E</u>DTA (TAE) buffer (10x)

Tris-base	24.2	g
Glacial acetic acid	5.71	ml
$Na_2EDTA \cdot 2H_2O$	3.72	g
ddH_2O	ad 1000.0	ml

Tris/HCl stock solution (1 M)

Tris-base	121.0	g
ddH_2O	ad 1000.0	ml

Dissolve Tris-base in 800 ml, adjust to desired pH with concentrated HCl, adjust volume to 1000 ml with ddH_2O, filter-sterilize if necessary. Store at 4°C or at room temperature.

2.1.11.2 DNA buffers

DNA Gel loading buffer (6x)

Bromphenol blue	0.25	% (w/v)
Xylene cyanol FF	0.25	% (w/v)
Sucrose	40.0	% (w/v)
or Ficoll 400	15.0	% (w/v)
or Glycerol	30.0	% (v/v)

Store at 4°C (room temperature if Ficoll is used). Sucrose, Ficoll 400, and glycerol are interchangeable in this recipe.

DNA extraction buffer

Tris-HCl (pH 8.5)	100.0	mM
NaCl	100.0	mM
EDTA (pH 8.0)	50.0	mM
SDS	2.0	%
Proteinase K	0.1	mg/ml (added at the time of use)

Ethidium bromide stock solution (10 mg/ml)

Ethidium bromide	0.2	g
ddH$_2$O	ad 20	ml

Do not sterilize. Store at 4°C in dark or in a foil-wrapped bottle.

STETL buffer

Saccharose	8.0	%
Triton -100	5.0	%
EDTA	50.0	mM
Tris-HCL (pH 8.0)	50.0	mM
Lysozyme	0.5	mg/ml (added at the time of use)

Store at room temperature. Lysozyme store at 4°C.

2.2 Methods

2.2.1 Nucleic acid manipulations

2.2.1.1 Polymerase chain reaction (PCR) amplification

PCR amplification Puffer (10x)

Tris-HCl (pH 8.4)	200.0	mM
KCl	500.0	mM
$MgCl_2$	25.0	mM

Stock solution is sterilised by autoclaving.

Plasmid or genomic PCR (*Taq* polymerase)

Basic PCR approach

Template DNA (genomic or plasmid)	50-300	pg
Upstream primer (100 pmol/µl)	0.5	pmol/µl
Downstream primer (100 pmol/µl)	0.5	pmol/µl
dNTP-mix (dATP, dGTP, dCTP, dTTP)	0.2	mM (each)
Taq DNA polymerase (2.5 U)	1.0	U
PCR amplification buffer (10x)	1/10	of reaction volume
Nuclease free water	variable	

Thermal profile

Stage	Temperature (°C)	Time period	No. of cycles
Initial denaturation	94	3 min	1x
Denaturation	94	30 sec	
Annealing	50-65	30 sec	25-50x
Extension	72	1 min per 1 kb amplified nucleotides	
Final extension	72	3 min	1x

E. coli colony PCR:

Essentially follow the plasmid or genomic PCR protocol except that one µl LB-medium containing *E. coli* was used as template.

PCRs with other polymerases, e.g., *Pfu, Pfx,* and *Pwo* were performed according to the manufacturer's protocol.

2.2.1.1.1 Quantitative real-time PCR

A quantitative real-time PCR kit (Brilliant SYBR Green QPCR Core Kit, Stratagene) was used to determine the amount of transcript accumulation of a gene of interest. Reactions were carried out according to the manufacturer's protocol. Primer combinations that specifically amplify the investigated gene and a gene serving as an internal standard were used in independent reactions performed on an ABI PRISM 7700 Sequence Detection System (Applied Biosystems, Foster City, California, USA). Data were analysed by the comparative $\Delta\Delta C_T$ method (ABI PRISM 7700 User Bulletin).

Quantitative real-time PCR approach

Template cDNA	2	µl
Upstream primer (100 pmol/µl)	50	nM
Downstream primer (100 pmol/µl)	50	nM
dNTP-mix (dATP, dGTP, dCTP, dTTP)	0.2	mM (each)
Taq DNA polymerase (2.5 U)	2.5	U
PCR amplification buffer (10x)	1/10	of reaction volume
Glycerol solution (50%)	8	% (v/v)
DMSO (100%)	3	% (v/v)
Diluted SYBR green (1:3000)	2.5	µl
Nuclease free water	ad 50.0	µl

Thermal profile

Stage	Temperature (°C)	Time period	No. of cycles
Initial denaturation	95	10 min	1x
Denaturation	95	30 sec	
Annealing	50-60	30 sec	40x
Extension	72	1.5 min	
Final extension	72	3 min	1x

2.2.1.2   Restriction endonuclease digestion of DNA

All restriction digests were carried using the manufacturers recommended conditions. Typically, reactions were carried out in 1.5 ml eppendorf reaction tubes using 1-2 Units of restriction enzyme per 10-20 µl reaction. All digests were carried out at the appropriate temperature in incubators with proper temperature for a minimum of 30 minutes.

2.2.1.3   Site-specific recombination of DNA in GATEWAY®-compatible vectors

Basic BP reaction approach

*att*B-PCR Product (75 ng/µl)	1	µl
GATEWAY® BP clonase	1	µl
BP reaction buffer (5x)	1	µl
pDONR™201 vector (75 ng/µl)	1	µl
ddH₂O	1	µl

Basic LR reaction approach

Entry clone (75 ng/µl)	1	µl
GATEWAY® LR clonase	1	µl
LR reaction buffer (5x)	1	µl
Destination vector (150 ng/µl)	1	µl
ddH₂O	1	µl

Typically, reactions were carried out in 200 µl PCR tubes. Reactions were incubated at room temperature for at least 12 h, before completely transformed into *E. coli* strain DH5α.

2.2.2   DNA analysis

2.2.2.1 Plasmid DNA isolations

Plasmid DNA was isolated by the boiling preparation method (Holmes and Quigley, 1981). High quality DNA for single-cell transient gene expression assays or sequencing was isolated using Qiagen or Macherey-Nagel Mini-, Midi- or Maxi-preparation kit.

2.2.2.2   Plant genomic DNA isolation

Plant materials were transferred into a 1.5 ml eppendorf reaction tube together with 150 µl of 25 mM NaOH and approximately 20 steal beats. Plant materials were grinded for 30 seconds in a "beatbeater" and subsequently boiled at 100°C for 30 seconds. 150 µl of 25 mM HCL and 75 µl of 0.5 M Tris/HCL (pH 8.0) containing 0.25% (w/v) Nonidet P40 (Roche) were added. Cell debris was pelleted by centrifugation at 13.000 rpm for 2 minutes and room temperature in a bench top centrifuge. 1-2 µl of supernatant were used for PCRs.

2.2.2.3   Isolation of DNA fragments from Agarose-gels

The Nucleospin Extract-Kit (Macherey-Nagel) was used to extract DNA fragments from Agarose-gels according to the manufacturer's protocol.

2.2.2.4   DNA sequencing

DNA sequences were determined by the <u>A</u>utomatische <u>D</u>NA <u>I</u>solierung und <u>S</u>equenzierung (ADIS) service unit at the MPIZ on Applied Biosystems (Weiterstadt, Germany) Abi Prism 377 and 3700 sequencers using Big Dye-terminator chemistry (Sanger *et al.*, 1977). PCR products were purified with the Nucleospin Extract-Kit (Macherey-Nagel) or Qiagen Extract Kit, ensuring sufficient amount at appropriate concentration to be directly sequenced.

2.2.2.5   DNA sequence analysis

Sequence data were analysed mainly using Clone Manager 6, version 6.00 and alignment made using Align Plus 4, version 4.10 from Scientific & Educational Software. Alternatively, the GCG Program (Version 10.0) from Genetics-Computer-Group, Inc., University of Wisconsin, Madison, or ClustalW (http://www.ebi.ac.uk/clustalw/) was used.
Treeview (http://www.taxonomy.zoology.gla.ac.uk./rod/rod.html) and Phylip (http://evolution.gs.washington.edu/phylip.html) were used for phylogenetic analysis.

2.2.2.6   Database searching

DNA sequence data were directly used for database searching using NCBI Blast (http://www.ncbi.nlm.nih.gov/BLAST/), or translated into polypeptide for motif similarity searching. Other used databases include the Phytopathogenic fungi and oomycete EST database (Version 1.4) (http://cogeme.ex.ac.uk/), TAIR (http://www.Arabidopsis .org/), TIGR (http://www.tigr.org) and IPK barley ESTs database (http://pgrc.ipk-gatersleben.de/).

2.2.3   RNA analysis

2.2.3.1   Isolation of total RNA from plant tissues

Plant materials were finely ground in liquid nitrogen, re-suspended in the total RNA extraction buffer, and incubated at 37°C for 1 hour. Following three phenol/chloroform extractions, RNA was precipitated with 1 volume 8 M LiCl prepared in Diethyl-polycarbonate (DEPC) water, washed with 70% ethanol and re-suspended in DEPC treated water.

Alternatively, harvested plant material, previously stored at -80°C, was transferred to a pre-chilled, autoclaved mortar, and ground to a fine powder in the presence of liquid nitrogen. Approximately 0.5 ml of tissue was transferred to an RNase-free 2 ml centrifuge tube, before 1 ml of Tri reagent (Sigma) was added. The sample was vortexed for 10 seconds and can be placed on dry ice until resumption of the process. All homogenised samples were left at room temperature for 10 minutes. 200 µl of chloroform was subsequently added, vortexed for 15 seconds and allowed to stand for 2-15 minutes at room temperature. The samples were spun for 20 minutes, at 13.000 rpm and 4°C, in a bench-top centrifuge. The upper aqueous phase was carefully transferred to a fresh RNase free 2 ml centrifuge tube. The RNA was precipitated by adding 500 µl of isopropanol, mixing well and leaving at room temperature for 10 minutes. Centrifuging at 13.000 rpm for 10-15 minutes and 4°C helped to pellet the RNA. The supernatant was removed and the white pellet was washed with 1 ml of 75% ethanol (absolute ethanol diluted with DEPC treated water 1:3). The samples were briefly vortexed to dislodge the pellet and centrifuged again for 10 minutes at 4°C and 13.000 rpm. The supernatant was removed and the pellet air-dried for 10 minutes. The RNA was re-suspended in 40-60 µl of DEPC water.

2.2.3.2   RT-PCR

Reverse transcription (RT)-PCR was carried out by a two-steps method. Reverse transcriptase Superscript II (Invitrogen) was used for the first strand cDNA synthesis by combining 2 µg template total RNA, 2 µl 10 µM oligo dT-18. The sample was incubated at 70°C for 10 minutes before immediately cooling on ice. Subsequently

the reaction was filled up to 20 µl by adding the following components: 4 µl first strand buffer (250 mM Tris (pH 8.3) / 375 mM KCl / 15 mM $MgCl_2$), 2 µl 0.1 M DTT, 1 µl 10 mM dNTPs mix and proper amount of DEPC treated water. The mix was incubated at 42°C for 2 min before adding 1 µl (200u) Superscript II. Subsequently, the reaction was incubated at 25°C for 10 minutes, at 42°C for 50 minutes and finally at 70°C for 15 minutes to inactivate the enzyme.

For subsequent normal PCR, 2 µl of the above mixture was used as cDNA template and 2.5 µl of DMSO added for 50 µl of reaction volume before PCR (for disrupting potential secondary structures of the single strand DNA).

2.2.4   Transformation of *E. coli*

2.2.4.1.1   Preparation of electro-competent *E. coli* cells

10 ml of an over night culture of *E. coli* strain DH5α were added to 1000 ml of LB broth and shaken at 37°C until the bacterial growth reached an OD_{600} 0.5-0.6. The bacteria were pelleted at 5000 x g for 20 minutes at 4°C and the pellet gently re-suspended in ice-cold sterile water. The cells were pelleted as before and again re-suspended in ice-cold water. The process was repeated twice. Finally the cells were gently re-suspended in a 1/100 volume of the initial culture in 10% sterile glycerol, pelleted once more and then re-suspended in 5 ml 10% glycerol. 50 µl aliquots of cells were frozen in liquid nitrogen and stored at -80°C until use.

2.2.4.1.2   Transformation of electro-competent *E. coli* cells

20 to 50 ng of salt-free ligated plasmid DNA (or ~ 1 µl of ligated mix from 10 µl ligation reaction) was mixed with 50 µl of electro-competent cells, and transferred to the a cold BioRad electroporation cuvette (1 mm electrode distance). The BioRad gene pulse apparatus was set to 25 µF capacitance, 1.8 kV and the pulse controller to 200 Ω. The cells were pulsed once at the above settings for a few seconds and 500 µl of SOC medium was immediately added to the cuvette and the cells were

quickly re-suspended and incubated at 37°C for 1 hour. A fraction (~ 150-300 µl) of the transformation mixture was plated onto selection media plates.

2.2.4.2.1   Preparation of chemo-competent *E. coli* cells (Hanahan, 1983)

5 ml of an over night culture of *E. coli* strain DH5α was added to 100 ml of LB broth and shaken at 37°C until the bacterial growth reached an OD_{600} 0.5-0.6. The bacteria were pelleted at 5000 x g for 10 minutes at 4°C. The pellet was gently re-suspended in 30 ml ice-cold TfBI solution and subsequently incubated for 10 minutes on ice. The cells were pelleted as before and re-suspended in ice-cold TfBII solution. 1.5 ml eppendorf reaction tubes containing 50 µl aliquots of cells were frozen in liquid nitrogen and stored at -80°C until use.

2.2.4.2.2   Transformation of chemo-competent *E. coli* cells

50 µl aliquot of chemo-competent cells was thawed on ice. 20 to 50 ng of salt-free ligated plasmid DNA (or ~ 1 µl of ligated mix from 10 µl ligation reaction) was mixed with the aliquot and incubated on ice for 30 minutes. The mixture was heat-shocked for 30 seconds at 42°C and again incubated on ice for 2 minutes. 500 µl of SOC medium was immediately added to the eppendorf tube and incubated at 37°C for 1 hour. A fraction (~ 150-300 µl) of the transformation mixture was plated out onto selection media plates.

2.2.5   High-throughput generation of ihpRNA constructs

*att*B-PCR products amplified from epidermal cDNA library clones were used in BP reactions with pDONR™201 according to Chapter 3.2.2.1 in a 96 deep-well (300 µl) microtiter plate with conical bottom. After site-specific recombination, 50 µl of ice-cold chemo-competent cell solution was added to each well. The microtiter plate was incubated for 30 minutes at 4°C. The mixture was heat-shocked for 2 minutes at 42°C and again incubated 5 minutes at -20°C. 200 µl of SOC medium was

immediately added to each well and the microtiter plate was incubated for 2 h at 37°C on a plate shaker. Each transformation was completely plated onto selection media plates.

Single colonies of each reaction were picked for plasmid isolation using the Millipore™ montage plasmid miniprep$_{96}$ kit. Preparation was carried out according to the manufacturer's protocol.

Resulting cDNA-containing pDONR™201 clones were used in LR reactions with ihpRNA vectors (pUAMBN or pUAMBN-i) according to the procedure described for BP reactions.

2.2.6   Single-cell transient gene expression/gene silencing assay in barley epidermal cells using particle bombardment

The Biolistic particle delivery is a method for transformation that uses helium pressure to introduce DNA coated on gold or tungsten particles (microcarriers) into living cells.

2.2.6.1   Preparation of microcarriers (for 10 bombardments)

30 mg of gold microcarriers (0.9-1.0 µm diameter) were transferred into a 1.5 ml eppendorf tube. 1 ml of 70% EtOH was added. The suspension was vigorously vortexed for 3-5 minutes on a platform vortexer. The suspension was left alone for 15 minutes to sediment the microcarriers. The microcarriers were pelleted by spinning for 5 seconds in a bench-top centrifuge. The supernatant was removed and discarded. The pellet was rinsed for three times by adding 1 ml of sterile water, vigorously vortexing for 1 minute, sedimentation of the particles for 1 minute, pelleting the microparticles by spinning for 5 seconds in a bench-top centrifuge and subsequent removal of the supernatant. After washing, 500 µl sterilised glycerol (50% (v/v)) was added to adjust microparticle suspension to a concentration of 60 mg/ml. The microcarriers can be stored at 4°C for up to 2 weeks.

2.2.6.2   Coating of microcarriers with DNA (for one bombardment)

The previously prepared microcarriers (see Chapter 2.2.6.1) were vortexed for 5 minutes on a platform vortexer to resuspend sedimented particles. 50 µl of the microcarrier suspension were removed while vortexing and transferred to a 1.5 ml eppendorf tube. A *GUS* reporter gene containing plasmid (pUbi-GUS-nos) and respective effector plasmids were mixed prior to the coating of particles (ratio 1:1, respectively, maximum of 5 µg DNA). While vigorously vortexed, the prepared DNA mixture, 50 µl $CaCl_2$ (2.5 M), and 20 µl spermidine (0.1 M) were added to microcarrier suspension. The microcarriers were spun down for 2 seconds in a bench-top centrifuge and the supernatant was discarded. 140 µl of 70% EtOH were added and the suspension was vortexed at low speed for 2 seconds before spinning the suspension for 2 seconds. The supernatant was removed and discarded. 140 µl of 100% EtOH were added and the suspension was again vortexed at low speed for 2 seconds before spinning the suspension for 2 seconds. The coated gold particles were resuspended in 50 µl of 100% EtOH.

2.2.6.3   Preparation for the bombardment

One-week old barley seedlings, grown in a phyto-chamber under controlled conditions (18°C, 60% relative humidity, and 16 h light / 8 h darkness), were cut off and placed on 1% agar plates supplemented with 85 µM Benzimidazol and stored in a light chamber at 18°C for 4 h prior bombardment.

2.2.6.4   The particle bombardment

Seven macrocarriers were placed inside the macrocarrier holder of the Hepta Adapter™ (BioRad). 6 µl aliquots of DNA-coated microcarriers were removed from the suspension while vortexing and transferred to each of the seven macrocarriers. After complete evaporation of the EtOH, the Hepta Adapter™ was placed inside the BioRad particle delivery system (Biolistic-PDS-1000/He) and a vacuum of 27 mm Hg was applied. Rupture discs bursting at a pressure of 900 psi were used in the

bombardment process. The bombarded leaves were placed in a light chamber at 18°C for 4 h for regeneration before high-density inoculation with *Bgh, Bgt,* or *Erysiphe pisi* spores. In the gene silencing experiments the bombarded leaves were incubated at 18°C for 96 h before high-density inoculation to allow turnover of preformed proteins.

2.2.6.5 GUS staining of bombarded leaves

The bombarded leaves were transferred after 48-96 h post powdery mildew fungus inoculation into 15 ml Falcon tubes containing the GUS staining solution. Falcon tubes were placed in an exicator and a vacuum of 30 mm Hg was applied for at least 5 minutes. This procedure was repeated four-times. The Falcon tubes were closed and incubated over night at 37°C. After incubation of the leaves, the GUS staining solution was exchanged with the GUS destaining solution. After 1 day at RT leaves were rinsed with water and transferred for max. 2 minutes into the Coomassie blue solution to stain epiphytic fungal structures for microscopic evaluation. Leaves can be stored in destaining solution for up to 6 months.

Spermidine solution (0.1 M)

Spermidine	73.0	mg
ddH$_2$O	ad 50.0	ml

GUS staining solution

Na$_2$HPO$_4$ (1M)	57.7	ml
NaH$_2$PO$_4$ (1M)	42.3	ml
Na$_2$EDTA (0.5 M)	20.0	ml
K$_4$Fe[CN]$_6$	2.11	g
K$_3$Fe[CN]$_6$	1.65	g
Triton X-100	0.1	% (v/v)
Methanol	20.0	% (v/v)
X-Gluc	1.0	g

X-Gluc: 5-bromo-4-chloro-3-indoxyl-β-D-glucuronic acid, cyclohexylammonium salt (Roth).

Destaining solution stock solution

Glycerol	50.0	%
Lactic acid	25.0	%
H$_2$O	50.0	%

Stock solution was diluted with ethanol 1:3 (v/v) for use.

Coomassie solution

Coomassie blue	0.6	% (w/v)
in ethanol		

Coomassie: Serva Blue R, (Serva).

2.2.7   Cytological methods

2.2.7.1   Cytochemistry of actin filaments

Actin microfilaments were stained as described previously (Kobayashi *et al*., 1997a) with slight modifications (Krystina S. Opalski, personal communication). Leaf segments (4x4 mm in size) were fixed in 3.7% formaldehyde in 1xPIPES buffer, pH 6.8, at room temperature for 1 h. After washing in 1xPIPES and in 1xPBS (pH 6.8), leaf segments were treated with 0.5% Triton X-100 in 1xPBS (pH 6.8) at room temperature for 1 h. The specimens were washed with 1xPBS (pH 6.8) then with 1xPBS (pH 7.4). Following a three times rinse cycle, leaf segments were stained with Alexa-Fluor® 488 phalloidin (Molecular Probes, Eugene; 0.66 µM in 1xPBS (pH 7.4)). To promote uptake of the dye vacuum infiltration was performed three times for 20 sec at 27 mm Hg. Subsequently, samples were stored at RT for 2-3 h in the dark. Finally, the leaves were rinsed with 1xPBS (pH 7.4). The specimens were mounted in 1xPBS (pH 7.4) on glass slides and observed by confocal laser scanning microscopy.

2.2.7.2 Callose staining in *Arabidopsis* and barley leaves

48 hpi with powdery mildew conidiospores, barley leaves were transferred into destaining solution (see Chapter 2.2.6.5) whereas *Arabidopsis* leaves were transferred into the lactophenol destaining solution. 1 day before microscopic evaluation of callose deposition leaves were washed with 50% (v/v) EtOH and subsequently with pure H_2O before transfer in the aniline blue staining solution. For microscopic evaluation leaves were rinsed with water, floated in Comassie blue solution to stain epiphytic fungal structures and mounted in 50% (v/v) glycerol.

Lactophenol destaining stock solution

Phenol (90%)	111.0	ml
Lactic acid	100.0	ml
Glycerol	200.0	ml
ddH$_2$O	ad 500.0	ml

Stock solution was diluted with ethanol 1:3 for use.

Aniline blue staining solution

KH$_2$PO$_4$	10.23	g
Aniline blue	50.0	g
ddH$_2$O	ad 500.0	ml

Adjust to pH 9.5.

Coomassie solution

Coomassie blue	0.6	% (w/v)
in ethanol		

Coomassie: Serva Blue R, (Serva).

3   Establishment of a dsRNAi-based high-throughput screen for genes implicated in barley powdery mildew resistance

3.1   Introduction

The aim of this work was to identify genes that play a role in the pathways of barley *Mlo*-mediated basal defence and/or *mlo* broad-spectrum resistance to *Blumeria graminis* f.sp. *hordei*, the barley powdery mildew fungus.

So far, forward genetic screens for mildew resistant plants only identified alleles of *mlo* in chemical- or radiation-mutagenised wild-type barley (Jørgensen, 1992). Additionally, two genes (*Ror1* and *Ror2*) were obtained by forward genetics in mutagenised *mlo* plants that were screened for compromised broad-spectrum resistance (Freialdenhoven *et al.*, 1996). Nevertheless, overall yield from these screens was low. Several causes can be assumed as possible explanation, like mutation-induced lethality or genetic redundancy. However, also the screening setup might be a limiting factor. Plant resistance against pathogens is a multi-layered process. Knock-out of individual "resistance" or "susceptibility" genes does not consequently render a plant fully resistant or susceptible. Large-scale genetic screens designed to unravel predominantly presence or absence of pathogen growth might miss subtle effects contributing to defence responses.

In this work, a reverse genetic screen was set up that might circumvent these putative limitations. Mutant lethality and gene redundancy were tried to avoid by application of the dsRNAi technology via transient effector construct expression in single barley leaf epidermal cells. Transfection of epidermal cells was achieved by particle bombardment (Nielsen *et al.*, 1999; Schweizer *et al.*, 1999; Schweizer *et al.*, 2000).

3.1.1   The patho-system: Barley and powdery mildew

Blumeria graminis f.sp. *hordei* (*Bgh*) belongs to the class of obligate biotrophic ascomycetes that are responsible for foliar diseases on grass species. *Bgh* causes

severe reductions in yield provoked by premature leaf senescence. Therefore, *Bgh* can be considered as an economically significant pathogen of barley.

The prevalent haploid asexual life cycle of *Bgh* can be distinguished in strictly adhered temporally stages. The first step is the development of a primary germ tube (PGT). This happens one hour after a fungal spore (conidium) landed on the surface of a barley leaf [Fig. 3]. The role of the PGT for the barley powdery fungus remains enigmatic, since penetration of plant epidermal cells by the PGT has never been observed. Nevertheless, the primary germ tube elicits putative plant defence responses manifested in papilla formation and an oxidative microburst (Hückelhoven *et al.*, 1999; Piffanelli *et al.*, 2002) (see Chapter 1.1). Following the formation of the primary germ tube, a secondary germ tube emerges from the conidiospore, the so-called appressorial germ tube (AGT). The swollen end of the AGT is designated as appressorium (APP). After approx. twelve hours post inoculation (hpi), an appressorial infection peg (AIP) is formed beneath the appressorium to penetrate the leaf cuticle, the epidermal cell wall and the papilla. This is probably achieved by combinatorial means of hydrostatic pressure and cell wall-degrading enzymes. After contact, the AIP invaginates the host-cell plasma membrane and starts to differentiate into a digitate structure, termed haustorium. The haustorium is suggested to serve as feeding organ and/or to contribute to the maintenance of compatibility between host and fungus. About 24 hpi haustoria become microscopically visible. Putative successful funnelling of host-derived nutrients by the fungal haustorium allows 40 hpi the progress of the primarily epiphytic growth of the fungus. This can be recognised by the development of elongating secondary hyphae (ESH). ESHs spread over the leaf surface in order to colonise new epidermal cells. Later during development ESHs differentiate further into conidiophores, which expose the fungal conidia. Huge amounts of conidiophores also account for the macroscopically visible powdery mildew phenotype. The development of conidia terminates the asexual life cycle of the fungus after approx. five to six days post inoculation (Boyd *et al.*, 1995; Schulze-Lefert and Vogel, 2000; Panstruga, 2003).
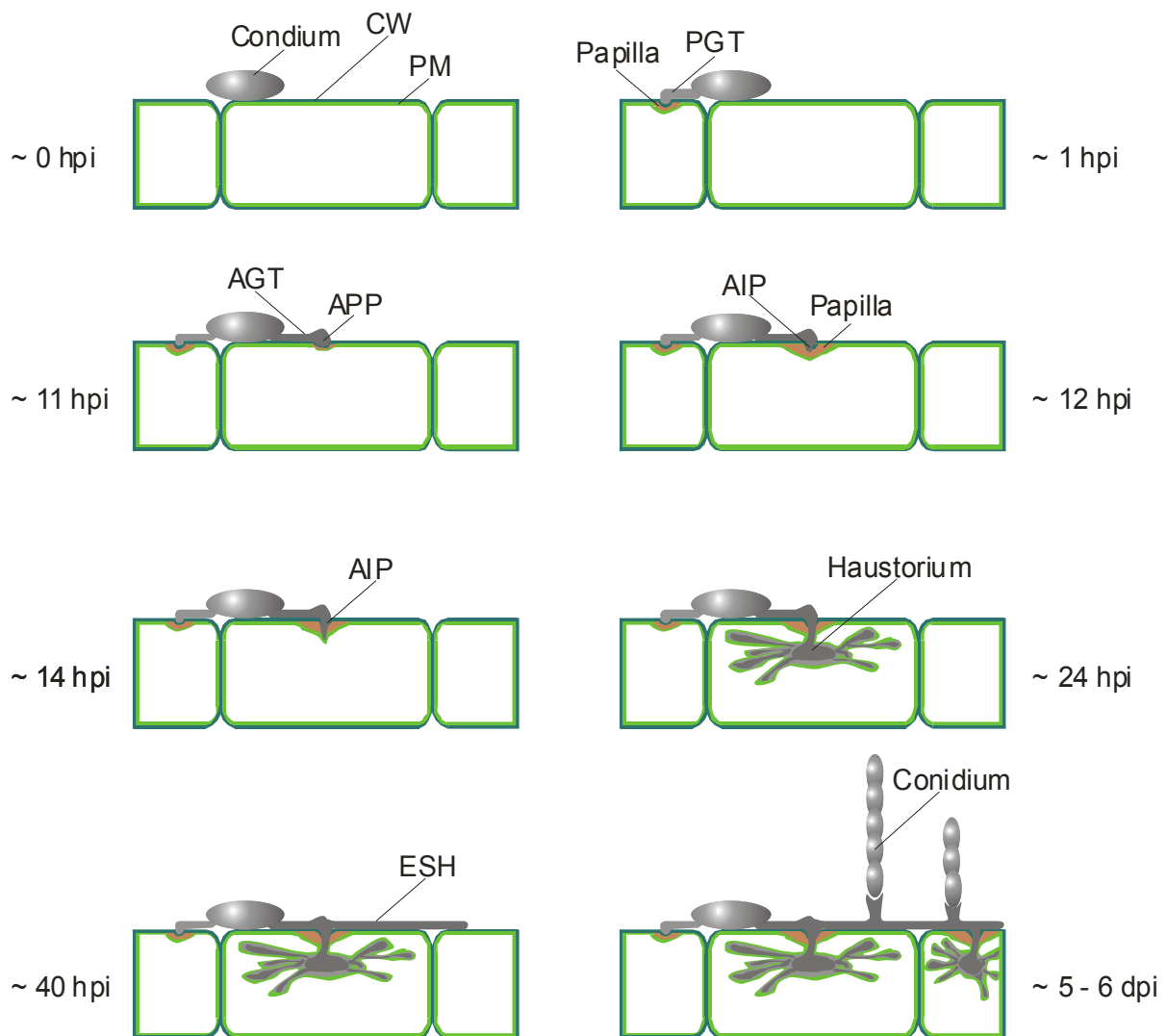
Figure 3. Schematic drawing of the asexual life cycle of *Bgh* on barley epidermal leaf cells.
For details, see text. Appressorial germ tube **(AGT)**; Appressorial infection peg **(AIP)**; Appressorium **(APP)**; Cell wall **(CW)**; Elongating secondary hyphae **(ESH)**; Plasma membrane **(PM)**.

Growth of *Bgh* on barley leaves of a *mlo* mutant ceases after approximately twelve hours. The arrest of growth coincides with the formation of papilla on the inner side of the cell wall (Aist and Israel, 1986). Consequently, the fungus forms neither haustoria nor elongating secondary hyphae [Fig. 3].

The microscopically easy distinguishable phenotypes of *Bgh* development on *Mlo* or *mlo* barley genotypes, apparently renders the *Bgh*-barley patho-system very applicable in a screen for both compromised *mlo*-mediated resistance and altered *Mlo*-mediated basal resistance/susceptibility.

3.1.2   Ballistic transfection of barley

Cereals like wheat and barley are not very suitable for forward genetic screens. Map-based cloning of genes is difficult in these grass species due to comparatively long generation times and the huge size of genomes. Therefore, only a limited number of cereal genes implicated in plant-pathogen interactions have been identified to date. Likewise, the generation of cereals stably expressing transgenes is laborious and might cause complications e.g. due to silencing effects (Panstruga, 2004). A faster and simpler way to study *in vivo* the impact of transgene expression or double stranded RNA interference (dsRNAi)-mediated post-transcriptional gene silencing (PTGS) (see Chapter 3.1.3) on barley-powdery mildew interactions is provided by the method of ballistic transformation of single epidermal cells (Nelson and Bushnell, 1997; Schweizer *et al.*, 1999; Shirasu *et al.*, 1999; Yu and Kumar, 2003). This method is based on particles that are coated with effector constructs. The constructs can consist of DNA or *in vitro* transcribed RNA. Nucleotide-coated tungsten or gold particles are high-pressure accelerated under vacuum conditions and delivered onto surfaces of detached leaves of seven-day old barley or wheat seedlings. From the excess of particles delivered, some enter the nucleus of single epidermal cells. There, the particles release their cargo load and the DNA or RNA message is converted by the plant cell. To identify transfected cells, the particles are co-coated with reporter constructs, containing either a gene encoding β-glucuronidase (GUS), staining the cells green-bluish upon X-Gluc infiltration [Fig. 4] or a fluorescent protein, e.g. GFP or YFP, detectable by epifluorescence microscopy (Nielsen *et al.*, 1999; Schweizer *et al.*, 1999; Shirasu *et al.*, 1999). Post transfection, the detached leaves are inoculated with conidiospores of *Bgh* and microscopically evaluated after a defined fungal growth period [Fig. 4]. Thereby, the ratio between numbers of reporter gene expressing cells, successfully penetrated by the fungus (visible by haustoria and ESH formation [Fig. 4B] and attacked transfected cells where fungal penetration was arrested (recognisable by presence of an appressorial germ tube on the cell surface [Fig. 4C], is determined. Information about the impact of the bombarded effector construct on the plant-microbe interaction is obtained by comparison to leaves transfected with the reporter construct only.
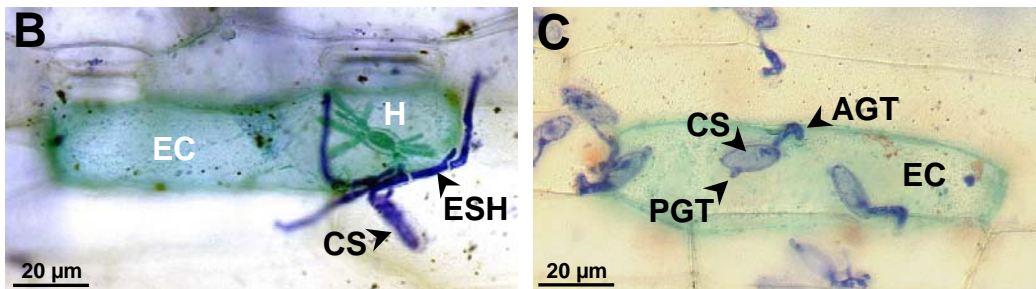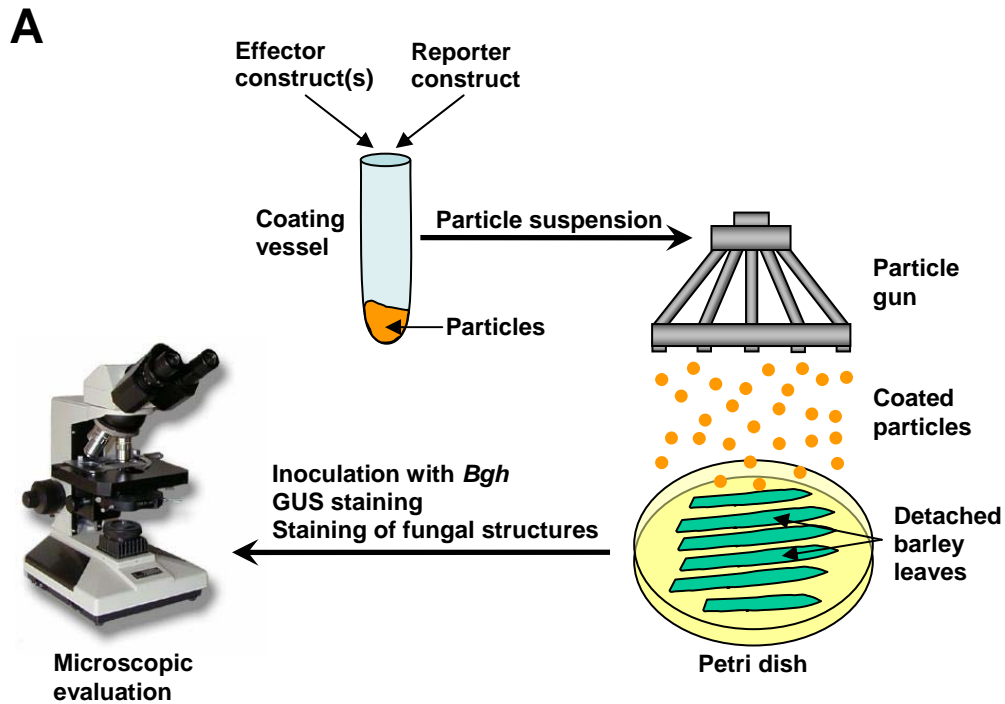
Figure 4. Scheme of the bombardment procedure.

   (A) For details, see text.
   (B) Micrograph of *Bgh* inoculated on a barley *Mlo* genotype: The *Bgh* conidiospore **(CS)** successfully penetrated into an barley epidermal cell **(EC)**, formed a haustorium **(H)** and initiated elongating secondary hyphae **(ESH)**.
   (C) Micrograph of *Bgh* inoculated on a barley *mlo* genotype: The *Bgh* conidiospore **(CS)** has formed a primary germ tube **(PGT)** and an appressorial germ tube **(AGT)**, but failed to penetrate into the epidermal cell **(EC)**.

ECs were stained for GUS reporter activity; epiphytic fungal structures were highlighted by Comassie brilliant blue staining. Micrographs were taken 48 hpi. The scale bars in the bottom left corners indicate absolute sizes.

3.1.3 Post-transcriptional gene silencing by means of inverted repeat RNA

Homologous recombination is exploited for reverse genetics in many species from prokaryotes to eukaryotes including lower plants. In higher plants, this tool is not available for the targeted knock-out of specific genes. To circumvent this problem in higher plants, huge libraries of plant mutants have been generated. For this, plants were randomly mutagenised by the insertion of Transfer (T)-DNAs into their genomes. Identification of single T-DNA insertion loci lead to an indexed catalogue of lines in which individual genes are disrupted by T-DNA insertions. These libraries enormously facilitate reverse genetics, but there are also some restrictions. First, not every gene knock-out can be found in the libraries, despite of huge collections of T-DNA insertion lines from *Arabidopsis*, e.g. the GABI-Kat collection (www.mpiz-koeln.mpg.de/GABI-Kat). Second, these libraries are confined to certain plant species. Concerning cereals, respective libraries are currently under development (Koprek *et al.*, 2000), but no easily accessible mutant libraries are available at the moment.

Another possibility to specifically switch off genes via reverse genetics is provided by the mechanism of post-transcriptional RNA silencing which causes the degradation of homologous target mRNA. Nematodes of the species *Caenorhabditis elegans* showed interfered regulation of single endogenous genes by injection of gene-homologous double-stranded RNA (dsRNA) (Fire *et al.*, 1998). Because injected RNA was instable and therefore not heritable in the nematode, it was proposed to generate dsRNA from inverted repeat DNA *in vivo*. This method proved very effective and also adaptable to other organisms (Tavernarakis *et al.*, 2000). Designated as dsRNAi in animals, the mechanism apparently is evolutionarily conserved throughout different kingdoms. It naturally occurs in plants as a defence response to attacking viruses and plays an important role in the regulation of endogenous gene expression (Kasschau and Carrington, 1998; Voinnet, 2002). The dsRNAi mechanism of plants is termed as post-transcriptional gene silencing (PTGS) (Turner and Schuch, 2000; Vaucheret *et al.*, 2001; Yu and Kumar, 2003) Consequently, the method of inverted-repeat DNA transformation was transferred to higher plants. It was initially demonstrated in rice, tobacco and *Arabidopsis* that the transformation of plants with inverted repeat DNA constructs leads to interference with the expression of specific genes (Chuang and Meyerowitz, 2000; Waterhouse *et al.*, 2001).

Interestingly, DNA constructs have not to contain the homologous full-length sequence of the target gene for initiation of dsRNAi-mediated gene silencing. Constructs containing only gene fragments, the 5'-untranslated or 3'-untranslated region of a specific gene were also capable to trigger transcript and consequently protein depletion (Bosher and Labouesse, 2000; Wesley *et al.*, 2001).

Due to knowledge of the *Arabidopsis* genome sequence (Arabidopsis GenomeInitiative, 2000) and accumulating data from cereals, dsRNAi-mediated PTGS additionally became an important tool in reverse genetics. In the barley-powdery mildew interaction, silencing of specific genes like *Mlo*, *Sgt1, Rar1*, *RacB*, *CaM* and the small trimeric G-protein subunit (*Gα*) was successfully performed upon ballistic transfection of single epidermal cells with both *in vitro* transcribed RNA or inverted repeat DNA constructs (Schweizer *et al.*, 2000; Azevedo *et al.*, 2002; Kim *et al.*, 2002; Schultheiss *et al.*, 2002).

Furthermore, first steps have been made in the large-scale application of the dsRNAi technology *in planta*. "pHELLSGATE", a vector in which specific, gene homologous DNA sequences can be easily cloned tandem in sense and antisense orientation via a recombinase system has been generated (Wesley *et al.*, 2001).

3.2   Results

3.2.1   pUAMBN, a vector suitable to transiently trigger PTGS in barley

As stated in the introduction (see Chapter 3.1) the intention of this work was to deplete single genes contained in a barley epidermal <u>c</u>opy <u>D</u>NA (cDNA) library via PTGS, to identify genes having an impact on the outcome of the barley-powdery mildew interaction. To induce dsRNAi-mediated PTGS in the transient expression system, a vector (pUAMBN; Fig. 5) was constructed to facilitate a high-throughput cloning procedure. It is conceivable that the cloning of barley ESTs (<u>e</u>xpressed <u>s</u>equence <u>t</u>ags) in sense and antisense orientation by means of restriction enzymes was not feasible for a large-scale approach. For this reason, an <u>att</u>achment site <u>R</u> (*att*R)-cassette from a commercially available bacteriophage lambda (λ) site-specific recombinase system (Invitrogen[™]/GATEWAY[®]; (Walhout *et al.*, 2000)), was amplified via polymerase chain reaction (PCR). A GATEWAY[®] destination vector (pDEST[™]14)

served as PCR template. The *att*R-cassette is flanked by two distinct *att*R-sites (*att*R1 and *att*R2), which guide the desired orientation of the inserted DNA fragment within the cassette. Enclosed between the *att*R-sites is the *ccd*B gene whose gene product interferes with the gyrase of most *Escherichia coli* strains (e.g. DH5α), thus inhibiting bacterial growth (Bernard and Couturier, 1992). Upon recombination, *ccd*B is replaced by the cDNA of interest, allowing a reliable recovery of desired clones after transformation in *E. coli*. Two copies of the cassette were cloned into the vector backbone pUbi-*Mla1*(3rd intron)-nos (Zhou *et al.*, 2001), containing the strong monocot maize <u>ubi</u>quitin promoter (Ubi) (Nielsen *et al.*, 1999), the 3rd intron of the *Mla1* gene including functional splice sites and the <u>no</u>palin <u>s</u>ynthase termination sequence (nos). The intron separated the sense-oriented from the antisense-oriented *att*R-cassette. Upon transcription, this arrangement of cassettes and intron is supposed to result in an <u>i</u>ntron-containing <u>h</u>air<u>p</u>in RNA (ihpRNA), which proved to be more efficient in mediating silencing in plants than simple self-complementary 'hairpin' RNA (hpRNA) (Smith *et al.*, 2000; Wesley *et al.*, 2001).
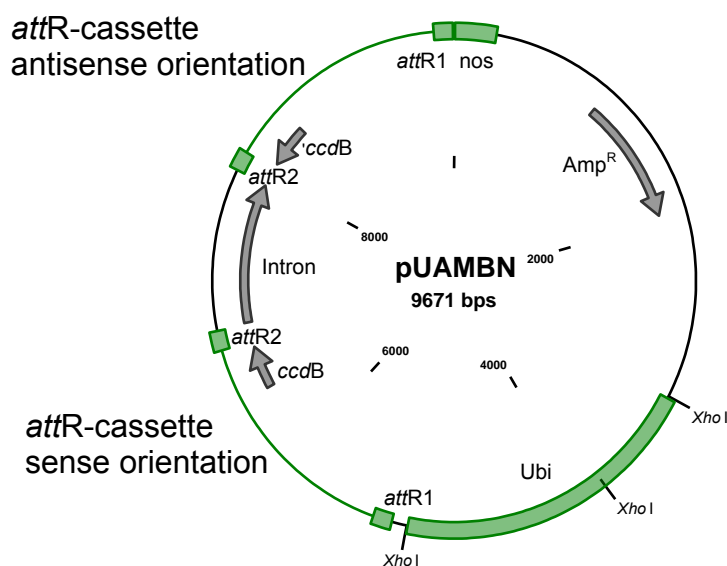

Figure 5. Plasmid map of the ihpRNA-Vector pUAMBN.
Essential features and restriction sites are depicted in the map. **(*att*R1)** attachment site R1; **(*att*R2)** attachment site R2; **(*ccd*B)** negative selection marker; **(Ubi)** maize ubiquitin promoter; **(nos)** transcription termination; **(Intron)** *Mla1* 3rd intron; **(Amp[R])** β-lactamase gene conferring ampicillin resistance.

In addition, the following derivatives of pUAMBN were generated; pUAMBN-i, in which the orientation of both *att*R-cassettes is simultaneously altered into the opposite direction and pUAMBN-35S, in which the strong monocot maize ubiquitin promoter (Ubi) is substituted by the cauliflower mosaic virus 35S promoter, suitable for high gene expression in dicot species.

3.2.1.1 Functionality and efficiency of pUAMBN

pUAMBN was tested for its ability to mediate gene silencing by knock-down of barley *Mlo*. Transient dsRNAi-mediated PTGS of endogenous *Mlo* in wild-type barley resulted previously in reduced penetration success of epidermal cells (approximately 50% compared to epidermal cells only transfected with the GUS reporter construct; Schweizer *et al.*, 2000). For this reason, a cDNA fragment of 997 bps from barley *Mlo* (accession number: Z 83834) was recombined into pUAMBN, resulting in the vector pHvMlo-dsR. The vector was bombarded on barley wild-type *Mlo* leaves alone or co-bombarded with a construct for the overexpression of *Mlo* (pUbi-Mlo-nos NEW; kindly provided by Ralph Panstruga), that, when expressed alone, renders cells super-susceptible (Kim *et al.*, 2002). Penetration success of wild-type barley epidermal cells transfected with pHvMlo-dsR was compared with cells transfected with the GUS reporter construct only [Fig. 6]. Reduction of super-susceptibility in barley due to silencing of the endogenous and transiently co-expressed *Mlo* was compared with samples only expressing the *Mlo* overexpression construct plus the reporter plasmid. Additionally, samples were compared with barley leaf epidermal cells transfected with a conventional restriction enzyme-cloned ihpRNA vector construct containing the full-length cDNA of a wheat *Mlo* orthologue (pTaMlo-dsRNAi; kindly provided by Ralph Panstruga) [Fig. 6]. Wheat *Mlo* shares more than 90% homology to barley *Mlo* (Elliott *et al.*, 2002) and the respective silencing construct was previously found to be efficient in dsRNAi-mediated gene silencing of barley *Mlo* (Patrick Schweizer, personal communication).
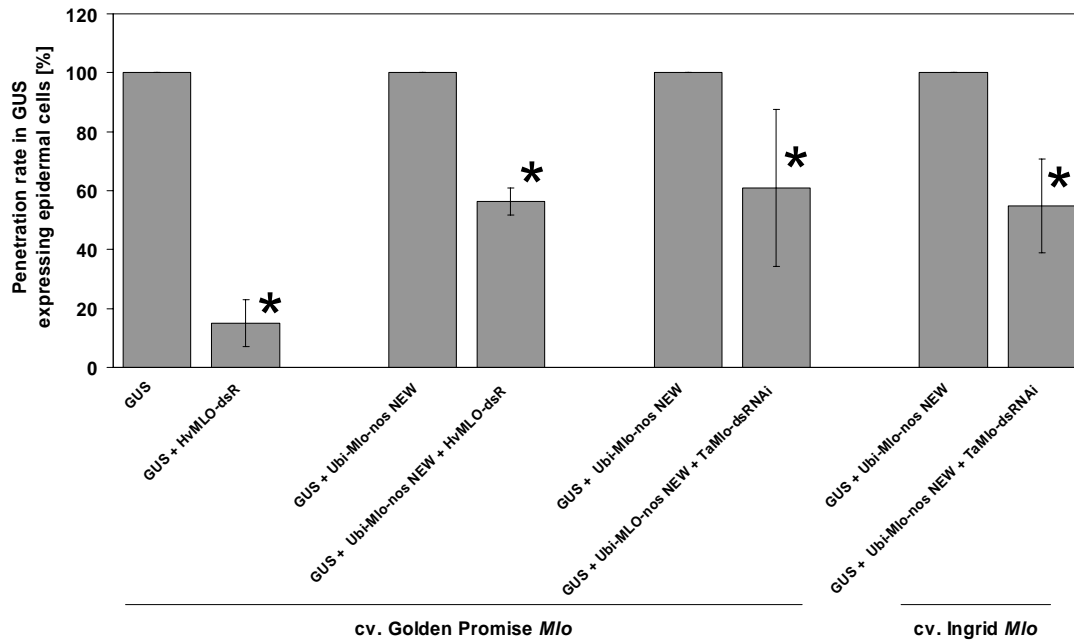
Figure 6: Silencing of endogenous and transiently expressed *Mlo* confers enhanced resistance of barley epidermal cells to *Bgh*.
Leaves of the susceptible barley cultivar Golden Promise were bombarded with the silencing construct pHvADF-dsR. Additionally, the cultivars Golden Promise and Ingrid were ballistically co-transfected with the *Mlo*-overexpressing construct (pUbi-Mlo-nos NEW) and a construct mediating silencing of *Mlo* (pHvMlo-dsR or pTaMlo-dsRNAi).
To allow a maximum of protein turnover, leaves were incubated for 96 h prior to *Bgh* inoculation. Columns represent percentage of successful penetration attempts of *Bgh* (isolate K1) 48 hpi of *Hordeum vulgare* leaves, scored by formation of haustoria in ß-glucuronidase marker gene expressing cells, in relation to the control (GUS or GUS + pUbi-Mlo-nos NEW), set as 100% [%]. Columns represent the average of a minimum of three independent experiments (± standard deviation) in which at least 100 interaction sites of single *Bgh* sporelings attacking epidermal barley cells were microscopically evaluated. Asterisks indicate $P < 0.05$ (Student's *t* test) compared with GUS or GUS + pUbi-Mlo-nos NEW.

Experiments revealed that pUAMBN-based silencing of transiently overexpressed *Mlo* by pHvMlo-dsR was as efficient as silencing of overexpressed *Mlo* by the conventional restriction enzyme-cloned silencing construct pTaMlo-dsRNAi. Furthermore, silencing of endogenous *Mlo* upon ballistic transfection of susceptible barley epidermal cells by pHvMlo-dsR reduced the penetration rate of *Bgh* to ~ 15%. Therefore, pUAMBN was considered as functional and efficient in mediating gene silencing via site-specific recombined cDNAs.

3.2.2   Establishment of a high-throughput system (HTPS) for the transient silencing of single barley epidermal genes by ballistic transfection

3.2.2.1   Generation of a pUAMBN-based ihp-RNA construct library

The basis for the PTGS screen was a barley epidermal cDNA library (HO library; kindly provided by Uwe Zierold and Patrick Schweizer), which was generated from epidermal tissue adaxially stripped from seven day old *mlo*-5 barley seedling leaves 6 and 24 hpi with the powdery mildew fungi *Bgh* and *Bgt*. The inoculation should have helped to increase expression of barley defence-related genes implicated in both broad-spectrum and non-host resistance, respectively. In total the redundant cDNA library contained approximately 12.000 clones.

Two consecutive GATEWAY® recombination steps are necessary to recombine single cDNAs form the barley epidermal cDNA library into pUAMBN [Fig. 7].

First, the cDNA had to be shuttled into a so-called GATEWAY® entry vector (pDONR™201) containing the recombination attachment sites P1 and P2 (*att*P1, *att*P2). To generate suitable PCR amplicons for the subsequent use in a BP recombination reaction, attachment sites *att*B1 and *att*B2 had to be incorporated into PCR products of the cDNAs. Since orientation of cDNAs in the library vector was predefined in sense from 5'-end to 3'-end direction, the primer combination Gate-*att*B1 and Gate-*att*B2 was designed accordingly. *att*B1 resides at the 5'-end of the EST and *att*B2 at the 3'-end. The 3'-ends of the primers are complementary to cDNA flanking regions of the vector pBluescript™ SK(+) that was used for library construction.

It proved practicable to use colonies of *Escherichia coli*, containing single cDNA clones, directly from storage microtiter plates as a template in the PCR reactions ("colony PCR"). On average, 95% of all reactions of 96 simultaneous colony PCRs showed successful amplification of the respective cDNAs. Thereby, it was possible to circumvent the laborious isolation of cDNA-containing plasmids from *E. coli* for subsequent use as PCR templates.

Amplified PCR fragments were used in combination with the GATEWAY® donor vector pDONR™201 in a 96 well format BP recombination reaction in microtiter

plates. After over night recombination at ~ 20°C (room temperature), each BP reaction was transformed into *E. coli* strain DH5α. Transformation approaches were plated on separate Petri dishes with agar containing kanamycin for selection. After over night incubation at 37°C, each plate contained on average 200 *E. coli* colonies. One colony from each plate was transferred into a 96 deep-well microtiter plate for growth. After over night incubation at 37°C, plasmids were recovered using a microtiter plate-compatible purification kit from Millipore™. Extracted plasmids were analysed by restriction enzyme digest to verify the correct insertion of the cDNAs into the pDONR™201 vector.

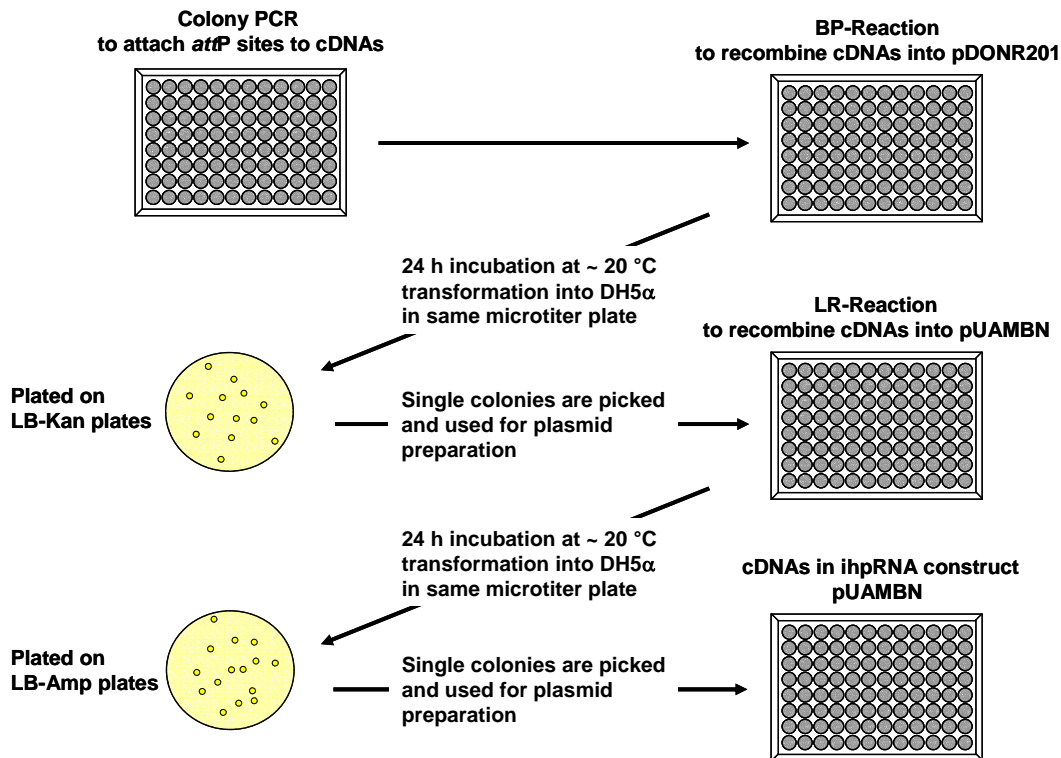On average, 80% of the resulting clones showed the expected restriction pattern and were used in the subsequent steps.

Figure 7. Scheme of simultaneous cloning of 96 ESTs into pUAMBN.
For details, see text.

During a BP recombination event, *att*B1 and *att*P1 as well as *att*B2 and *att*P2 fuse and result in *att*L1 and *att*L2 sites. These can be exploited for the site-directed recombination of the cDNA from the donor vector pDONR™201 into pUAMBN. cDNA-

containing pDONR™201 clones were used together with pUAMBN in an LR recombination procedure. LR reactions were carried out as the above described BP reactions except that transformants were plated on ampicillin-containing agar plates for selection.

After restriction enzyme digest of the recovered pUAMBN plasmids, on average ~ 85% of the clones showed the correct restriction pattern.

As a final result of the two-step recombination process an average of 62 clones, representing ~ 65% of the originally 96 recombination approaches, could be used for transient expression of ihpRNAs in barley leaf epidermal cells.

A further vector (pASSASSIN) was generated which contained the GATEWAY® pDONR™201 *att*P sites instead of pUAMBN *att*R sites. The intention of generating this construct was to skip the LR recombination step; so that the *att*B sites-flanked cDNA derived PCR products could be directly recombined into the *att*P sites-containing ihpRNA vector pASSASSIN. Unfortunately, the yield of correct clones after the BP recombination reaction was very low and not suitable for the simultaneous generation of multiple ihpRNA constructs. Therefore, the pASSASSIN approach was rejected in favour of pUAMBN.

3.2.2.2   The bombardment procedure

The bombardment procedure was performed in accordance with the protocol provided BioRAD™, the manufacturer of the particle delivery system Biolistic® PDS-1000/He (see Chapter 2.2.6).

Variables that influence the bombardment efficiency include the kind of particles (gold or tungsten) and the applied pressure. Preliminary tests revealed that tungsten particles were not suitable in combination with the GUS reporter system. Needle-like structures were occasionally formed inside tungsten-bombarded barley epidermal cells upon GUS staining. These needles masked the potential presence of haustoria and rendered the microscopic evaluation process more difficult. Therefore, gold particles were used for bombardment throughout all experiments.

The speed of the gold particles determines how deep the particles penetrate into the barley leaf tissue. A pressure of 900 psi was determined as being optimal, accelerating the gold particles to an extent that only the epidermal cell layer was penetrated.

3.2.3 Optimisation of the screening process

3.2.3.1 Determination of ihpRNA construct pool sizes

The microscopic evaluation of transfected barley leaf samples (Chapter 4.1) is time-consuming (approximately 30 to 60 minutes per sample) and therefore represents the rate-limiting step in the screening process. It was envisaged to bombard pools consisting of several pUAMBN-based ihpRNA constructs on one leaf sample each as a possibility to facilitate a high-throughput of silencing constructs. In case of phenotypic alterations upon microscopic evaluation of the samples, the pool could be divided in its single components. Then, the individual pool constituents could be independently used for transfection. In this way, pool-provoked effects could be traced back to a single construct responsible for the alteration of the defence response. Bombardments of ihpRNA construct-containing pools would accelerate the screening procedure but it might also negatively influence other aspects of the screening approach.

A possible limitation is that the number of simultaneously bombarded constructs does interfere with the silencing ability of an individual ihpRNA construct. This possibility was investigated by exploiting a two fluorescent protein reporter system (TRS) in the transient expression system (Panstruga *et al.*, 2003). The method is based on a reporter construct that consists of two tandem-oriented genes [Fig. 8A]. One encodes a green fluorescent protein (GFP) and the other a red fluorescent protein RFP. Both fluorescing proteins can be distinguished in epifluorescence microscopy by their different emission spectra. The two genes fulfil distinct functions in the test. For this reason, each gene is flanked by its own promoter and termination sequence. While GFP serves as a reference dye and as a marker to identify transfected barley epidermal cells, the RFP-encoding gene is the actual reporter for silencing efficiency.
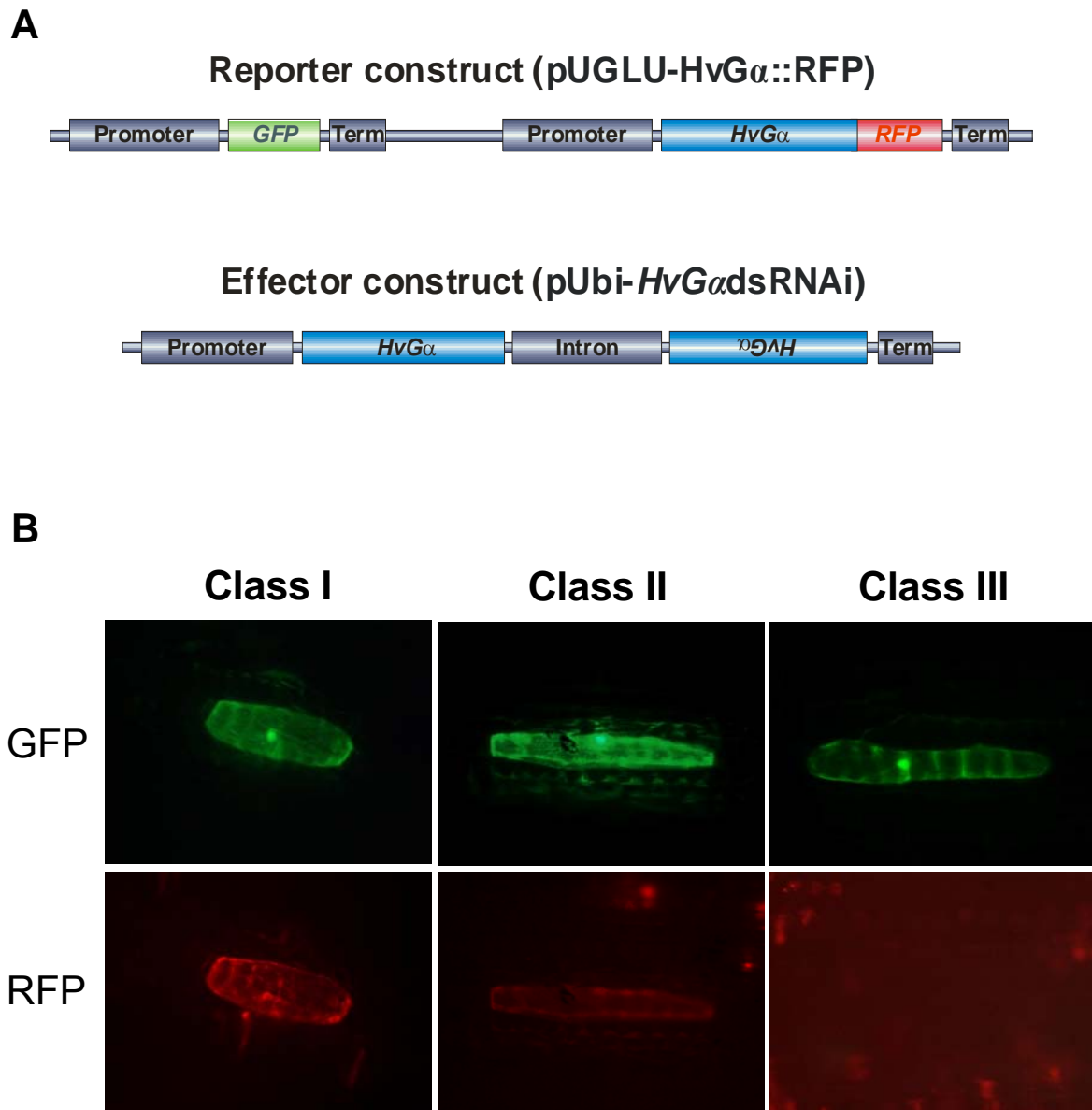
A

B

Figure 8. The two fluorescent protein reporter system.

(A) Scheme of both the reporter and the effector construct.

The reporter construct pUGLU-HvGα::RFP possesses two tandem-oriented gene cassettes, both consisting of a promoter, a fluorescent-protein encoding gene (*GFP*, *RFP*) and a termination sequence (Term). In case of the *RFP*-containing cassette, a gene, encoding the small heterotrimeric G-protein α subunit from barley (*HvGα*) is fused to *RFP*.

The effector ihpRNA construct consists of two *HvGα* cDNA sequences in sense and antisense orientation, separated by an intron. (Modified from (Panstruga *et al.*, 2003).

(B) The three classes of RFP fluorescence intensity.

Class I represents fluorescence of RFP at levels comparable to barley epidermal cells ballistically transfected with the reporter construct only. In epidermal cells co-bombarded with reporter and effector, this RFP fluorescence intensity is considered as inefficient silencing capacity of the ihpRNA construct.

Class II represents a reduced RFP fluorescence. The ihpRNA-vector is capable to mediate silencing, but the silencing efficiency is suboptimal.

Class III shows complete absence of RFP fluorescence. This indicates that the ihpRNA-vector possesses the capacity to efficiently suppress RFP expression by PTGS.

GFP fluorescence serves in all cases as marker to identify transfected barley epidermal cells. (Modified from Panstruga *et al.*, 2003)

For this, a gene of interest has to be fused to RFP. The heterotrimeric G-protein α subunit of barley (HvGα) was fused to RFP in this study (Kim *et al.*, 2002; Panstruga *et al.*, 2003). An effector ihpRNA construct, whose functionality and/or efficiency shall be tested, has to target the gene sequence N-terminally fused to RFP [Fig. 8A]. Bombardment of the reporter construct pUGLU-HvGα::RFP (Kim *et al.*, 2002) alone is expected to result in barley epidermal cells expressing both GFP and RFP. Contrary, co-transfection of the reporter construct and the effector construct (here: pUbi-*HvGα*dsRNAi; (Kim *et al.*, 2002)) should predominantly result in *GFP* expression. This would indicate the efficient silencing of the *RFP*-fused gene. Distinction between three groups of RFP fluorescence intensity, depicted in [Fig. 8B], allows a semi-quantitative estimation of the ihpRNA construct functionality and efficiency.

In order to determine the silencing efficiency of the effector construct in the presence of further ihpRNA constructs, pUbi-*HvGα*dsRNAi was simultaneously bombarded with the reporter construct (pUGLU-HvGα::RFP) and up to six additional ihpRNA constructs. Each of the additional ihpRNA constructs has been previously shown to be effective in silencing of a specific target gene (Table 1).

Table 1. Overview of target genes used in the TRS to determine the efficiency of single ihpRNA constructs.

Silenced gene	Putative function of encoded protein	ihpRNA construct name	Reference
Sgt1	Defence signalling	RNAi-SGT1	Azevedo *et al.*, 2002
Rar1	Defence signalling	RNAi-RAR1	Azevedo *et al.*, 2002
CaM	Calmodulin sensor	pUbi-*HvCaM*dsRNAi	Kim *et al.*, 2002
Gα	G protein subunit	pUbi-*HvGα*dsRNAi	Kim *et al.*, 2002
Cs1	Callose synthase	pAJ2	Jacobs *et al.*, 2003
Cs2	Callose synthase	pAJ3	Jacobs *et al.*, 2003
TaMlo	Defence modulator	pTaMlo-dsRNAi	Ralph Panstruga, personal communication

This experiment revealed that at least six additionally co-bombarded ihpRNA constructs do apparently not interfere with the silencing efficiency of an individual ihpRNA construct [Fig. 9], in this case pUbi-*HvGα*dsRNAi.
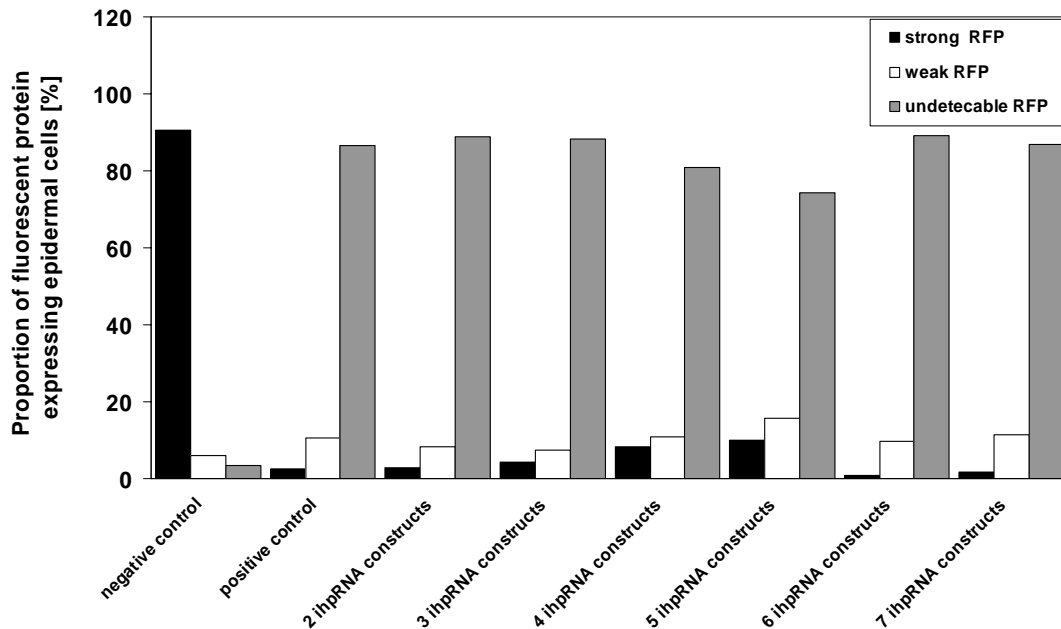

Figure 9. Efficiency of the ihpRNA construct pUbi-*HvGα*dsRNAi in mediating silencing in the presence of up to six additional ihpRNA constructs.
Detached leaves of the barley cultivar Ingrid were ballistically transfected with the reporter construct pUGLU-HvGα::RFP (negative control); with the reporter construct plus the effector construct pUbi-*HvGα*dsRNAi (positive control) and both reporter and effector together with up six additional ihpRNA constructs (2 - 7 ihpRNA constructs). Compositions of ihpRNA construct pools: *HvGα*dsRNAi + pUbi-*HvCaM*dsRNAi (2 ihpRNA constructs); + RNAi-RAR1 (3 ihpRNA constructs); + RNAi-SGT1 (4 ihpRNA constructs); + pJA2 (5 ihpRNA constructs); + pJA3 (6 ihpRNA constructs); + p*TaMlo*-dsRNAi (7 ihpRNA constructs).
Columns represent percentage of GFP-expressing epidermal cells, scored by appearance of RFP fluorescence as shown in Figure 8B. Class I: GFP and strong RFP fluorescence (black columns); Class II: GFP and weak RFP fluorescence (white columns); Class III: GFP and apparent absence of RFP fluorescence (grey columns) in [%]. Columns result from one experiment in which at least 100 GFP-fluorescing epidermal barley cells were microscopically evaluated.
To allow a maximum of RFP and GFP accumulation, leaves were evaluated 48 h after bombardment. Single cell fluorescence was analysed by using a Zeiss Axiophot microscope equipped with the GFP2 filter (HQ 480/20 excitation filter, Q 495 beam splitter, and HQ 510/20 nm emission filter) or an RFP filter (D 546/10 excitation filter, 565 DCLP beam splitter, and 600/40 emission filter; AHF Analysentechnik AG, Tübingen, Germany).

To corroborate this result complementary experiments were conducted. This should reveal whether five or ten co-bombarded pUAMBN-based ihpRNA constructs interfere with the efficiency of the pTaMlo-dsRNAi silencing construct. The ihpRNA

constructs comprised randomly chosen barley cDNAs from the barley epidermal cDNA library. In these experiments, the penetration rate of *Bgh* in transfected barley epidermal cells served as an indicator for the silencing construct efficiency described in Chapter 3.2.1.1 and previously shown to effectively silence barley *Mlo* expression. The cells were rendered super-susceptible by *HvMlo* overexpression upon ballistic transfection (see Chapter 3.2.3.2, Fig. 12).

The result of the TRS experiment could be substantiated in these experiments, since the number of simultaneously bombarded ihpRNA constructs did not significantly influence the silencing efficiency of pTaMlo-dsRNAi [Fig. 10].
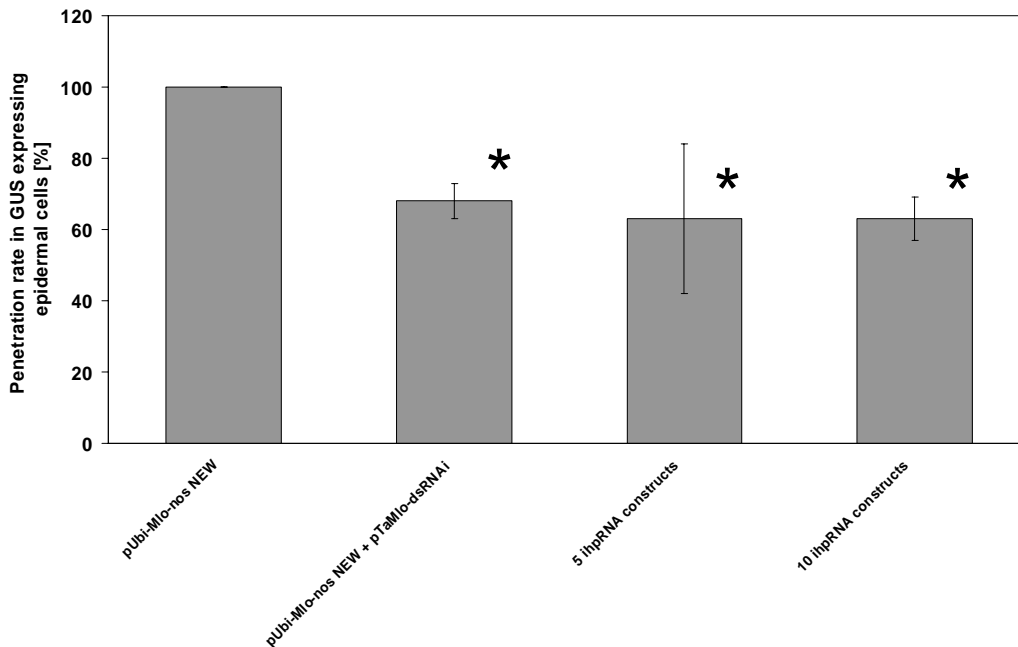

Figure 10. Efficiency of the ihpRNA construct pTaMlo-dsRNAi in mediating silencing in presence of up to ten additional ihpRNA constructs.
Barley wild-type cultivar Golden Promise was ballistically transfected with an *HvMlo* overexpression construct (pUbi-Mlo-nos NEW) (negative control); together with the effector construct pTaMlo-dsRNAi (positive control); plus 5 (5 ihpRNA constructs) or 10 (10 ihpRNA constructs) randomly chosen pUAMBN-based ihpRNA constructs. To allow a maximum of protein turnover, leaves were incubated for 96 h prior to *Bgh* inoculation.
Columns represent percentages of successful penetration attempts of *Bgh* (isolate K1) 48 hpi of *Hordeum vulgare* leaves, scored by formation of haustoria in marker gene (ß-glucuronidase (GUS)) expressing cells, in relation to the negative control, set as 100% [%]. Columns represent the average of a minimum of three independent experiments (± standard deviation) in which at least 100 interaction sites of single *Bgh* sporelings attacking epidermal barley cells were microscopically evaluated. Asterisks indicate *P* < 0.05 (Student's *t* test) compared with the negative control.

However, it turned out in these experiments that the number of GUS-expressing cells in barley leaves co-bombarded with ten ihpRNA constructs varied considerably [Fig. 11]. Usually, at least 100 GUS-expressing cells per sample were microscopically evaluated. Due to the spatial restriction of a Petri dish, one sample consisted of a maximum of eight detached barley seedling leaves. In the case of samples ballistically transfected with ten ihpRNA constructs, all leaves had to be inspected to obtain a sufficient number of marker gene-expressing cells. Nevertheless, even by evaluating all available leaves, on average only 65 GUS-expressing cells per sample were obtained [Fig. 11].
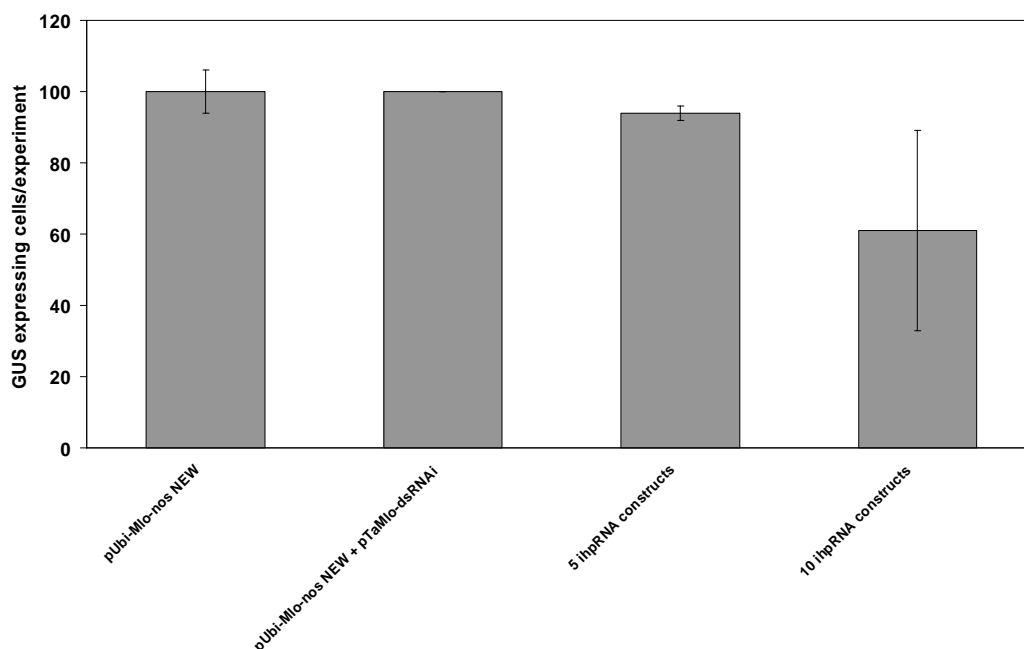

Figure 11. Number of GUS-expressing cells obtained upon simultaneous bombardment of additional pUAMBN-based ihpRNA constructs.
Detached leaves of the barley wild-type cultivar Golden Promise were ballistically transfected with an *HvMlo* overexpression construct (pUbi-Mlo-nos NEW) (negative control); the overexpression construct together with the effector construct pTaMlo-dsRNAi (positive control); plus five (5 ihpRNA constructs) or plus ten (10 ihpRNA constructs) randomly chosen pUAMBN-based ihpRNA constructs. Leaves were inoculated with *Bgh* 96 h after bombardment.
Columns represent numbers of ß-glucuronidase (GUS) expressing cells showing interaction with *Bgh* (isolate K1) 48 hpi of *Hordeum vulgare* leaves. Data represent the average of a minimum of three independent experiments (± standard deviation) in which the number of GUS-expressing cells showing an interaction with single *Bgh* sporelings was microscopically evaluated.

The high deviation in the number of cells expressing the GUS reporter gene suggested that co-bombardment with ten ihpRNA is unsuited for the screening procedure.

In conclusion, the experiments revealed that five constructs did not interfere with the silencing efficiency of a single construct and did not affect the total number of reporter gene-expressing cells. For this reason, a pool size of five pUAMBN-based ihpRNA constructs was considered as optimal for the subsequent screening process.

3.2.3.2   Avoidance of masked PTGS effects caused by protein half-life periods

The stability of proteins that are supposed to be depleted by ihpRNA constructs has to be considered upon transient PTGS in plants. Before ballistic transfection, the endogenous gene subsequently targeted by PTGS is transcribed and translated to a normal extent in the plant cells. Pre-existing target protein levels remain unaffected by PTGS and might compensate for the lack of newly synthesised proteins, so that silencing effects affecting the barley-powdery mildew interaction become not apparent. Since proteins are known to possess a certain half-life period, it was tried to circumvent this potential pitfall by the reduction of pre-existing proteins by their natural degradation processes. To allow a maximum of protein turnover resulting in target protein depletion in the screening procedure, detached barley leaves were inoculated not before 96 h after ballistic transfection with *Bgh*.

An undesired effect associated with the 96 h pre-inoculation phase is an elevated resistance of detached barley *Mlo* leaves to *Bgh*, which interfered with a reliable assessment of dsRNAi-mediated silencing effects. In the screening process for compromised *Mlo* function this problem was circumvented by rendering leaf epidermal cells super-susceptible [Fig. 12] via co-bombardment of ihpRNA constructs with a *HvMlo* overexpressing construct (pUbi-Mlo-nos NEW).
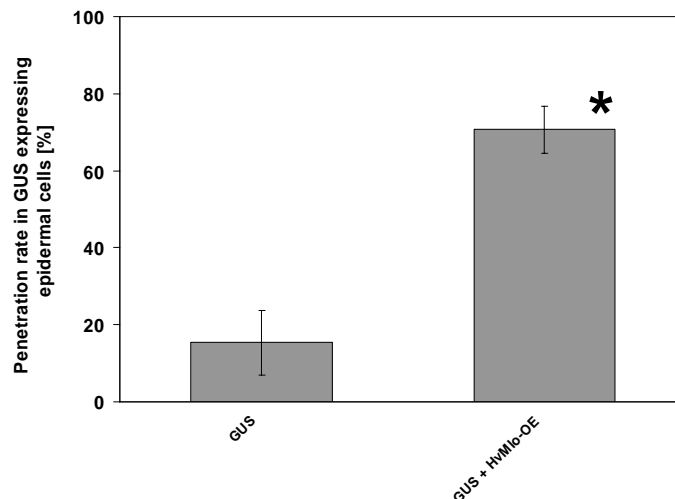
Figure 12. Overexpression of *HvMlo* enhances the basal susceptibility in the *Mlo* genotype.
The overexpression construct of wild-type *HvMlo* (HvMlo-OE) was ballistically delivered in barley epidermal cells of a *Mlo* genotype. Inoculation with *Bgh* (isolate K1) was performed 96 h after bombardment. Control cells were transfected with the marker gene-expressing vector (GUS) only. Columns represent the percentage of successful penetration attempts of *Bgh* (isolate K1) 48 hpi of detached leaves, scored by formation of haustoria in marker gene (ß-glucuronidase (GUS))-expressing cells [%]. Columns represent the average of three independent experiments (± standard deviation) in which at least 100 interaction sites of single *Bgh* sporelings attacking epidermal barley cells were microscopically evaluated. The asterisk indicates *P* < 0.05 (Student's *t* test) compared with GUS.

3.3   Discussion

Due to the poor knowledge of genes implicated in the barley *Mlo* or *mlo* resistance pathways, it was intended to perform a dsRNAi-based reverse genetic screen to identify further factors involved in this biological process.

Induction of gene silencing requires a trigger dsRNAi (Fire *et al.*, 1998) which may be transcribed *in vivo* from an inverted repeat DNA construct (Tavernarakis *et al.*, 2000). The commercially available GATEWAY® recombinase system makes it feasible to generate a library of ihpRNA constructs within a reasonable time span (Walhout *et al.*, 2000; Sijen *et al.*, 2001; Wesley *et al.*, 2001).

Therefore, an ihpRNA vector (termed pUAMBN) was generated that fulfils the requirements for site-directed cloning by means of the GATEWAY®-system. pUAMBN was proven to be functional and efficient in gene silencing. The large-scale recombination process to shuttle clones from a barley epidermal cDNA library into pUAMBN resulted in a yield of approximately 65% of correct pUAMBN-based

ihpRNA constructs in a single 96 well microtiter plate approach. Generation of incorrect clones could be traced back to failures in recombination events. To minimise the loss rate, different alterations in the recombination process, including usage of different vectors, were attempted. No significant improvement was achieved by these measures. It is conceivable that intramolecular structures of single cDNAs from the original barley epidermal cDNA library might hamper efficient recombination. However, the exploited barley epidermal cDNA library was not a true unigene set. Many cDNAs were represented by at least two copies in the library. The loss of single cDNAs due to failures in recombination reactions might therefore be compensated by other ESTs clones representing the same cDNA.

For this reason, the established procedure for fast and easy generation of pUAMBN-based ihpRNA constructs (see Chapter 3.2) was considered as sufficient and was further used.

Optimisation of the screening procedure was focused on the acceleration of the overall process. This was achieved by both, the already mentioned high-throughput generation of pUAMBN-based ihpRNA constructs and by the simultaneous bombardment of five pUAMBN constructs. Especially the co-bombardment had an impact on the microscopic evaluation time. Investigation time of one sample ranged from 30 minutes up to one hour. The co-bombardment of five constructs therefore saved on average three hours of microscopic evaluation. Simultaneous bombardment of ten ihpRNA constructs was also tested and showed no disadvantageous effects with respect to the silencing efficiency of single constructs. Despite this, the approach was rejected since the variation in the quantity of reporter gene-expressing cells was too large. GUS-staining is a process that requires living tissue. High numbers of simultaneously bombarded ihpRNA constructs mediating silencing of multiple endogenous gene functions might interfere with cell viability. Thus, the insufficient quantity of GUS-stained cells might result from cell lethality induced upon co-silencing of multiple genes.

The inoculation period with *Bgh* was defined to 96 hours post bombardment. This time span was determined to allow a maximum of protein turnover, which due to pUAMBN-mediated PTGS of specific genes should result in the depletion of

respective pre-existing proteins. Extended incubation periods were not feasible due to the limited viability of detached barley leaves on agar plates.

In case of the *Mlo* genotype, the incubation caused an increased resistance of leaf epidermal cells to *Bgh* attack. This most likely results from the induction of systemic defence mechanisms due to an abiotic stress response triggered by detachment of the leaves. Decreased susceptibility impairs the distinction of ihpRNA construct-mediated silencing effects from naturally deviations in susceptibility. Overexpression of *Mlo*, which renders barley epidermal cells super-susceptible (Kim *et al.*, 2002), is exploited in the screen to overcome this obstacle.

However, in *mlo* resistant leaves this increased resistance can not be avoided and might be responsible for the miss of subtle effects produced by the knock-down of genes.

4   The role of ADFs in barley-powdery mildew interactions

4.1   Introduction

The eukaryotic actin cytoskeleton participates in a plethora of intracellular processes including cellular morphogenesis, organelle translocation, actin-based motility processes, and signalling events in responses to versatile environmental stimuli (Rogers and Gelfand, 2000; Martin *et al.*, 2001; Khaitlina *et al.*, 2003; Drøbak *et al.*, 2004). An involvement of the actin meshwork in these processes requires the ability of actin filaments to form a variety of distinct assemblies with specific biophysical and biochemical properties (Gungabissoon and Bamburg, 2003). The dynamic character of the polymeric actin framework is warranted by its assembly from monomeric G-actin subunits. Further, the structure of actin filaments is characterised by its polarity. The plus or barbed end is more dynamic than the minus or pointed end in respect to loss and addition of G-actin. Different classes of ABPs regulate actin dynamics by maintaining the optimal equilibrium between unpolymerised G-actin and assembled F-actin. One class of actin dynamics-regulating ABPs comprises ADF/cofilins (Maciver and Hussey, 2002; Dos Remedios *et al.*, 2003). A major property of ADF/cofilins is to enhance the turnover rate (treadmilling) of actin filaments by accelerating the dissociation rate of actin monomers at the pointed ends whereas the dissociation rate of G-actin at the barbed ends of filaments remains unchanged (Carlier *et al.*, 1997; Carlier, 1998). Another putative function of ADF/cofilins is the severing of actin filaments, thereby increasing the monomer release rate by providing more pointed ends. However, this function is controversially discussed (Carlier *et al.*, 1997; Maciver and Hussey, 2002).

The specificity of ADF/cofilins for distinct actin dynamics-dependent intracellular processes is supposedly achieved by differential tissue-specific expression of the respective mRNAs and/or by a variety of regulatory post-transcriptional / post-translational control mechanisms (Lopez *et al.*, 1996; Jiang *et al.*, 1997; Bamburg, 1999; Bowman *et al.*, 2000; Maciver and Hussey, 2002). For example, in plants, some *ADF*s appear to be expressed specifically in reproductive tissues, whereas others are expressed either constitutively and/or in vegetative tissues only (Hussey *et al.*, 2002). Moreover, intracellular pH values (Gungabissoon *et al.*, 1998; Bernstein *et*

al., 2000; Chen *et al.*, 2004), reversible phosphorylation (Agnew *et al.*, 1995; Arber *et al.*, 1998; Smertenko *et al.*, 1998; Allwood *et al.*, 2001; Niwa *et al.*, 2002), small monomeric GTPases (Arber *et al.*, 1998; Yang *et al.*, 1998; Chen *et al.*, 2003) a tryptophan-aspartate (WD) repeat containing protein (AIP) (Iida and Yahara, 1999; Okada *et al.*, 1999; Allwood *et al.*, 2002; Ketelaar *et al.*, 2004), and direct binding of phospholipids (Gungabissoon et al., 1998) have been reported to influence ADF/cofilin activities throughout all kingdoms.

With the exception of ADF/cofilins from *Acanthamoeba* (Maciver *et al.*, 1998) and starfish (Mabuchi, 1983), the ability of ADF/cofilins to assemble or disassemble F-actin *in vitro* is dependent on the prevalent pH milieu (Yonezawa *et al.*, 1987). Plant ADF/cofilins preferably bind to F-actin at acidic conditions less than pH 6.8, whereas raise of the pH value results in an increased depolymerisation activity of ADF/cofilins and higher affinity for monomeric actin at alkaline pH values around 9.0 (Gungabissoon *et al.*, 1998). Similar ADF/cofilin properties were observed in vertebrate cells, although the transition of monomeric actin-binding to filamentous actin-binding occurs at lower pH values compared to plants (Gungabissoon *et al.*, 1998; Dos Remedios *et al.*, 2003).

Vertebrate ADF/cofilins have been shown to be regulated via reversible phosphorylation. Responsible for phosphorylation are the metazoan-specific LIM kinases 1 and 2 (Arber *et al.*, 1998; Yang *et al.*, 1998; Bamburg, 1999) and the testicular protein kinases TESK1 and TESK 2 (Toshima *et al.*, 2001b; Toshima *et al.*, 2001a), whereas the Slingshot phosphatase has been shown to reverse this process (Niwa *et al.*, 2002). Some plant ADFs are likely regulated by reversible phosphorylation as their metazoan counterparts, but in contrast to animals phosphorylation is supposed to be mediated by calcium-stimulated calmodulin-like domain protein kinases (CDPKs) unique to plants (Smertenko *et al.*, 1998; Allwood *et al.*, 2001; Allwood *et al.*, 2002; Gungabissoon and Bamburg, 2003). This would imply that plant ADFs exhibit a level of control different from that of metazoan ADFs, by cytoplasmic calcium levels indirectly controlling plant ADF function (Allwood *et al.*, 2002; Hussey *et al.*, 2002).

Phosphatidyl-inositol 4,5-bisphosphat (PIP_2) directly inhibits ADF function by preventing its binding to actin filaments (Yonezawa *et al.*, 1990). It is known that PIP_2 is an important regulator of several signal transduction processes besides its function as a precursor for the second messengers inositol 1,4,5-triphosphate and

diacylglycerol (Takenawa and Itoh, 2001). Inhibition of ADF function by phospholipids raises the intriguing possibility of ADF regulation via the phosphoinositide signal transduction pathway.

A plethora of GTPases has been implicated in signal transduction of external stimuli (Agrawal *et al.*, 2003; Burridge and Wennerberg, 2004). The activity of metazoan LIM kinases is regulated by the small Rho-type GTPases Rho, Rac, and c̲ell d̲ivision c̲ycle protein 42 (Cdc42) (Yang *et al.*, 1998; Gungabissoon and Bamburg, 2003). Overexpression of Rho family-like GTPases promoted actin remodelling in plant cells (Fu and Yang, 2001). Furthermore, a Rac/Rop GTPase is suggested to modulate ADF activity in pollen tubes (Chen *et al.*, 2003).

Due to the number of putative direct or indirect ADF/cofilin effectors a vast amount of regulation scenarios is conceivable. These complex regulatory mechanisms render ADF/cofilins potential convergence points of multiple signalling pathways. Thus, ADF/cofilins may transduce the received stimuli into a single outcome, an enhanced or reduced F-actin turnover with modulated spatial and temporal precision, which is a prerequisite for many actin-dependent biological processes.

4.2   Results

4.2.1   Identification of ihpRNA constructs conferring partially compromised penetration resistance of barley cells to *Bgh*

Approximately 700 randomly chosen ihpRNA clones have been used for ballistic transfection. This resulted in the identification of two different pools mediating an enhanced *Bgh* penetration rate in cells of resistant barley *mlo*-3 leaves. Interestingly, each pool contained a pUAMBN-based ihpRNA construct harbouring a cDNA with 100% homology to barley *HvADF3* (TIGR database accession number TC146245). The cDNAs were derived from the two distinct epidermal cDNA library clones HO00E08 (GenBank accession number CD054609) and HO02C05 (GenBank accession number CD054021), respectively. Repeated bombardments of the first identified pool confirmed the enhanced penetration rate compared with control

experiments in which leaves were transfected with the GUS reporter construct only [Fig. 12].
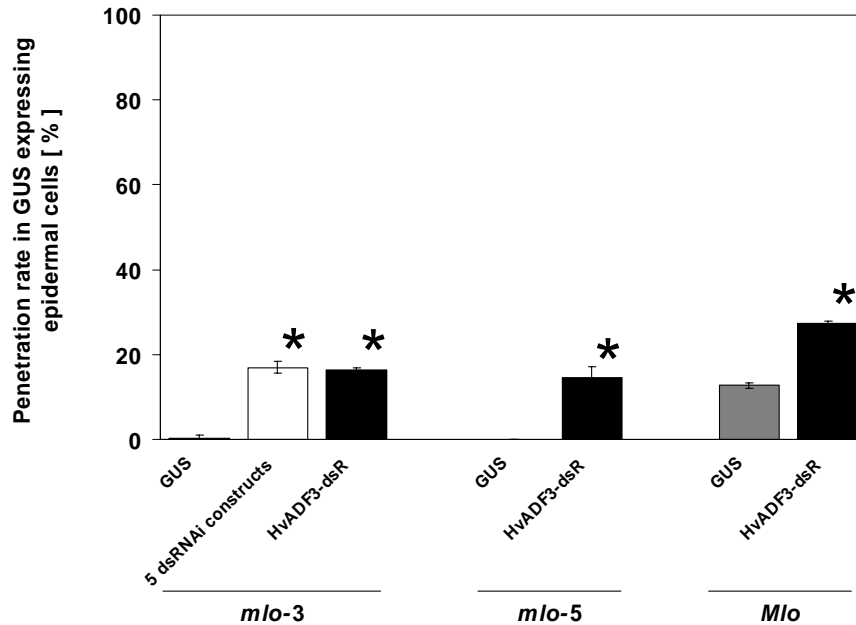

Figure 12. An ihpRNA construct of *HvADF3* mediates enhanced *Bgh* penetration success in barley leaf epidermal cells.

Two powdery mildew resistant near-isogenic barley lines (Ingrid *mlo*-3 and *mlo*-5) and the susceptible cultivar Golden Promise (*Mlo*) were ballistically transfected with a *HvADF3* cDNA-containing ihpRNA construct (pHvADF3-dsR, black columns). To allow a maximum of protein turnover, leaves were subsequently incubated for 96 h prior to inoculation with *Bgh*.

Columns represent percentage of successful penetration attempts of *Bgh* conidia (isolate K1) 48 h after inoculation of *Hordeum vulgare* leaves, scored by formation of haustoria in marker gene (ß-glucuronidase (GUS); grey columns) expressing cells [%]. Data represent the average of a minimum of three independent experiments (± standard deviation) in which at least 100 interaction sites of single *Bgh* sporelings attacking epidermal barley cells were microscopically evaluated. The asterisks indicate $P < 0.05$ (Student's *t* test) compared with GUS.

Additionally, results for the pool containing 5 different ihpRNA constructs including pHvADF3-dsR, originally identified in the PTGS screen in the *mlo*-3 genetic background, are displayed (white column).

After testing the five constructs of the pool in individual bombardments, the enhanced penetration efficiency could be assigned to the single *HvADF3* cDNA-containing ihpRNA construct (designated as pHvADF3-dsR). Sequencing of pHvADF3-dsR revealed that in addition to the *HvADF3* coding region parts of the 5'-untranslated region (UTR) and of the 3'-UTR were present in the silencing vector [Fig. 13].

```
     EcoRI
  1  GAATTCGGCACGAGGCCCCCCCTCTCCTTTCCCCTCCCCCTCCCCCTCCCCGCCGGATTCCTCCTTCCCCTCCCGACTCC
     CTTAAGCCGTGCTCCGGGGGGGAGAGGAAAGGGGAGGGGGAGGGGGAGGGGCGGCCTAAGGAGGAAGGGGAGGGCTGAGG

           HvADF3
 81  CGAGCTCGGCAATGGCAAACGCTTCATCAGGTGCTGGGATCCATGACGACTGCAAGCTGAGGTTCGTGGAGCTCAAGTCC
     GCTCGAGCCGTTACCGTTTGCGAAGTAGTCCACGACCCTAGGTACTGCTGACGTTCGACTCCAAGCACCTCGAGTTCAGG

161  AAGAGGATGCACCGCTTCATAACCTACAGGCTGGAGAACCAGAAGGAGGTCATTGTGGACCAAACCGGGCAGCGCGATGC
     TTCTCCTACGTGGCGAAGTATTGGATGTCCGACCTCTTGGTCTTCCTCCAGTAACACCTGGTTTGGCCCGTCGCGCTACG

241  CACCTATGAGGATTTCACCAAGACCCTCCCTGAAAACGACTGCCGATTCGCAGTGTTTGACTTCGACTTCACCACCCCGG
     GTGGATACTCCTAAAGTGGTTCTGGGAGGGACTTTTGCTGACGGCTAAGCGTCACAAACTGAAGCTGAAGTGGTGGGGCC

321  AGGATGTGCCAAAGAGCAGGATCTTCTATATCTTCTGGTCCCCGGACACCGCAAAGGTGAGGAGCAAGATGACGTACGCG
     TCCTACACGGTTTCTCGTCCTAGAAGATATAGAAGACCAGGGGCCTGTGGCGTTTCCACTCCTCGTTCTACTGCATGCGC

401  AGCACCAACGAGAAGTTCAAGAGGACCCTGGACGGCATCCAGATCGAGATGCAGGCCACCGACCCCAGCGAAATCAGCCT
     TCGTGGTTGCTCTTCAAGTTCTCCTGGGACCTGCCGTAGGTCTAGCTCTACGTCCGGTGGCTGGGGTCGCTTTAGTCGGA

481  GGACGTGATCAAGGAGCGCGCACACTAGGGCGGCAAACCAACCATCCATCCAATGCTCTGCCCTTTGGACGCCTCACGGC
     CCTGCACTAGTTCCTCGCGCGTGTGATCCCGCCGTTTGGTTGGTAGGTAGGTTACGAGACGGGAAACCTGCGGAGTGCCG

561  GACATGGATTTATTATGTCAATTATAGATTTGGCGGTGTGACTCTTGAAACTTTCTTGATGATTTGTNGGCTTTGTTACC
     CTGTACCTAAATAATACAGTTAATATCTAAACCGCCACACTGAGAACTTTGAAAGAACTACTAAACANCCGAAACAATGG

641  GTGTCGAAAGATCCCCGTGGTGAGACCACCACGGCGGTCTTGTTCTAAGTTCTATCATGTAATCCGTTCCTTCTTCCGCT
     CACAGCTTTCTAGGGGCACCACTCTGGTGGTGCCGCCAGAACAAGATTCAAGATAGTACATTAGGCAAGGAAGAAGGCGA

721  GCCCATTTATATGCCGGGCGTTATGCTGCTGCACTGTTCTTCCAAGTTCTGGTTATAAATAATTAAATGTTCTAAAAAAA
     CGGGTAAATATACGGCCCGCAATACGACGACGTGACAAGAAGGTTCAAGACCAATATTTATTAATTTACAAGATTTTTTT

           XhoI
801  AAAAAAAAAAAACTCGAG
     TTTTTTTTTTTTGAGCTC
```

Figure 13. Nucleotide sequence of the *HvADF3* cDNA introduced into pUAMBN.
The translation initiation of *HvADF3* is indicated by an arrow; boldface letters mark the coding region
of *HvADF3*; underlined, boldface letters mark flanking restriction enzyme recognition sites used for
cloning in the barley epidermal cDNA library.

Therefore, it was assumed that the partially impaired resistance response could be
caused by depletion of at least one *ADF* via PTGS triggered upon pHvADF3-dsR
transfection [Fig. 12].

To exclude that side-effects caused by second-site mutations in the mutagenesis-
derived cv. Ingrid *mlo*-3 backcross line contributed to enhanced *Bgh* penetration,
HvADF3-dsR was additionally tested in leaves of the near-isogenic backcross line
Ingrid containing the *mlo*-5 null allele. These experiments further corroborated the
results obtained in the *mlo*-3 genotype, indicating that the enhanced *Bgh* penetration
could be assigned to pHvADF3-dsR [Fig. 12].

Likewise, the impact of pHvADF3-dsR on *Bgh* penetration was tested in the susceptible *Mlo* cultivar Golden Promise. In these experiments, cells were rendered super-susceptible compared with control bombardments with the GUS reporter construct only [Fig. 12].

4.2.2   The *HvADF3* coding region is unaltered in *ror1* mutants

Enhanced penetration rates of *Bgh* in pHvADF3-dsR-transfected barley epidermal cells were highly reminiscent of the phenotypes observed in barley *Mlo* or *mlo* plants carrying mutations in the *Ror1* or *Ror2* genes (Freialdenhoven *et al.*, 1996; Collins *et al.*, 2003). While *Ror2* has been recently cloned and was shown to encode a syntaxin (t-SNARE; Collins *et al.*, 2003; see Chapter 1.1.4), the molecular nature of *Ror1* is still unclear. To examine whether *HvADF3* corresponds to the *Ror1* gene, cDNAs of *HvADF3* were isolated from 5 independent *ror1* alleles (A39/1a (*ror1*-1), A89/1a (*ror1*-2), C36/1b (*ror1*-3), C69/1 (*ror1*-4), C88/1b (*ror1*-5)) by RT-PCR. Sequence analysis of the complete coding region revealed that none of the *ror1* mutants carried mutations in the *HvADF3* coding region, suggesting that *HvADF3* does not correspond to *Ror1*.

4.2.3   Overexpression of *HvADF3* confers enhanced accessibility to *Bgh* in *mlo* genotypes

The role of ADF in rapid treadmilling of actin filaments requires a tight regulation of cellular ADF protein levels (Carlier, 1998). Experiments with different species revealed that alteration of endogenous ADF levels have drastic effects on the actin cytoskeleton architecture. In a single cell experiment, longitudinal actin cables were reorganised into thick, transverse arrays by injection of maize ADF (ZmADF1) into stamen hair cells of *Tradescantia* (Hussey *et al.*, 1998). Overexpression of a tobacco *ADF* (*NtADF1*) in *Nicotiana tabacum* pollen tubes resulted in the disruption of the actin cytoskeleton (Chen *et al.*, 2002). A similar effect was observed upon overexpression of an *ADF* (*AtADF1*) in *Arabidopsis* hypocotyl cells (Dong *et al.*,

2001b). In contrast, *Arabidopsis* antisense lines with reduced transcript levels of *AtADF1* showed a stimulated formation of actin cables (Dong *et al.*, 2001b).

Cofilin has been shown to be essential for viability of *Dictyostelium discoideum* (Aizawa *et al.*, 1995). Interestingly, in contrast to the actin cytoskeleton-disrupting property of overexpressed *ADF*s *in planta*, overexpression of cofilin in the soil-living amoeba increased F-actin and actin bundles, enhanced cell movement, and resulted in membran*e* ruffling (Aizawa *et al.*, 1996).

To test whether *HvADF3* overexpression has a different impact on barley resistance to *Bgh* than the putatively *HvADF3*-depleting ihpRNA construct pHvADF3-dsR, a construct for transient *HvADF3* overexpression was generated (pHvADF3-OE) [Fig. 14]. The full-size coding region (417 bps) of *HvADF3* was amplified via PCR from the original epidermal cDNA library clone HO00E08 and introduced into the overexpression vector backbone pUbi-nos (kindly provided by Ralph Panstruga) in which high-level expression is driven by the strong maize ubiquitin promoter (Nielsen *et al.*, 1999) [Fig. 14].
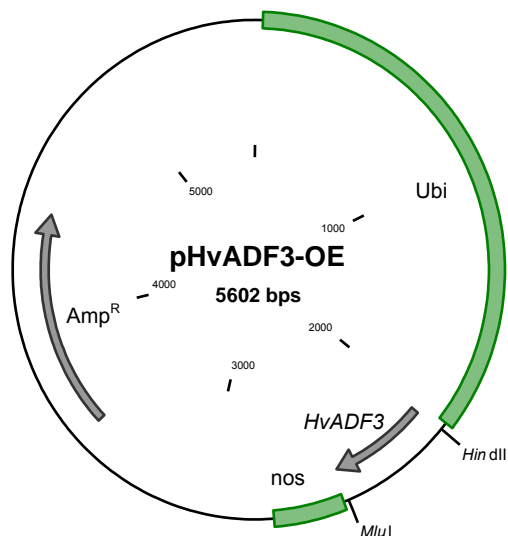

Figure 14. Plasmid map of the *HvADF3* overexpression vector pHvADF3-OE.
Essential features and restriction sites are depicted in the map. (***HvADF3***) cDNA coding region of the *HvADF3*; **(Ubi)** maize ubiquitin promoter; **(nos)** transcription termination; **(Amp^R)** β-lactamase gene conferring ampicillin resistance. The 5'-end of the *HvADF3* cDNA was modified by changing the context immediately 5' to the initiator ATG codon to a "Kozak consensus" sequence (Kozak, 1989) for optimal translation initiation.

Surprisingly, ballistic delivery of pHvADF3-OE in cells of barley *mlo*-3 leaves caused partial breakdown of broad-spectrum penetration resistance to a similar extent as observed with ihpRNA construct pHvADF3-dsR [Fig. 12 and Fig. 15].
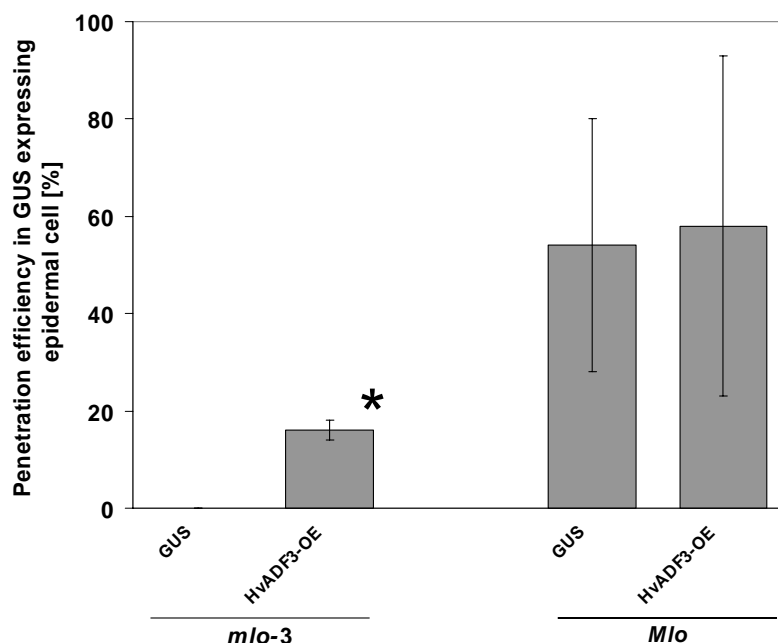

Figure 15. Overexpression of *HvADF3* confers enhanced *Bgh* penetration success in *mlo*-3 leaf epidermal cells.
The overexpression construct of wild-type *HvADF3* (pHvADF3-OE) was ballistically delivered in barley epidermal cells of *mlo*-3 and *Mlo* genotypes. Inoculation with *Bgh* conidiospores (isolate K1) was performed 4 h after bombardment. Control cells were transfected with the marker gene expressing vector (GUS) only. The asterisk indicates $P < 0.05$ (Student's *t* test) compared with GUS. Experimental procedures not explicitly mentioned are as described in Figure 12.

However, transfection of susceptible barley wild-type leaf epidermal cells with pHvADF3-OE showed no reproducible enhanced penetration rate compared with control samples [Fig. 15]. High variation among independent experiments with *Mlo* genotypes are unusual (Elliott *et al.*, 2002; Kim *et al.*, 2002) and cannot be explained. The elevated penetration rates in the *Mlo* genotype compared with experiments with construct pHvADF3-dsR [Fig. 12] were likely due to the different duration of incubation periods before inoculation with *Bgh*. Protein turnover rates have not to be considered upon transient gene overexpression. Therefore, the time period between bombardment and subsequent inoculation was generally set to four hours in

overexpression experiments to diminish time-dependent enhanced resistance in susceptible barley genotypes (see Chapter 3.2.3.2).

4.2.4 Visualisation of the actin cytoskeleton upon transient single cell expression of pHvADF3-dsR and pHVADF3-OE

As already mentioned above, alterations of ADF levels by gene silencing or overexpression have been described to have contrary effects on actin cytoskeleton architecture *in planta.* Since unexpectedly both *HvADF3* constructs (pHvADF3-dsR and pHvADF3-OE) had the same effect on *Bgh* penetration rates in ballistically transfected leaf epidermal cells, specific staining of filamentous actin in combination with confocal laser scanning microscopy was used to visualise the impact of pHvADF3-dsR and pHvADF3-OE on the architecture of the actin cytoskeleton.
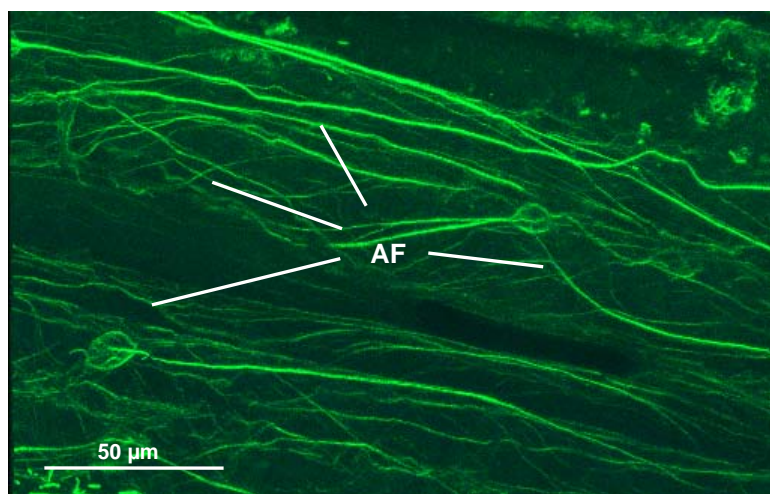

Figure 16. Barley epidermal cells stained with ALEXA-Fluor phalloidin 488[®].
Leaf segments of a barley wild-type genotype were stained with ALEXA-Fluor as described in the Material and Methods (see Chapter 2.2.7.1). Green structures represent the ALEXA-Fluor phalloidin 488[®]-labelled actin meshwork (**AF**, actin filaments) of adjacent barley epidermal cells. Fluorescence of actin/phalloidin complexes was visualised by using a confocal laser microscopy system (CLSM 510 META; Carl-Zeiss, Jena, Germany) equipped with an Argon ion laser and a HFT 488 beam splitter. The 488 nm Argon ion laser line was used to excite ALEXA-Fluor phalloidin 488[®]. The emitted light was collected in the lambda spectrum mode between 494 and 580 nm. The micrograph was taken immediately after the phalloidin staining procedure. The scale bar in the bottom left corner represents the absolute size.

Barley cells were ballistically transfected with pHvADF3-dsR or pHvADF3-OE and a reporter construct (pUbi-RFP-nos; kindly provided by Ralph Panstruga) expressing a red fluorescent protein (RFP) for the identification of transfected cells. Leaves were fixed with formaldehyde 48 h after transfection and subsequently stained with ALEXA-Fluor phalloidin 488®. Alexa dyes, which are derivatives of phalloidin, decorate F-actin with high specificity (Wulf *et al.*, 1979; Panchuk-Voloshina *et al.*, 1999) [Fig. 16]. Microscopic analysis revealed that in cells transfected with the reporter construct alone, the actin cytoskeleton appeared unaltered compared with adjacent non-transfected cells [Fig. 17A].

In cells containing the reporter construct and the *HvADF3* overexpression construct pHvADF3-OE, phalloidin-stainable F-actin cables and filaments were completely absent compared with surrounding non-transfected cells [Fig. 17B]. A similar result was obtained with the suspected silencing construct pHvADF3-dsR, although cells apparently contained few residual actin arrays [Fig. 17C].
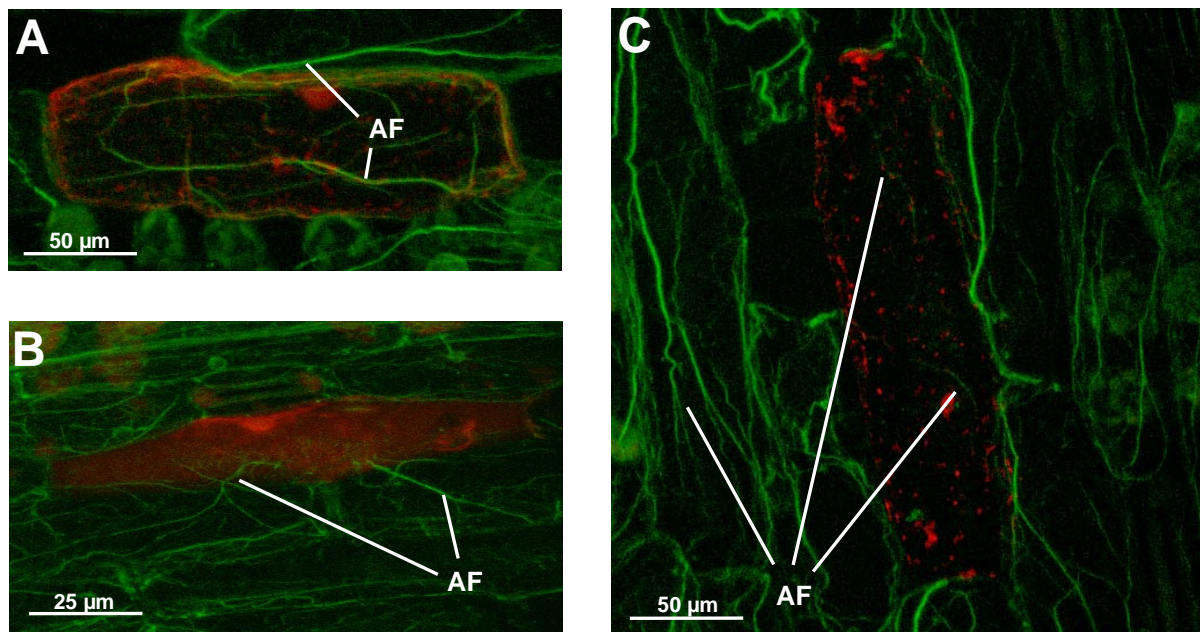

Figure 17. Impact of pHvADF3-dsR and pHvADF3-OE on phalloidin-stainable actin filaments in barley epidermal cells.
(A) Barley epidermal cell of a detached barley leaf ballistically transfected with pUbi-RFP-nos for the expression of RFP, serving as a reporter for successful transformation. The whole leaf segment was stained with ALEXA-Fluor phalloidin 488® 48 h after transfection. Green structures represent stained actin filaments **(AF)**.
(B) Barley epidermal cell ballistically co-transfected with a *HvADF3* overexpression construct (pHvADF3-OE) and the RFP reporter construct.
(C) Co-transfection of a barley epidermal cell with pHvADF3-dsR and the RFP reporter construct.
All micrographs were taken by confocal laser scanning microscopy immediately after the phalloidin staining procedure. The scale bars in the bottom left corners represent the absolute sizes.

In conclusion, this set of experiments revealed that bombardment of either pHvADF3-dsR or pHvADF3-OE led to a similar disappearance of phalloidin-stainable actin filaments, most likely due to a depolymerisation of the actin cytoskeleton.

4.2.5 Perturbation of the actin cytoskeleton impedes trafficking of peroxisomes

A limitation of the phalloidin-based F-actin staining method is that it can be applied to fixed tissue only. Therefore, dynamic alterations of the actin cytoskeleton scaffold, like the rearrangement towards sites of fungal penetration attempts (see Chapter 1.4), cannot be monitored over time. Actin cytoskeleton dynamics in living cells have been visualised by the transient expression of ABPs, like fimbrin or talin, fused to fluorescing proteins (McCann and Craig, 1997; Kovar *et al.*, 2001).

It was attempted to decorate actin filaments with GFP-talin and GFP-fimbrin (both constructs kindly provided by Volker Lipka) by ballistic delivery of corresponding constructs into barley leaf epidermis cells. Though these constructs had been shown to be functional in *Alium cepa* (monocot) and *Arabidopsis* (dicot) cells, fluorescence in barley cells was not sufficient for microscopic analysis. Fluorescent proteins targeted to peroxisomes were used as an alternative approach to visualise indirectly the integrity of the actin cytoskeleton in living cells.

Plant peroxisomes stream through the cytoplasm at peak velocities approaching 10 µm s^{-1} (Jedd and Chua, 2002). In contrast to mammalian peroxisomes, which are shuttled along microtubules, plant peroxisomes move along actin microfilaments (Jedd and Chua, 2002; Mathur *et al.*, 2002), possibly independently of myosin motor proteins (Mathur *et al.*, 2002). Attachment of a peroxisome targeting signal (PTS) to a protein results in reliable localisation to peroxisomes (Mullen and Trelease, 2000). The prototypical PTS type 1 of higher plants, encoding the tripeptide motif serine (S), arginine (R) and leucin (L) (Jedd and Chua, 2002; Reumann, 2004), was C-terminally attached to both GFP and RFP via PCR. Respective PCR products were cloned into the monocot overexpressing vector backbone pUbi-nos (kindly provided by Ralph Panstruga), resulting in the plasmids pGFPTS and pRFPTS [Fig. 18].
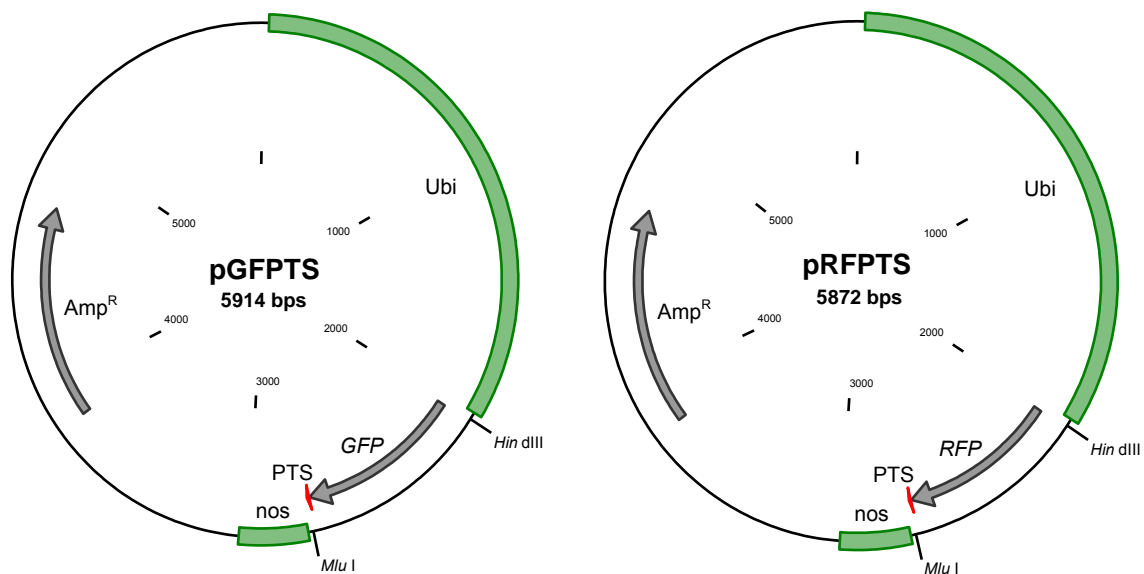
Figure 18. Plasmid maps of the vectors pGFPTS and pRFPTS for the expression of peroxisome-targeted GFP and RFP, respectively.
Essential features and restriction sites are depicted in the map. **(*GFP*)** coding region of the green fluorescent protein; **(*RFP*)** coding region of the red fluorescent protein; **(PTS)** peroxisome targeting sequence (SRL-motif) fused in-frame to marker proteins; **(Ubi)** maize ubiquitin promoter; **(nos)** transcription termination; **(Amp^R)** β-lactamase gene conferring ampicillin resistance. The 5'-end of *GFP* and *RFP* was modified by changing the context immediately 5' to the initiator ATG codon to a "Kozak consensus" sequence (Kozak, 1989) for optimal translation initiation.

Visualisation of peroxisome movement by epifluorescence microscopy was achieved upon delivery of either of these constructs into barley leaf epidermal cells [Fig. 19A]. Co-bombardment of the *HvADF3*-overexpressing construct resulted in the disruption of the actin cytoskeleton (Chapter 4.2.4) and consequently removed actin tracks required for peroxisome trafficking. The limited mobility of GFP-labelled peroxisomes became apparent by the formation of compact globular peroxisome aggregates distributed in the cytoplasm [Fig. 19B] Motility of peroxisomes inside aggregates was reduced to random oscillation. Nevertheless, single peroxisomes were occasionally able to move short distances away from accumulation sites. Remaining amounts of polymerised G-actin or newly synthesised F-actin allowing residual peroxisome trafficking might account for this phenomenon.

These findings corroborate the actin-disrupting function of *HvADF3* overexpression. Moreover, the results are consistent with previous reports showing that interference with actin polymerisation by application of the pharmacological drugs cytochalasin D or latrunculin B to plant cells leads to similar effects as impaired peroxisomal mobility

and the formation of peroxisome aggregates (Jedd and Chua, 2002; Mathur *et al.*, 2002).
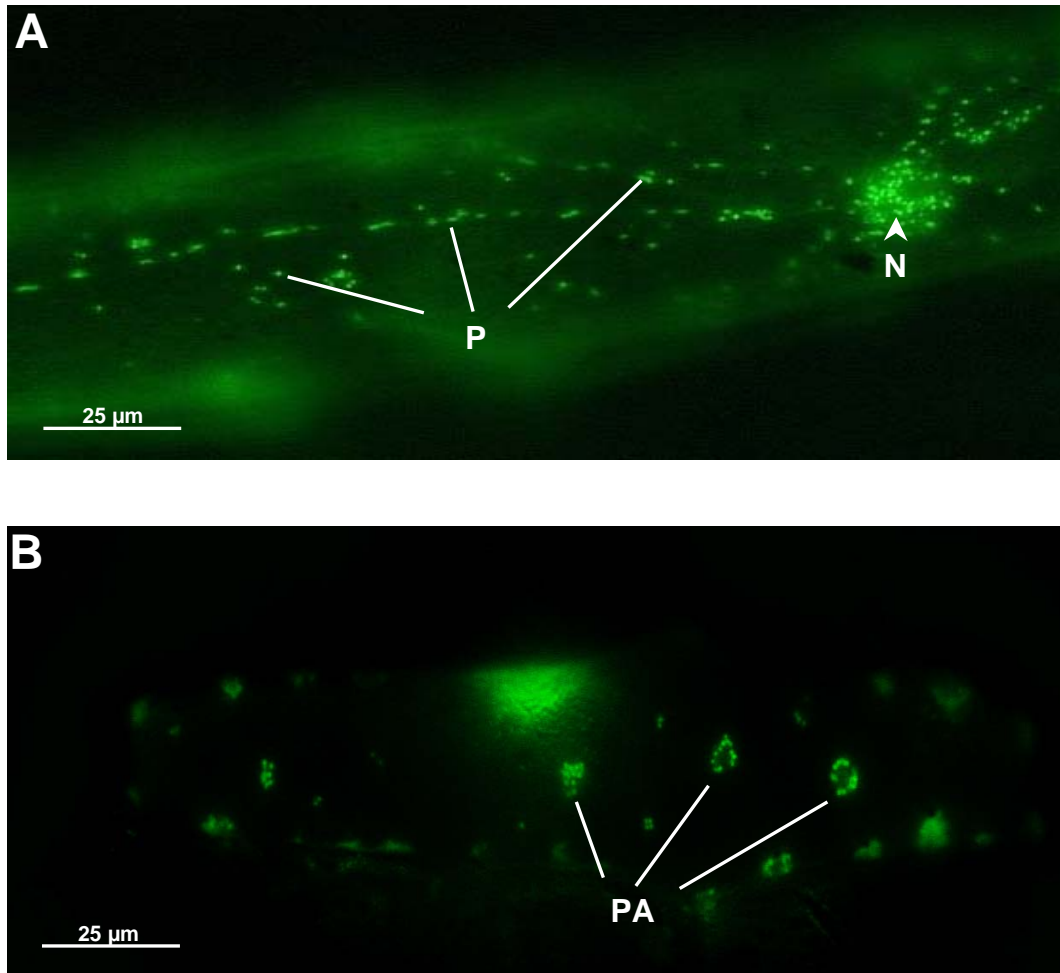
Figure 19. Alterations of peroxisome dynamics upon overexpression of *HvADF3*.
(A) Peroxisomes were labelled by particle bombardment of a GFP fusion construct (pGFPTS) containing a C-terminal peroxisome targeting sequence (PTS1) into barley epidermal cells. Green fluorescing dots represent single mobile peroxisomes **(P)**; Peroxisomes accumulating around the nucleus **(N)**.
(B) Co-transfection of the GFP-PTS construct and the *HvADF3* overexpression construct (HvADF3-OE). Bright green areas represent peroxisome aggregates **(PA)**.
The scale bars in the bottom left corners represent the absolute sizes. The micrographs were taken 60 h after transfection.

4.2.6   Callose deposition upon pathogen challenge requires an intact actin cytoskeleton

Perturbation of actin dynamics by application of actin polymerisation inhibitors in barley resulted in absence of callose-containing papillae in response to pathogenic attack. Since this effect was only observed upon interference with the actin cytoskeleton but not upon disruption of microtubules, deposition of callose in papillae was suggested to be an actin-dependent process (Kobayashi *et al.*, 1997b).
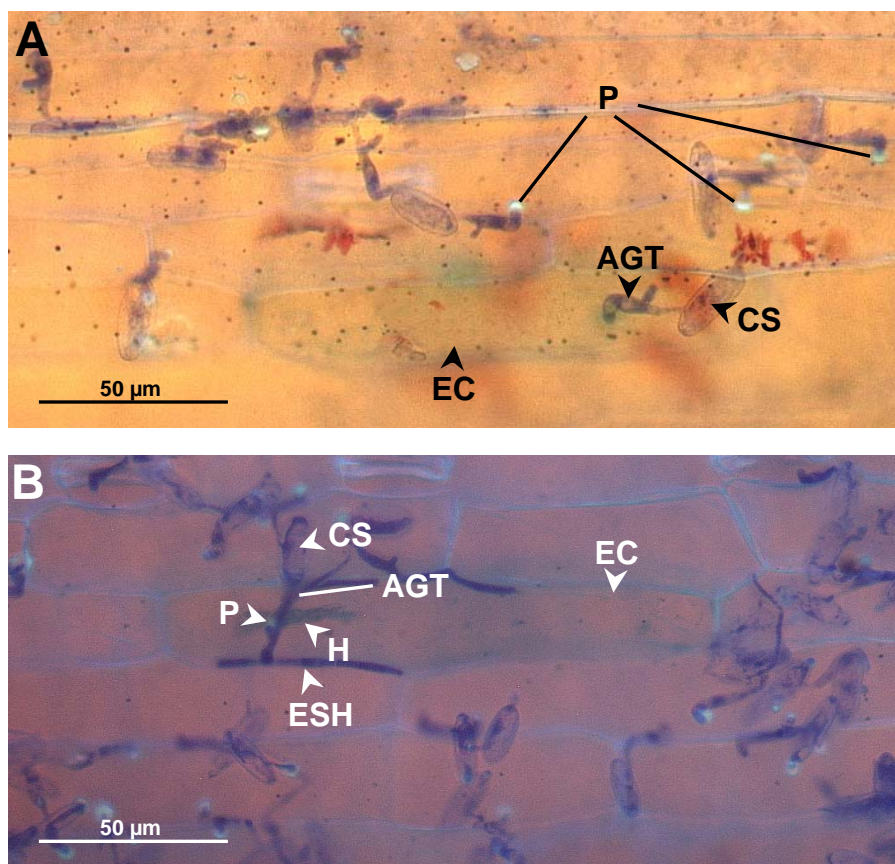
Figure 20. Disruption of actin filaments by *HvADF3* overexpression reduces callose deposition.
Barley leaves of the resistant line Ingrid (*mlo*-3) were ballistically transfected with the *HvADF3*-overexpressing construct pHvADF3-OE. Leaves were inoculated with *Bgh* conidiospores 4 h post transfection and stained for ß-glucuronidase activity of transfected epidermal cells **(EC)** 48 hpi. Papillae **(P)** subtending appressorial germ tubes **(AGT)** of *Bgh* conidiospores **(CS)** were subsequently stained for callose deposition with aniline blue.
>   **(A)** Failed *Bgh* penetration attempt.
>   **(B)** Successful *Bgh* penetration attempt. Haustorium **(H)** and elongating secondary hyphal **(ESH)** are formed.

Micrographs represent an overlay of UV-excited aniline blue fluorescence of callose and bright-field microscopy of epiphytic fungal structures stained with Comassie brilliant blue, analysed by using a Zeiss Axiophot microscope. The scale bars in the bottom left corners represent the absolute sizes.

To test whether this phenomenon also occurs upon genetic interference with the actin cytoskeleton, resistant barley epidermal cells transfected with the *HvADF3* overexpression construct were investigated for impaired callose accumulation in response to *Bgh* attack. After aniline blue staining, transfected GUS-expressing epidermal cells showed in ~ 80% of all cases no callose deposition at sites of failed *Bgh* penetration attempts. In contrast, neighbouring untransfected epidermal cells accumulated callose underneath almost all fungal appressorial germ tubes [Fig. 20A]. Interestingly, more than 50% of successfully penetrated cells showed a faint fluorescence at the tips of appressorial germ tubes, indicative of some residual callose deposition. These putative papillae were extremely small in diameter [Fig. 20B]. Additional actin-independent mechanisms for callose deposition might account for this phenomenon.

In conclusion, these findings corroborate the ability of HvADF3 overexpression to disrupt actin filaments and substantiate the notion that focal callose deposition requires intact actin cytoskeleton architecture.

4.2.7   Effects mediated by the *HvADF3* ihpRNA construct are likely to be overexpression artefacts

The observed disruption of F-actin upon *HvADF3* overexpression is in accordance with previous reports (Dong *et al.*, 2001b; Chen *et al.*, 2002). However, reduced ADF protein levels are generally not correlated with disappearance of actin filaments (Carlier, 1998; Dong *et al.*, 2001b).

As described earlier (see Chapter 4.2.1), the cDNA insertion of the suspected *HvADF3* silencing construct pHvADF3-dsR included parts of the 5'- and 3'-UTR in addition to the complete coding region. This cDNA portion was integrated in sense orientation adjacent to the ubiquitin promoter of the vector, possibly allowing undesired *HvADF3* overexpression rather than dsRNAi-mediated silencing.

To investigate whether silencing or overexpression caused pHvADF3-dsR-mediated effects, a full-size cDNA coding region of *HvADF3* introduced into pUAMBN-i (see Chapter 3.2.1), giving rise to an ihpRNA silencing construct in which the first cDNA of

the repeat was oriented in antisense adjacent to the promoter. This arrangement should exclude the possibility of *HvADF3* overexpression.

Furthermore, the cDNA in the original ihpRNA construct pHvADF3-dsR was replaced by a corresponding sequence encoding a putatively non-functional HvADF3 due to lack of the first six amino acids (Met-Ala-Asn-Ala-Ser-Ser). Repeated bombardments of these constructs showed no impact on the penetration efficiency of *Bgh* in transfected resistant (*mlo*) barley leaf epidermal cells (data not shown).

Provided that both constructs were functional, this data suggest that disruption of the actin cytoskeleton and resulting enhanced *Bgh* penetration efficiency might be exclusively due to overexpression of *HvADF3* and that dsRNAi-mediated PTGS does not affect these processes.

4.2.8 Overexpression of barley *HvADF6* impairs barley defence against *Bgh*

To investigate whether the *HvADF3* overexpression-mediated enhanced *Bgh* penetration rates were provoked by a HvADF3 isoform-specific function, the barley epidermal cDNA library was searched for further ADF isoforms that could be tested for altering accessibility of ballistically transfected leaf epidermal cells to *Bgh*. The library contained only one additional *ADF*, designated as *HvADF6*, which was amplified from library clone HO06M01 (GenBank accession number CD057834) via PCR and cloned into the ihpRNA-vector pUAMBN. This experiment was performed to further investigate whether undesired overexpression by pUAMBN is a general phenomenon or was special for *HvADF3*. The *HvADF6* full-size coding region was amplified by means of the specific primer pair (HvADF6-Gate-For and HvADF6-Gate-Rev) containing GATEWAY® *att*B-sites for insertion of the cDNA into the overexpression vector pUbiGATE (see below).

To facilitate the rapid generation of overexpression constructs, the GATEWAY®-based overexpression vector pUbiGATE was generated. pUbiGATE consists of an *att*R-cassette (see Chapter 3.2.1) in sense-orientation adjacent to the maize ubiquitin promoter [Fig. 21]. The functionality of the construct was tested by fluorescence protein expression. A GFP-encoding gene was recombined into the vector and

subsequent ballistic delivery of barley leaf epidermal cells with pUbiGATE-GFP revealed fluorescence of transfected cells.
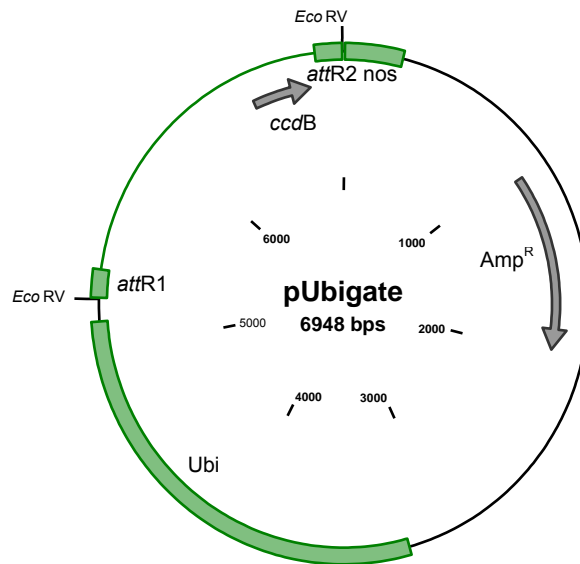

Figure 21. Plasmid map of the overexpression vector pUbiGATE.
Essential features and restriction sites are depicted in the map. **(*att*R1)** attachment site R1; **(*att*R2)** attachment site R2; **(*ccd*B)** negative selection marker; **(Ubi)** maize ubiquitin promoter; **(nos)** transcription termination; **(Amp^R)** β-lactamase gene conferring ampicillin resistance.

Ballistic delivery of the *HvADF6* overexpression construct pHvADF6-OE into resistant barley epidermal cells revealed an enhanced accessibility of transfected cells to *Bgh* [Fig. 22]. Penetration rates were comparable to those observed upon overexpression of *HvADF3* [Fig. 12]. Surprisingly, in contrast to the *HvADF3* ihpRNA construct (pHvADF3-dsR) suspected to mediate enhanced *Bgh* penetration by *ADF* overexpression (see Chapter 4.2.3), exchange of *HvADF3* cDNAs to *HvADF6* cDNAs resulted in unaltered penetration rates of *Bgh* compared with control experiments [Fig. 22]. Structural intramolecular differences between *HvADF3* and *HvADF6* might facilitate undesired overexpression of *HvADF3* but not of *HvADF6* by the corresponding ihpRNA constructs.
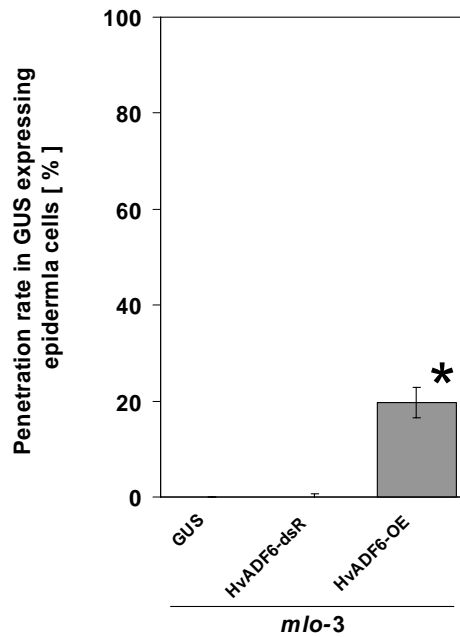
Figure 22. Overexpression but not silencing of *HvADF6* impairs *mlo* penetration resistance in barley leaf epidermal cells.
Barley epidermal cells (*mlo*-3 genotype) were inoculated with *Bgh* conidiospores (isolate K1) either 4 hours after ballistic transfection of the *HvADF6* overexpressing construct (HvADF6-OE) or 96 h after delivery of the ihpRNA construct (HvADF6-dsR). Results for the cells only transfected with the GUS gene expressing vector (GUS) inoculated 4 h after transfection are depicted as control. Data for control cells inoculated 96 h after transfections were identical to cells inoculated 4 h after transfection (data not shown). The asterisk indicates $P < 0.05$ (Student's *t* test) compared with GUS. Experimental procedures not explicitly mentioned are as described in Figure 12.

Enhanced *Bgh* penetration rates upon transient *HvADF6* overexpression in ballistically transfected barley cells suggested for both isoforms (HvADF6 and HvADF3) an unspecific function in the disruption of actin filaments mediated by ectopic expression.

4.2.9 Compromised barley defence is an unspecific effect triggered upon overexpression of both monocot and dicot *ADF*s

Phylogenetic analysis of known ADF sequences of monocotyledonous plants as such barley, wheat, rice, maize and the twelve ADFs of dicotyledonous *Arabidopsis* revealed the existence of a clade of monocot-specific ADFs. While HvADF3 belongs to this cluster, HvADF6 groups in a distinct branch of the phylogentic tree [Fig. 23]. It

remains questionable, whether the ADF isoform of the monocot-specific clade exert a specific function in mediating actin dynamics.

Ectopic expression of ADFs from a heterologous plant species can interfere with actin cytoskeleton dynamics (Dong *et al.*, 2001a). To test whether ADF isoform-unspecific F-actin disruption by heterologously expressed *ADFs* is sufficient to induce the enhanced *Bgh* penetration phenotype, different *Arabidopsis* ADF isoforms were assayed in the barely single cell transient gene expression system.

Nine of the twelve known *Arabidopsis ADF*s were successfully amplified via PCR from single strand cDNAs generated from wild-type *Arabidopsis* leaves (ecotype Columbia-0). The identity at the amino acid level of the nine ADFs (AtADF1, AtADF2, AtADF3, AtADF5, AtADF4, AtADF6, AtADF7, AtADF9, AtADF11) isolated from *Arabidopsis* ranges from 54% to 67% compared with HvADF3.

AtADF cDNAs were recombined into pUbiGATE via GATEWAY®-cloning. The resulting overexpression constructs were individually used for ballistic transfection of resistant barley epidermal cells which were subsequently inoculated with *Bgh*.

Evaluation of these experiments revealed that six out of the nine overexpression constructs mediated an enhanced penetration rate of *Bgh*, most likely by impairing actin structures [Fig. 24].
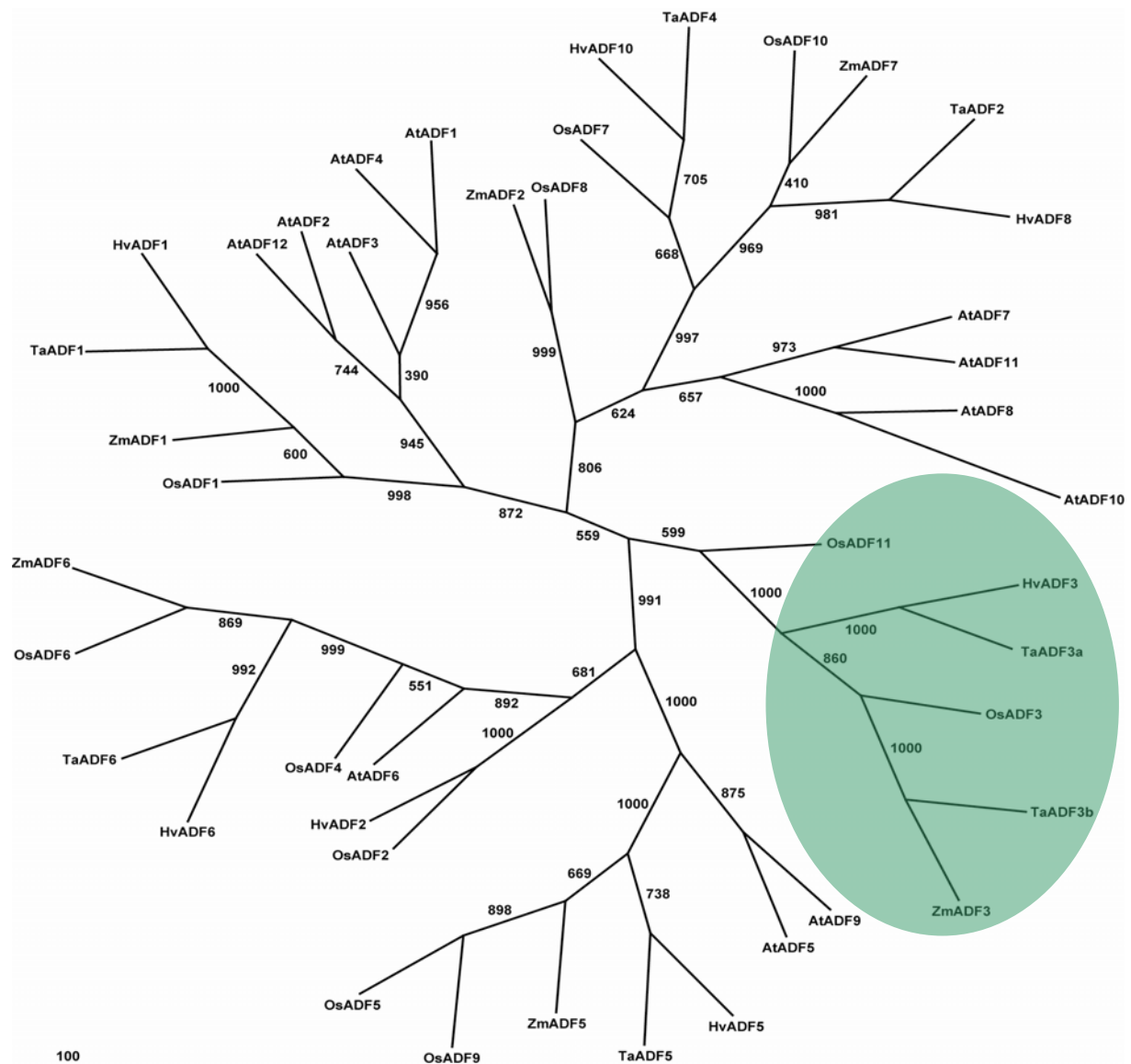
Figure 23. Unrooted phylogenetic tree of ADFs from different monocot species and the dicot plant *Arabidopsis thaliana*.

A phylogenetic tree was constructed by bootstrapping (1.000 reiterations, Phylip, see Chapter 2.2.2.5) from an alignment of the complete amino acid sequences with ClustalW (EMBL-EBI). The unrooted output tree was plotted using the Treeview program; numbers indicate bootstrap values. The shaded area highlights the monocotyledonous-specific ADF clade.

The *Arabidopsis* sequence data were taken from the TAIR database:

AtADF1 (At3g46010), *AtADF2* (At3g46000), *AtADF3* (At5g59880), *AtADF5* (At2g16700), *AtADF4* (At5g59890), *AtADF6* (At2g31200), *AtADF7* (At5g52360), *AtADF8* (At4g00680), *AtADF9* (At4g34970), *AtADF10* (At1g01750), *AtADF11* (At4g25590), *AtADF12* (At3g45990).

Barley (Hv), maize (Zm), rice (Os) and wheat (Ta) ADF data originate from EMBL or TIGR (TI) EST databases:

HvADF1 (TI: TC46250), *HvADF2* (TI: TC60360), *HvADF3* (TI: TC146245), *HvADF5* (TI: TC46717), *HvADF6* (EMBL: CD057834) *HvADF8* (TI: TC49352) *HvADF10* (TI: TC62764), *ZmADF1* (TI: TC150616), *ZmADF2* (TI: TC150192), *ZmADF3* (TI: TC148556), *ZmADF5* (TI: TC150207), *ZmADF6* (TI: TC159321) *ZmADF7* (TI: TC150192), *OsADF1* (TI:TC201477), *OsADF2* (TI: TC208620), *OsADF3* (EMBL: AC104433), *OsADF4* (TI: TC192283), *OsADF5* (TI: TC202703), *OsADF6* (TI: TC185994), *OsADF7* (EMBL: AL606647), *OsADF8* (EMBL: AK072662), *OsADF9* (TI: TC106152), *OsADF10* (EMBL: AK069605), *OsADF11* (EMBL: AC104433), *TaADF1* (TI: TC88586), *TaADF2* (TI: TC70034), *TaADF3a* (EMBL: BJ284976), *TaADF3b* (EMBL: CA486380) *TaADF4* (TI: TC70035), *TaADF5* (TI: 66848), *TaADF6* (TI: TC86040)
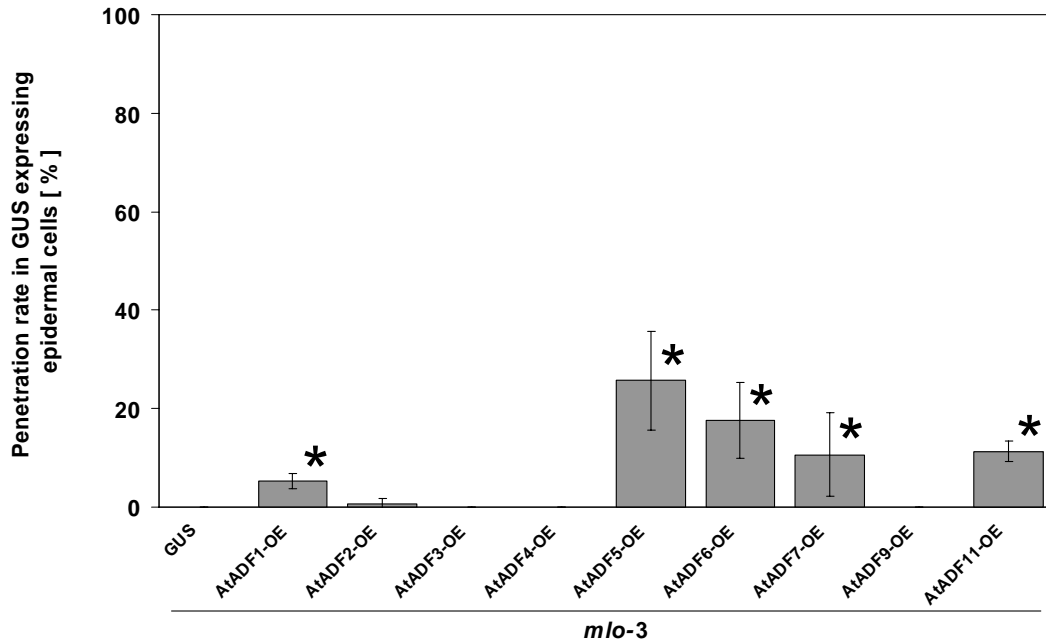
Figure 24. ***Bgh*** **penetration frequencies upon expression of nine** ***Arabidopsis*** ***ADF*s in barley leaf epidermal cells.**
Overexpression of nine different *AtADF*s (AtADF1-7; 9; 11-OE) upon ballistic delivery of respective pUbiGATE constructs into resistant *mlo*-3 mutant barley epidermal cells. Leaf segments were inoculated with *Bgh* conidiospores 4h after bombardment. The asterisks indicate $P < 0.05$ (Student's *t* test) compared with GUS. Experimental procedures not explicitly mentioned are as described in Figure 12.

Expression of *AtADF3, AtADF4,* and *AtADF9* showed no impact on the *Bgh* penetration efficiency in transfected cells. To investigate whether these proteins were efficiently expressed in barley cells, cDNAs of the respective ADFs where inserted into the GATEWAY®-based vector pUbi-YFP-GW-nos (Riyaz Bhat, unpublished) to generate in-frame fusions to the C-terminus of YFP. *HvADF3* was recombined into the same vector to test whether N-terminal fusion of YFP interferes with ADF function. Functionality of the YFP-ADF fusion proteins was determined by analysing their ability to induce the formation of peroxisome aggregates. Individual fusion protein expressing vectors were co-bombarded with RFPTS (see Chapter 4.2.5). Yellow fluorescence of epidermal cells indicated that all four YFP-ADF fusion proteins were expressed. However, the fluorescence intensity of YFP-AtADF9 was very low. In cells transfected with *YFP-AtADF3* and *YFP-AtADF4*, peroxisomal movement was attenuated to similar extents as in cells transfected with *YFP-HvADF3*, though the number of cells forming such aggregates was comparably low.

In epidermal cells expressing *YFP-HvADF9*, impairment of peroxisomal movement was not observed (data not shown).

The experiment was repeated using cDNAs without YFP fusion. Here, no influence on peroxisomal movement could be detected in cells ballistically transfected with the *Arabidopsis ADF*s, whereas *HvADF3* overexpression led to the expected formation of peroxisome clusters.

This set of experiments corroborated the assumption that enhanced *Bgh* penetration rates provoked by overexpression of either *HvADF3* or *HvADF6* are unspecific effects, since heterologous expression of a range of *ADF*s from *Arabidopsis* resulted in similar compromised resistance phenotypes. Furthermore, with the exception of *AtADF9*, all tested *AtADF*s were capable to interfere with F-actin dynamics as monitored by impaired peroxisome movement (data not shown), though AtADF3 and AtADF4 required protein stabilisation by an N-terminal tag. Low-level expression of YFP-AtADF9 or a highly unstable fusion protein recognisable by low YFP fluorescence of transfected epidermal may account for the putatively reduced functionality of this isoform.

4.2.10 HvADF3 might be regulated by posttranslational modification upon pathogen challenge

Plant cells respond to microbial challenge with the rearrangement of intracellular metabolic processes. A part of this reprogramming is controlled by spatial and/or temporal transcriptional suppression or activation of genes (Glazebrook, 2001). It is known from various plant-pathogen interactions that transcript accumulation of up to 10% of the host genes is altered upon pathogen attack (Schenk *et al.*, 2000 Collinge et al., 2001).

Real-time RT-PCR analysis was carried out to test a possible differential expression of *HvADF3* in response to *Bgh* challenge. Leaves of *mlo*-3 and *Mlo* barley genotypes were inoculated with *Bgh*. Infected epidermal tissue was stripped off at 6, 12 and 24 hpi with *Bgh*. cDNA was synthesised from poly(A)$^+$ total RNA derived from respective

samples and used as templates for real-time RT-PCR analysis with primer pairs (HvADF3-For and HvADF3-Rev) covering the complete *HvADF3* coding region (417 bps). Amplification of *HvADF3* from genomic DNA showed amplicon sizes of about 550 bps indicating that genomic *HvADF3* contains at least one intron. The size difference was exploited to check for genomic DNA contaminations in the cDNA preparations.
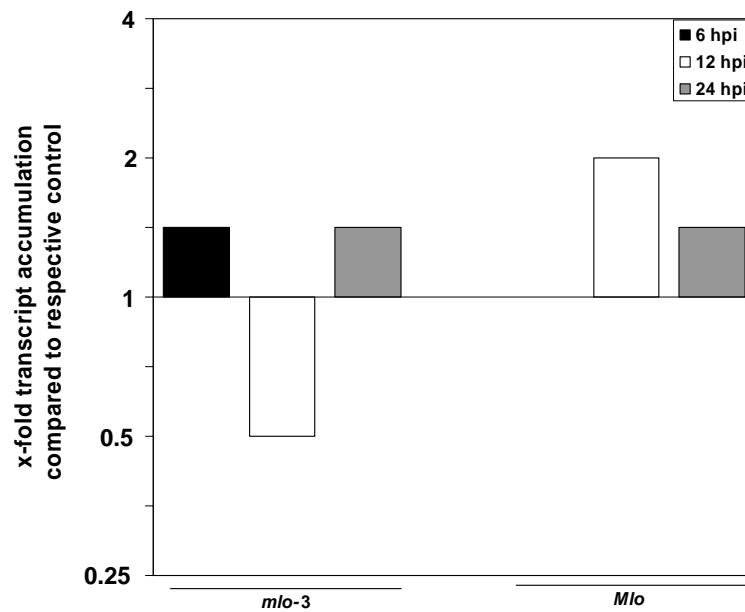
Figure 25. *HvADF3* **RNA accumulation in barley epidermal cells is constitutive and not altered upon** *Bgh* **inoculation.**
Epidermal tissue was peeled from barley leaves (*mlo*-3 null mutant or wild-type *Mlo*) at 6 h (black columns), 12 h (white columns) and 24 h (grey columns) post inoculation with *Bgh* and used for subsequent cDNA generation and real-time RT-PCR analysis. *HvADF3* transcript accumulation was compared with respective uninoculated control samples set to the value of 1. Constitutively expressed actin transcript accumulation served as an internal control for normalising *HvADF3* expression levels. An independent repetition of the experiment revealed similar expression levels (data not shown).

The amounts of *HvADF3*-specific amplification products were normalised against an actin PCR fragment obtained with *HvActin2/7*-specific (GenBank accession number AY145451) primers. Actin genes have been shown to be constitutively transcribed and were chosen as internal control. The *HvActin2/7* primer pair (Actin-intron-For and Actin-intron-Rev) was designed to span one intron resulting in distinguishable amplicon sizes obtained from cDNA and genomic DNA to monitor putative contaminations.

HvADF3 transcript accumulation of *Bgh* challenged leaves was compared with uninoculated leaf samples. No major alterations were observed at any time point in either genotype [Fig. 25]. From the results, it was concluded that *HvADF3* expression is constitutive and is not substantially regulated upon pathogen-challenge.

Since *HvADF3* was found to be constitutively expressed it was tested whether the protein may be regulated by posttranscriptional modification.

Reversible phosphorylation of a serine residue of the amino acid sequence at position 3 (Ser3) in vertebrate ADF/cofilin proteins is known to regulate their activity (Agnew *et al.*, 1995; Moriyama *et al.*, 1996). This Ser3 is structurally an equivalent to a conserved plant serine at position 6 (Ser6) (Lopez *et al.*, 1996). Previous studies on the function of a maize ADF isoform (*ZmADF3*) revealed that phosphorylation of Ser6 inactivates actin-binding *in vitro* and *in vivo* (Smertenko *et al.*, 1998; Allwood *et al.*, 2001; Chen *et al.*, 2002). Putatively functional inactive or constantly active forms of *ZmADF3* were created by mutating Ser6 to aspartate (mimicking phosphorylation) or to alanine (abolishing potential phosphorylation), respectively. The inactive ZmADF3 variant in which Ser6 was replaced by a negatively charged residue was demonstrated to be unable in binding to G- or F-actin and had a negligible effect in accelerating the dissociation rate of G-actin from filaments (Smertenko et al., 1998). Contrary, replacement of Ser3 to alanine prevented phosphorylation (Smertenko *et al.*, 1998; Allwood *et al.*, 2001). Analogous amino acid substitutions were introduced into *HvADF3* [Fig. 26] by PCR mutagenesis and both HvADF3 variants were cloned into the overexpression vector pUbi-nos (kindly provided by Ralph Panstruga), resulting in construct pHvADF3-S6A encoding a putatively constantly active variant and construct pHvADF3-S6D encoding a putatively constantly inactive variant.

Barley *mlo*-3 leaf epidermal cells were ballistically transfected with the respective plasmids and inoculated with *Bgh* 4 h after bombardment.

```
HvADF3        MANASSGAGIHDDCKLRFVELKSKRMHRFITYRLENQKEV        40
HvADF3-S6A    .....A.................................        40
HvADF3-S6D    .....D.................................        40


HvADF3        IVDQTGQRDATYEDFTKTLPENDCRFAVFDFDFTTPEDVP        80
HvADF3-S6A    .......................................        80
HvADF3-S6D    .......................................        80


HvADF3        KSRIFYIFWSPDTAKVRSKMTYASTNEKFKRTLDGIQIEM       120
HvADF3-S6A    .......................................       120
HvADF3-S6D    .......................................       120


HvADF3        QATDPSEISLDVIKERAH        138
HvADF3-S6A    .................        138
HvADF3-S6D    .................        138
```

Figure 26. Mutant variants of HvADF3 at serine 6.
Deduced amino acid sequence of wild-type HvADF3, a constantly active variant (HvADF3-S6A) and a constantly inactive variant (HvADF3-S6D). The alignment shows position and nature of mutations. Dots indicate identical residues.

Overexpression of the constantly active variant of *HvADF3* (HvADF3-S6A) gave rise to a significantly enhanced penetration rate compared with the overexpression of wild-type *HvADF3.* In contrast, epidermal cells expressing the putatively inactive variant of *HvADF3* (HvADF3-S6D) exhibited a significantly reduced penetration rate upon *Bgh* challenge compared with the wild-type overexpression construct [Fig. 27].

As described in Chapter 4.2.3 overexpression of wild-type *HvADF3* (pHvADF3-OE) rendered ballistically transfected cells of wild-type barley super-susceptible to *Bgh*. The putative constitutive active variant of HvADF3 apparently further enhanced the *Bgh* penetration frequency in susceptible barley cells compared with wild-type *HvADF3* [Fig. 28]. However, this effect was not statistically significant. The effect mediated by the putatively non-functional HvADF3 variant in susceptible barley leaf epidermal cells was indistinguishable from those of wild-type HvADF3.
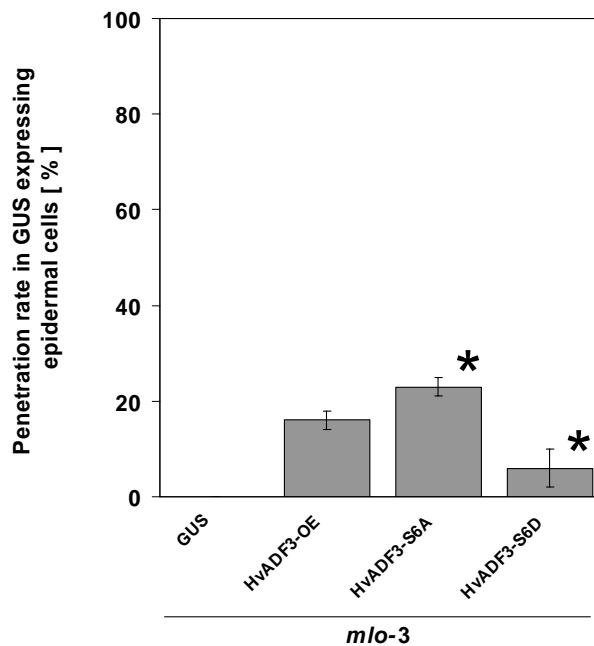
Figure 27. Overexpression of *HvADF3* variants confers enhanced *Bgh* penetration success in *mlo*-3 leaf epidermal cells.
Overexpression constructs of wild-type *HvADF3* (pHvADF3-OE), a putative constantly functional active variant (pHvADF3-S6A), and a putative constantly inactive variant (pHvADF3-S6D) were ballistically delivered in barley epidermal cells of the *mlo*-3 genotype. Inoculation with *Bgh* conidiospores (isolate K1) was performed 4 h after bombardment. Control cells were transfected only with the marker gene-expressing vector (GUS). The asterisks indicate $P < 0.05$ (Student's *t* test) compared with HvADF3-OE. Experimental procedures not explicitly mentioned are as described in Figure 12.

In conclusion, penetration rates of *Bgh* in *mlo*-3 epidermal cells individually transfected with each of the two mutated HvADF3 variants indicate that the activity of HvADF3 is likely modulated by the phosphorylation status of Ser6. However, this finding could not be unambiguously confirmed in the *Mlo* genetic background. Variations in basal susceptibility indicated by high standard deviations can not be explained but may mask potential differences between the effects mediated by single HvADF3 variants in this genotype.
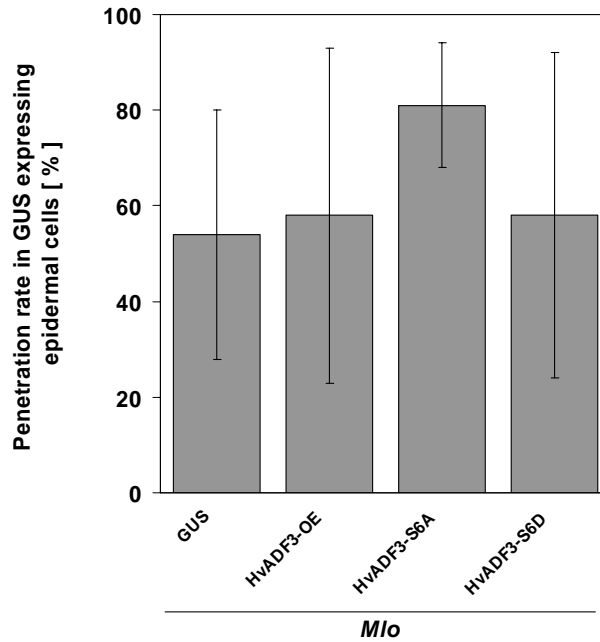
Figure 28. Overexpression of different *HvADF3* variants in *Mlo* leaf epidermal cells.
Overexpression constructs of wild-type *HvADF3* (pHvADF3-OE), a putative constantly active variant (pHvADF3-S6A) and a putatively constantly inactive variant (pHvADF3-S6D) of *HvADF3* were ballistically delivered in barley epidermal cells of a susceptible *Mlo* genotype. Inoculation with *Bgh* conidiospores (isolate K1) was performed 4 h after bombardment. Control cells were transfected only with the marker gene-expressing vector (GUS). Experimental procedures not explicitly mentioned are as described in Figure 12.

4.2.11 Actin dynamics are decisive for *forma specialis* and non-host resistance

From several pharmacological experiments it is known that actin dynamising processes contribute to resistance responses of (non-host) plants attacked by inappropriate pathogens (see Chapter 1.4). Therefore, the influence of *HvADF3* overexpression on both non-host resistance and *forma specialis* resistance was investigated.

Sporelings of *Erysiphe pisi* germinate on the surface of barley plants, but are normally not able to penetrate epidermal cells (Kobayashi *et al.*, 1997a). Barley can therefore be considered as a non-host plant with respect to *Erysiphe pisi*. Strict host specialisation of the wheat powdery mildew *Bgt* limits this fungus to the single host genus wheat and renders *Bgt* an inappropriate *forma specialis* of barley (Wyand and

Brown, 2003). The majority of attempted colonisations of *Bgt* in barley wild-type epidermal cells fail at the cell wall upon papilla formation, but occasionally spores are able to penetrate attacked non-host cells (approximately 2%) (Peterhänsel *et al.*, 1997). Despite the successful invasion of single epidermal cells and formation of haustoria, *Bgt* growth never proceeds beyond the formation of short secondary hyphae (Hückelhoven *et al.*, 2001). Interestingly, *Bgt* penetration was not observed in *mlo* barley plants (Peterhänsel *et al.*, 1997). In addition, transient overexpression of *Mlo* renders barley epidermal cells more accessible to *Bgt* (Elliott *et al.*, 2002), suggesting that the ineffective *forma specialis* resistance in barley wild-type leaves is mediated via MLO. These and other findings indicate that MLO also modulates host reactions in response to the inappropriate *forma specialis*.

To test the impact of *HvADF3* overexpression on *forma specialis* and non-host resistance, respectively, ballistically transfected *mlo*-3 and *Mlo* leaves were either inoculated with conidiospores of *Bgt* or *Erysiphe pisi.* In the *Mlo* genotype, *HvADF3* overexpression compromised penetration resistance to both powdery mildew species [Fig. 29A and Fig. 30A]. In the case of *Bgt* inoculated leaves, *HvADF3* overexpression resulted in penetration rates resembling the naturally occurring host-interaction between *Bgh* and susceptible barley [Fig. 15]. However, fungal growth was arrested at the latest after formation of short elongating secondary hyphae. These observations are reminiscent of the interaction of *Bgt* and with wild-type barley (Hückelhoven *et al.*, 2001).

In case of *Erysiphe pisi*, the penetration rate was significantly increased, although less drastic than in the *Bgt*-barley interaction. In contrast to the *Bgh* host powdery mildew fungus, enhanced *Bgt* and *Erysiphe pisi* penetration rates were not observed in *mlo* genotypes upon F-actin disruption [Fig. 29A and Fig. 30A].

A

B

Figure 29. Overexpression of *HvADF3* impairs *forma specialis* resistance in a *Mlo*-dependent manner.

(A) Barley leaf epidermal cells of two different genotypes (*mlo*-3; *Mlo*) were transfected with the *HvADF3* overexpression construct (pHvADF3-OE). 4 h after transfection leaves were inoculated with conidiospores of the wheat powdery mildew fungus, *Blumeria graminis* forma specialis *tritici* (*Bgt*). The asterisk indicates $P < 0.05$ (Student's *t* test) compared with the GUS control. Experimental procedures not explicitly mentioned are as described in Figure 12.

(B) Micrograph of a *Mlo* barley leaf inoculated with *Bgt*. The *Bgt* conidiospore **(CS)** has successfully penetrated a pHvADF3-OE-transfected barley epidermal cell **(EC)**, formed a haustorium **(H)**, and started to spread elongating secondary hyphae **(ESH)**. EC was stained for GUS reporter activity; epiphytic fungal structures were stained by Comassie brilliant blue. The scale bar in the bottom left corner represents the absolute size. The micrograph was taken 48 hpi.
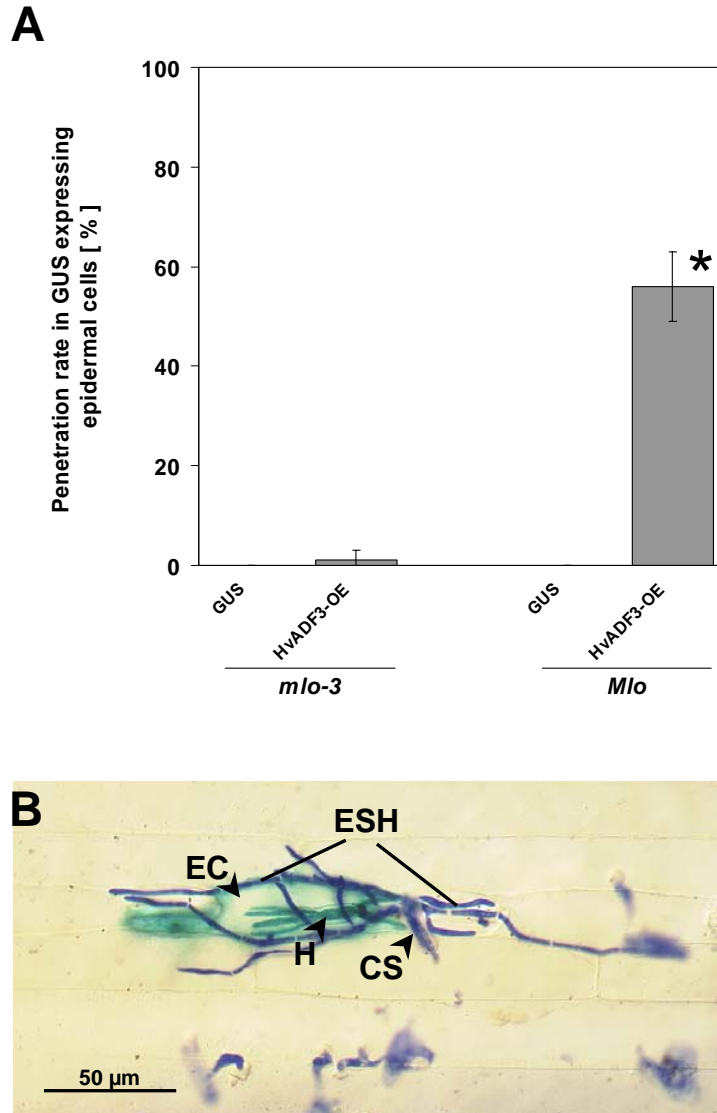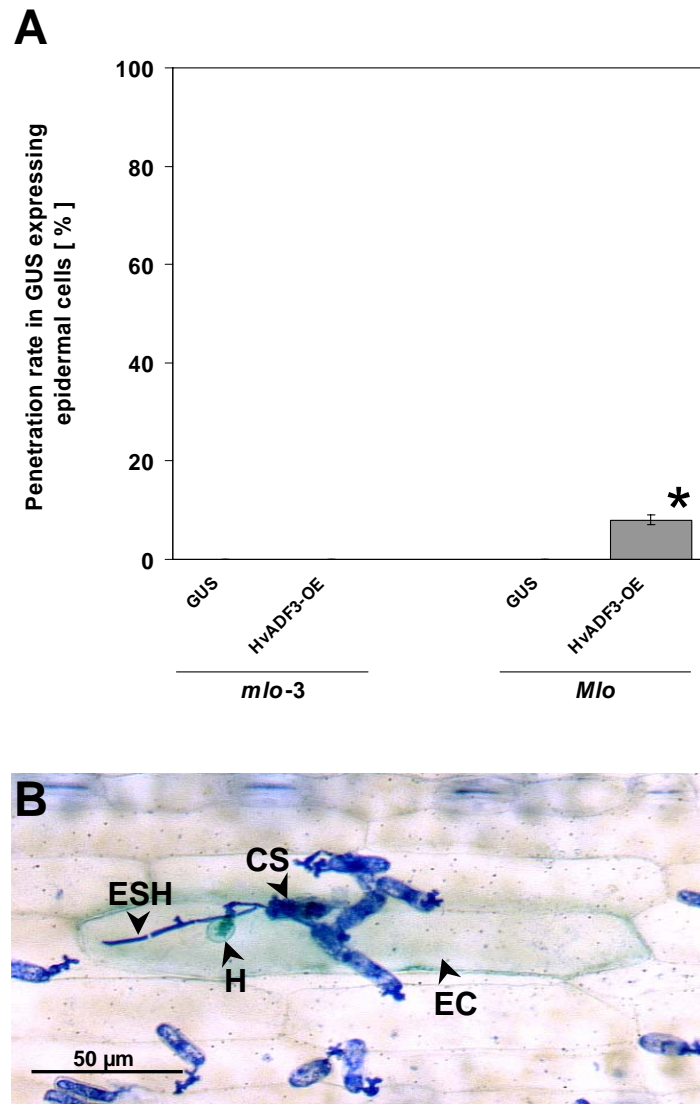
Figure 30. Overexpression of *HvADF3* impairs non-host resistance in a MLO-dependent manner.

(A) Barley leaf epidermal cells of two different genotypes (*mlo*-3; *Mlo*) were transfected with the *HvADF3* overexpression construct (pHvADF3-OE). 4 h after transfection leaves were inoculated with conidiospores of the inappropriate pea powdery mildew fungus, *Erysiphe pisi*. The asterisk indicates $P < 0.05$ (Student's *t* test) compared with the GUS control. Experimental procedures not explicitly mentioned are as described in Figure 12.

(B) Micrograph of growth of *Erysiphe pisi* on a barley *Mlo* leaf: The *Erysiphe pisi* conidiospore **(CS)** has successfully penetrated a pHvADF3-OE transfected barley epidermal cell **(EC)**, formed a haustorium **(H),** and started to spread elongating secondary hyphae **(ESH)**. EC was stained for GUS reporter activity; epiphytic fungal structures were stained by Comassie brilliant blue. The scale bar in the bottom left corner represents the absolute size. The micrograph was taken 48 hpi.

Simultaneous overexpression of a barley *Mlo* overexpression construct (pUbi-Mlo-nos NEW) and *HvADF3* in a *Mlo* null-mutant genotype confirmed the strict MLO-dependency of the compromised *forma specialis* resistance. Only epidermal cells overexpressing both genes showed *Bgt* penetration frequencies comparable to wild-type (*Mlo* genotype) barley leaf epidermal cells overexpressing *HvADF3* [Fig. 31]. Overexpression of *Mlo* was previously shown to render barley epidermal cells slightly more accessible to *Bgt* (Elliott *et al.*, 2002).
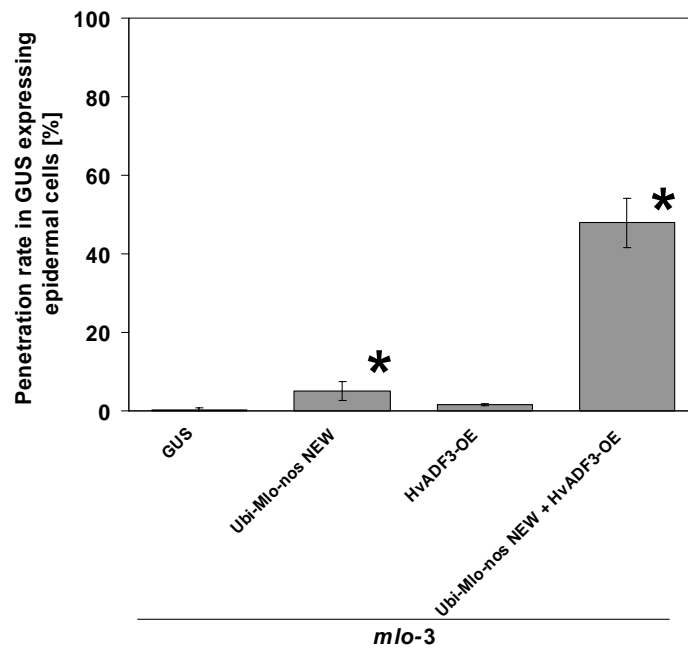
Figure 31. Overexpression of *HvADF3* compromises *forma specialis* resistance in a *Mlo*-dependent manner.
Barley leaf epidermal cells of the resistant line Ingrid (*mlo*-3) were transfected with an *HvMlo* overexpression construct (pUbi-Mlo-nos NEW); with a *HvADF3* overexpression construct (pHvADF3-OE), or with both constructs simultaneously (pUbi-Mlo-nos NEW + pHvADF3-OE). 4 h after transfection leaves were inoculated with conidiospores of the wheat powdery mildew fungus, *Blumeria graminis* f.sp. *tritici* (*Bgt*). The asterisks indicate $P < 0.05$ (Student's *t* test) compared with GUS. Experimental procedures not explicitly mentioned are as described in Figure 12.

4.2.12 Alteration of HvADF3 protein levels does not interfere with race-specific resistance

Overexpression of *ADF* in transgenic *Arabidopsis* lines resulted in morphological abnormalities but not in plant lethality (Dong *et al.*, 2001a). In yeast it was demonstrated that overexpression of *ADF* reduced cell viability (Iida and Yahara, 1999). Although plant cells remain alive, disruption of the actin cytoskeleton putatively interferes with a plethora of intracellular functions. Partially compromised *Mlo* or *mlo* resistance could therefore be an unspecific consequence of the perturbation of essential cellular processes. This would presumably affect other cell defence responses as well. One way to investigate this possibility was to test the efficiency of race-specific resistance to *Bgh* upon *HvADF3* overexpression.
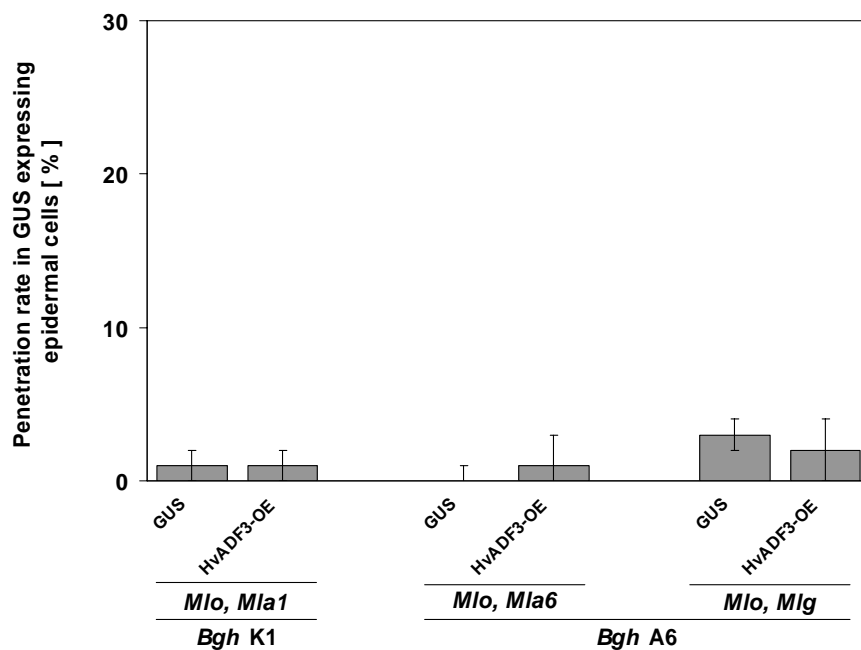
Figure 32. Overexpression of *HvADF3* does not impair race-specific resistance.
The *HvADF3* overexpression construct pHvADF3-OE was ballistically delivered in epidermal cells of three different barley genotypes comprising distinct race-specific resistance specificities, conferred by the equivalent *R* genes *Mla1, Mla6* and *Mlg*. 4 h after transfection of HvADF3-OE into epidermal cells, leaves were inoculated with conidiospores of the appropriate powdery mildew fungal isolates containing the *R* gene-matching *Avr* genes (*Bgh* K1 *AvrMla1*; *Bgh* A6 *AvrMla6* and *AvrMlg*). Results were compared with control cells transfected with the reporter gene expressing vector (GUS), only. Experimental procedures not explicitly mentioned are as described in Figure 12.

HvADF3-OE transfected epidermal cells of barley genotypes containing race-specific *R* genes were inoculated with *Bgh* isolates harbouring matching *Avr* genes. All tested race-specific resistances, namely *Mla1 / Bgh* isolate K1 (*AvrMla1*), *Mla6 / Bgh* isolate A6 (*AvrMla6*) and *Mlg / Bgh* isolate A6 (*AvrMlg*) (Görg *et al.*, 1993; Halterman *et al.*, 2001; Zhou *et al.*, 2001), were able to prevent fungal ingress. No significant differences could be observed by comparison of pHvADF3-overexpressing cells to control cells [Fig. 32]. Consequently, interference with the actin cytoskeleton upon *HvADF3* overexpression does not cause substantial perturbation of race-specific powdery mildew resistance, suggesting that the tested race-specific resistances functions independently of an intact actin cytoskeleton.

Additionally, pharmacological experiments were conducted to validate the actin cytoskeleton independence of barley race-specific powdery mildew resistance. Cytochalasin E interferes with the polymerisation of actin filaments and was previously shown to compromise non-host resistance to *Erysiphe pisi* in barley coleoptile cells (Kobayashi *et al.*, 1997a). Application of the drug to broad-spectrum resistant barley leaves (*mlo*-3) mimics the effect of overexpressing *HvADF3* by rendering epidermal cells accessible to *Bgh* [Fig. 33]. However, consistent with the findings of *HvADF3* overexpression, cytochalasin E does not impede race-specific resistance, corroborating the finding that actin dynamics are pivotal in broad-spectrum resistance and basal defence but are dispensable for race-specific resistance.

Furthermore, two well-characterised compounds known to depolymerise microtubules, oryzalin and propyzamid (Mathur *et al.*, 2002), were tested. Disruption of microtubules by oryzalin was previously shown to partially impair non-host resistance of barley coleoptile epidermal cells to *Erysiphe pisi* (Kobayashi *et al.*, 1997a). In contrast, application of these drugs apparently did not interfere with broad-spectrum resistance or race-specific resistance in barely leaf epidermal cells [Fig. 33]. Therefore, it was concluded that microtubules seemingly do not contribute to *Mlo-* or *mlo*-mediated defence processes and race-specific resistance. Nevertheless, inefficient infiltration of the drugs into leaf epidermal cells and/or a rapid metabolic turnover of the compounds cannot be excluded.
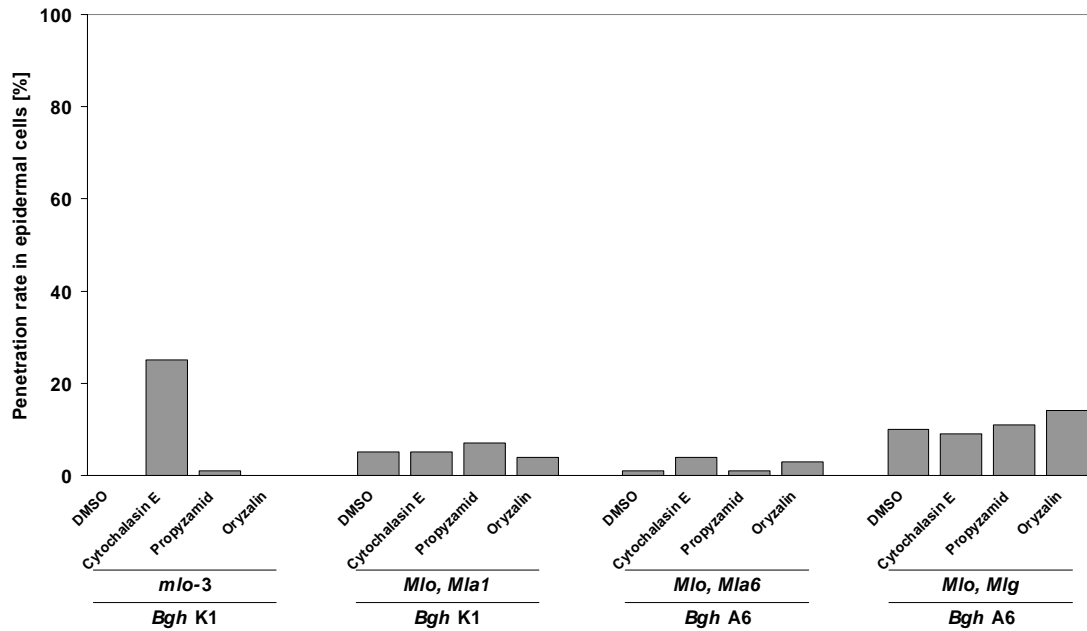
Figure 33. Cytochalasin E treatment resembles the enhanced *Bgh* penetration rate caused by overexpression of *HvADF3*.

mlo-3 null mutant barley leaves with abaxially peeled off epidermis were vacuum infiltrated for 10 minutes with solutions containing the following drugs: Cytochalasin E (5 µg ml^{-1}), propyzamid (15 µM) or oryzalin (30 µM). The drug solvent DMSO (0.25%(v/v)) served as an internal control. 1 hour after infiltration the leaf segments were adaxially inoculated with *Bgh* (isolate K1).

Leaves were microscopically evaluated 48 h after inoculation for the presence of fungal secondary hyphal growth serving as a marker for successful penetration by the powdery mildew fungus.

Additionally, the influence of the respective drugs on race-specific resistance mediated by the *R* genes *Mla1, Mla6 and Mlg* in combination with the appropriate fungal isolate *Bgh* K1 or *Bgh* A6 harbouring the *R* gene-matching *Avr* genes (*AvrMla1, AvrMla6 and AvrMlg*) was tested. The experiments were repeated once and showed similar results.

To test the influence of the pharmacological perturbation of actin filaments and microtubules on callose deposition in CWAs (see Chapter 4.2.6) drug-treated *mlo*-3 leaves were stained with the aniline blue fluorochrome after *Bgh* inoculation. Leaves treated with propyzamid, oryzalin (data not shown), or the solving agent DMSO [Fig. 34B] showed accumulation of callose at all sites of penetration attempts. Nevertheless, callose-derived fluorescence was weak in case of oryzalin treatment. In comparison, less than 30% of resistant cytochalasin E-treated epidermal cells showed callose deposition. Similar to the *HvADF3* overexpression experiment [Fig. 20B], successfully penetrated cells showed faint fluorescence at more than 50% of all successful interaction sites [Fig. 34A].
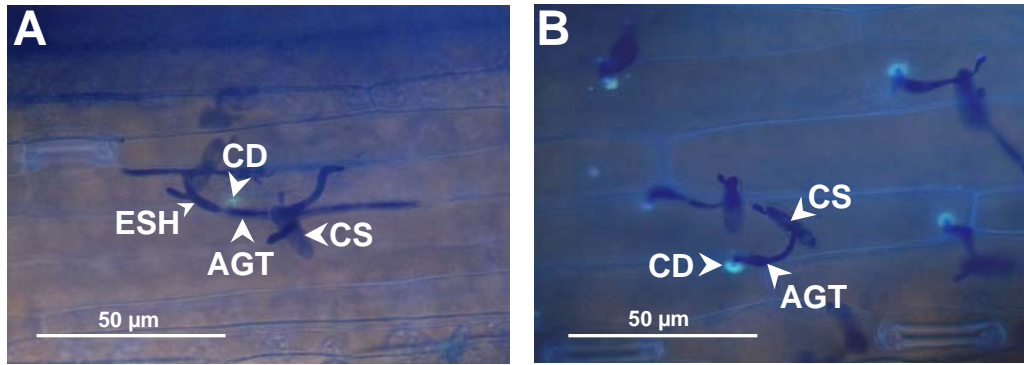
Figure 34. Callose staining in cytochalasin E-treated epidermal cells upon successful penetration.
Resistant (*mlo*-3) barley leaves of cultivar Ingrid were treated with cytochalasin E (5 µg ml^{-1}) **(A)** or DMSO (0.25%(v/v)) **(B)**. Leaves were inoculated with *Bgh* conidiospores 1 h post vacuum infiltration of drug-containing solutions. Callose deposition **(CD)** subtending appressorial germ tube **(AGT)** of *Bgh* conidiospores **(CS)** was subsequently stained by aniline blue 48 hpi. Elongating secondary hyphae **(ESH)** served as marker for successful host cell penetration by *Bgh*. Micrographs show an overlay of UV excited aniline blue fluorochrome-fluorescence of papillae and bright-field microscopy of Comassie brilliant blue stained epiphytic fungal structures, analysed by using a Zeiss Axiophot microscope. The scale bars in the bottom left corners represent the absolute size.

Similar results were obtained with pharmacologically treated barley leaves, harbouring the resistance gene *Mla1* (Zhou *et al.*, 2001) that mediates effective resistance against *Bgh* isolate K1 (*AvrMla1*). Callose depositions underneath *Bgh* appressorial germ tubes were present in all leaves treated with the microtubule-disrupting drugs. Again, the callose-derived fluorescence of oryzalin-treated leaves was weak compared with untreated leaves. Although callose deposition was visible in less than 30% of all evaluated interactions, race-specific resistance was not impaired by cytochalasin E treatment, suggesting that callose deposition is not required for mounting race-specific immunity.

Independently of the applied microtubule polymerisation inhibitor, most attacked cells showed a whole-cell callose accumulation, which is likely indicative of typical race-specific HR-like cell death (Dangl and Jones, 2001; Jacobs *et al.*, 2003). In contrast, cytochalasin E-treated cells only occasionally exhibited a weak auto-fluorescence, which was confined to cell margins [Fig. 35], suggesting that the majority of the cells, though still resistant, apparently did not react with a hypersensitive response/cell death. In conclusion, barley race-specific resistance does seemingly not require actin dynamics or microtubules. Consequently, barley race-specific immunity likely acts

independently of HR/cell death, since actin filaments seem to be essential for the execution of a hypersensitive cell death (Hazen and Bushnell, 1983).
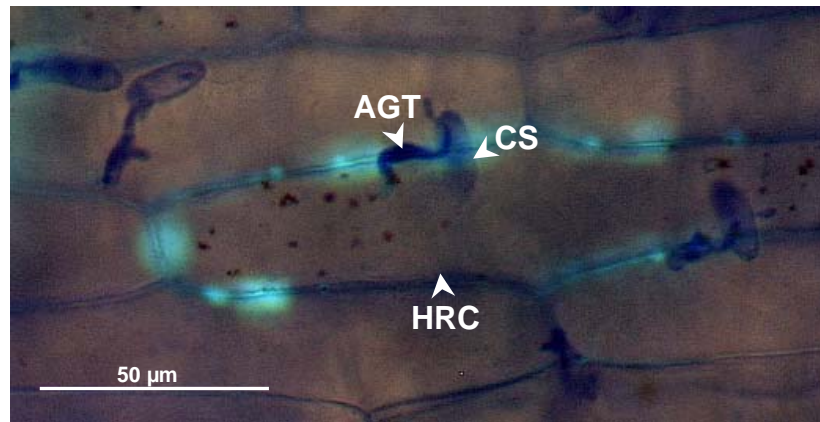
Figure 35. Perturbation of actin dynamics interferes with the HR of race-specific resistance.
Barley leaves of line Pallas01 (carrying the race-specific *R* gene *Mla1*) were treated with cytochalasin E (5 µg ml^{-1}). Leaves were inoculated with *Bgh* conidiospores (isolate K1) 1 h post vacuum infiltration of the drug-containing solution. Leaves were subsequently stained for callose with the aniline blue fluorochrome 48 hpi. **(AGT)** appressorial germ tube; **(CS)** *Bgh* conidiospore. The micrograph shows an overlay of UV-excited weak auto-fluorescence of an HR-expressing cell **(HRC)** and bright-field microscopy of Comassie brilliant blue-stained epiphytic fungal structures, analysed by using a Zeiss Axiophot microscope. The scale bar in the bottom left corner represents the absolute size.

4.2.13 Host actin dynamics – a pivotal factor for the maintenance of fungal biotrophy

The role of actin microfilament dynamics in plant-microbe interactions is not necessarily confined to plant defence processes at the host cell penetration stage. The pea powdery mildew fungus, *Erysiphe pisi*, rearranges the host actin cytoskeleton to close proximity of the fungal haustorium in successfully colonised pea epidermal cells (Green *et al.*, 2002). The actin cytoskeleton is thought to facilitate intracellular transport processes for funnelling host-derived nutrients to the haustorium.

Perturbing actin dynamics by *HvADF3* overexpression is sufficient to allow cell wall penetration and initial hyphal growth of *Bgh* in transfected barley *mlo*-3 cells. However, time-course experiments revealed that hyphal growth of sporelings exclusively penetrating transfected cells ceased at latest 3 days post inoculation,

suggesting that maintenance of fungal biotrophy requires intact host actin dynamics in the *Bgh*-barley interaction [Fig 36A].
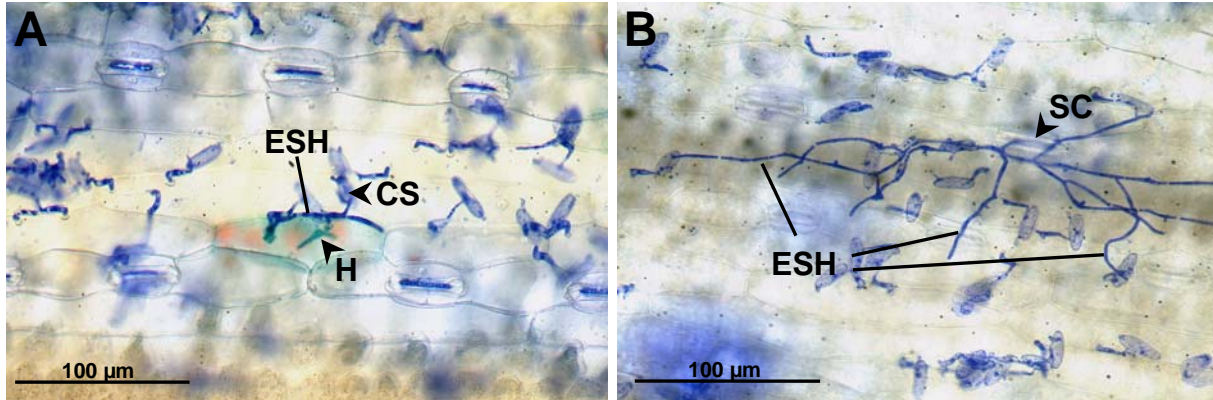
Figure 36. Retarded secondary hyphal growth in barley epidermal cells transfected with a constantly active variant of *HvADF3*.
    (A) Successful penetration and subsequent haustorium **(H)** formation of a *Bgh* conidiospore **(CS)** in a *mlo*-3 genotype epidermal barley cell which was ballistically transfected with the constantly active *HvADF3* overexpression construct (pHvADF3-S6A) and a GUS expressing plasmid, serving as a marker for successful transformation. Epiphytic fungal structures were highlighted by Comassie brilliant blue.
    (B) Elongating secondary hyphae **(ESH)** of a single *Bgh* conidiospore after successful penetration of a non-transfected stomatal cell **(SC)** of a *mlo*-3 leaf.
The scale bars in the bottom left corners represent absolute sizes. All micrographs were taken 72 hpi.

Restricted hyphal growth in pHvADF3-S6A-transfected cells was often masked by the subsequent colonisation of non-transfected subsidiary stomatal cells by elongating secondary hyphae [Fig 36B]. Due to the distinct cytology of stomatal cells (Lin and Edwards, 1974), the fungal pathogen was then able to efficiently form secondary haustoria (Lin and Edwards, 1974) seemingly accounting for hyphal growth maintenance. However, the susceptibility of stomatal cells can serve as an internal control for secondary hyphal growth in otherwise resistant *mlo* leaves.

Bombardment of barley wild-type leaves with the *HvADF3* overexpression construct demonstrated that arrest of fungal growth most likely resulted from impaired actin dynamics, independently of *mlo*-mediated resistance.
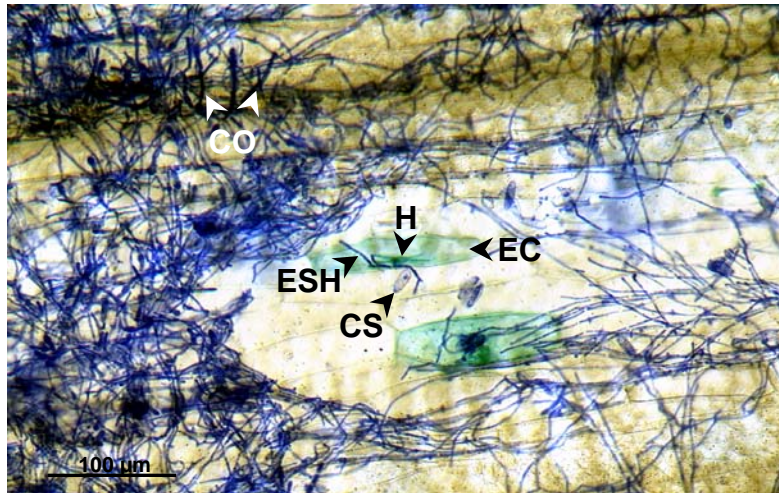
Figure 37. Impairment of fungal growth on barley *Mlo* leaves upon disruption of the actin cytoskeleton by *HvADF3* overexpression.

Barley leaves of the cultivar Golden Promise (*Mlo*) were ballistically transfected with the *HvADF3*-overexpressing construct pHvADF3-OE. Leaves were inoculated with *Bgh* conidiospores 4 h post transfection. The *Bgh* conidiospore **(CS)** has successfully penetrated a pHvADF3-OE-transfected barley epidermal cell **(EC)**, formed a haustorium **(H),** and started to spread elongating secondary hyphae **(ESH)**. *Bgh* conidiospores that penetrated untransfected cells were able to differentiate conidiospores **(CO)**. EC was stained for GUS reporter activity; epiphytic fungal structures were stained by Comassie brilliant blue. The scale bar in the bottom left corner represents the absolute size. The micrograph was taken 96 hpi.

In this scenario, fungal growth of transfected *HvADF3*-overexpressing cells was significantly reduced, illustrated by the highly retarded growth of elongating secondary hyphae 96h after inoculation. *Bgh* spores that colonised untransfected susceptible epidermal cells were able to cover the leaf surface with mycelium and developed conidiophores, which indicated that the fungus was able to complete its asexual life-cycle [Fig. 37].

4.3   Discussion

Many forward or reverse genetic screens conducted in plant science identified genes implicated in a variety of biological processes. The success of such genetic screens strongly depends on the simplicity and specificity of the biological read-out. For example, subtle mutation-induced effects on specific processes are often missed due to variability of the read-out by various parameters. Consequently, many genes were identified by the drastic effect caused by the respective mutants. This qualitative

read-out strategy is generally the most straightforward approach for successful gene identification. It was, for example, applied in a recent VIGS screen (Lu *et al.*, 2003a) for impaired disease resistance in pathogen-challenged tobacco plants (Lu *et al.*, 2003b). The screening procedure was simple because appearance or lack of HR was chosen as a read-out parameter resulting in more than 70 candidate plants after evaluation of approximately 5000 mutants. Closer inspection ultimately identified four different genes with the desired impact on disease resistance (Lu *et al.*, 2003b). Nevertheless, the pre-selection strategy involving an easily scorable trait (presence / absence of HR) facilitated the overall procedure. Another example for the qualitative read-out strategy is the identification of the six *pmr* complementation groups among 26.000 screened M2 e̲thyl m̲ethanes̲ulfonate (EMS) mutant *Arabidopsis* plants (Vogel *et al.*, 2002). In this approach, absence of macroscopically visible disease symptoms by the virulent pathogen *Erysiphe cichoracearum* on mutagenised plants was scored.

In contrast to this, a quantitative read-out was applied in the reverse screening strategy of the present study by utilising transient dsRNAi-mediated silencing of genes (Fire *et al.*, 1998; Tijsterman *et al.*, 2002) in combination with a single cell assay in barley (Nielsen *et al.*, 1999; Shirasu *et al.*, 1999; Schweizer *et al.*, 2000). Here, the highly efficient powdery mildew resistance of barley *mlo* mutants (Jørgensen, 1992) was exploited to screen for impaired broad-spectrum resistance. The microscopic evaluation process should allow identification of mutant phenotypes that would be likely missed in conventional genetic screens based on macroscopic scoring.

Screening of approximately 700 constructs did not result in the identification of an ihpRNA vector impairing *mlo* resistance by gene silencing. However, since the number of tested constructs (~ 6% of all available epidermal cDNA clones) was comparatively low, this result provides no evidence for the general inefficiency of the screen. In contrast to the results of this study, selection of epidermal cDNA library clones of genes that were transcriptionally upregulated upon pathogen challenge led to the identification of three candidate genes (partially) compromising *mlo* resistance (Patrick Schweizer, personal communication). However, a potential disadvantage of the pre-selection procedure compared to an unbiased approach is the likely miss of genes that contribute to resistance but are not differentially expressed.

Alterations in basal defence in *Mlo* genotypes upon PTGS were chosen as a second read-out in this study. During this screen it became apparent that natural variability in the susceptibility of *Mlo* leaf material that occurred independently of PTGS complicated the assessment of PTGS-mediated effects. In several cases, candidate clones initially selected because of altered infection phenotypes had to be discarded after independent repetitions. Therefore, it remains questionable if screens that require time-consuming sample evaluation processes are sensible if the read-out is based on comparatively small quantitative differences.

Unaware of the fact that an ihpRNA vector might trigger overexpression of inserted full-size coding regions, two constructs impairing *mlo*-mediated resistance were identified in the PTGS screening process. Both identified ihpRNA constructs contained cDNAs encoding the barley actin depolymerising factor HvADF3. ADFs are involved in actin filament dynamising process (Bamburg, 1999; Maciver and Hussey, 2002; Dos Remedios *et al.*, 2003). Expression of the originally identified "silencing" construct and overexpression of *HvADF3* both resulted in disruption of actin cytoskeleton architecture [Fig. 17B and C]. This surprising finding does not conform with proposed functions of ADFs (Carlier, 1998; Maciver and Hussey, 2002). Detailed analysis of the *HvADF3* pUAMBN-based ihpRNA construct revealed that enhanced *Bgh* penetration rates of ballistically transfected epidermal barley cells were most likely conferred by undesired overexpression of the gene. Responsible for this effect was presumably the disadvantageous combination of the topology of GATEWAY® cloning cassettes in pUAMBN and the inserted full-size coding region of *HvADF3*. Application of the ihpRNA vector pUAMBN-i instead of pUAMBN (see Chapter 3.2.1) will circumvent this problem in future and further optimise the PTGS screen.

While the genomes of most vertebrates encode only one ADF isoform and two cofilins, plants possess a large number of ADF genes (Maciver and Hussey, 2002). The multitude of ADF genes *in planta* may partially compensate for the lack of some factors known to regulate vertebrate ADF function, e.g. LIM kinases (Gungabissoon and Bamburg, 2003). Additionally, the surplus of ADFs in plants suggests that distinct ADF isoforms specifically controll actin-dependent biological processes. Isoform-specific functions have been proposed for two ADF isoforms of *Caenorhabditis elegans* (Ono *et al.*, 2003). However, in contrast to effects provoked by gene

silencing, enhanced epidermal cell accessibility to *Bgh* attack upon *HvADF3* overexpression is not necessarily indicative of an isoform-specific function in barley disease resistance. *Arabidopsis* ADFs are known to bind *in vivo* to cytosolic F-actin in a range of heterologous plant species. Binding of ectopically expressed ADF proteins resulted in a reduction of the number and/or the length of actin filaments (Dong *et al.*, 2001a) Therefore, different *Arabidopsis ADFs* and barley *HvADF6* were individually overexpressed in barley epidermal cells to clarify whether HvADF3 possesses unique actin-dynamising properties possibly implicated in defence against powdery mildew. The experiments revealed enhanced *Bgh* penetration rates triggered by *HvADF6* and six different *Arabidopsis ADF* isoforms, corroborating the assumption that HvADF3, at least when overexpressed, is not specifically implicated in barley defence mechanisms. In general, ectopic *ADF* expression seems to unspecifically interfere with actin-dependent processes, since AtADFs that are likely restricted to pollen tube or root tip tissue, like AtADF7 and AtADF5, respectively (Dong *et al.*, 2001a; Maciver and Hussey, 2002) and therefore proposed to be functionally distinct (Hussey *et al.*, 2002), also trigger enhanced *Bgh* penetration (see Chapter 4.2.9). N-terminal fusion of YFP to two of the three *Arabidopsis* ADFs that were apparently non-functional in the pathogen assay likely resulted in stabilisation of the proteins. Translational fusions of AtADF3 and 4 fusions to YFP were capable of impairing actin dynamics, whereas no function was found for AtADF9 in the available experimental assays (see Chapter 4.2.9). Impaired protein stability in the heterologous system could be the reason for the apparent lack of AtADF9 functionality.

ADF overexpression may represent a potentially valuable genetic tool that might be exploited for studies concerning the requirement of an intact actin cytoskeleton in distinct biological processes. Moreover, the generation of ADF-overexpressing transgenic plants would lead to reliable interference with the actin cytoskeletons in all cell types of the transgenic line. This would provide an advantage compared to investigations exploiting pharmacological drugs for interference with actin architecture, since drug application via infiltration might be heterogeneous. Another advantage is the specificity of ADFs for F-actin, since potential side effects of the drugs can generally not be excluded. Moreover, in plant-microbe interactions genetic interference provides the advantage of selective interference with the host, whereas pharmacological inhibition is not selective and might also affect the pathogen.

Results obtained in overexpression experiments do not exclude a contribution of HvADF3 in defence processes that might be manifested by differential gene expression or posttranslational protein modification. According to the real-time PCR results shown in Chapter 4.2.10, *HvADF3* does not seem to be differentially expressed upon pathogen challenge. Negative results, however, do not unequivocally exclude pathogen-induced alterations of *HvADF3* transcript levels. cDNA samples used in this study were generated from *Bgh*-inoculated epidermal tissue which contained comparably few cells that had been attacked by fungal sporelings. The background arising from surrounding unchallenged tissue may mask potential alterations of transcript levels caused upon powdery mildew attack. Transcript analysis of individual cells, e.g. on the basis of laser microdissection (Asano *et al.*, 2002), might provide a more sensitive approach to study changes of transcript levels in response to pathogen challenge (Gjetting *et al.*, 2004).

Alternatively or additionally to transcriptional regulation, HvADF3 may be regulated at the post-translational level. It has been shown that similar to vertebrate ADFs the phosphorylation status of a serine at position 6 is decisive for the *in vitro* activity of a maize ADF isoform (Smertenko *et al.*, 1998). However, presence of Ser6 does not necessarily indicate a phosphorylation-dependent regulation of an ADF (Allwood *et al.*, 2002). In the case of *HvADF3*, mutation of the putative phosphorylation site resulted in an increase of ADF activity as evidenced by a raise in the *Bgh* penetration rate. Likewise, mimicking a phosphorylation event reduced HvADF3 functionality (see Chapter 4.2.10) similar to previous observations in vertebrates and plants (Agnew *et al.*, 1995; Smertenko *et al.*, 1998). These findings suggest that HvADF3 activity is regulated by reversible phosphorylation. Moreover, it can be concluded that at least part of the overexpressed wild-type HvADF3 is likely to exist in the less-active phosphorylated state.

Despite unsuccessful loss-of-function experiments, detailed analysis of the impact of HvADF3 overexpression allowed conclusions about the role of the actin cytoskeleton in barley defence against different fungal pathogens.

It was previously shown that pharmacological disruption of F-actin impaired callose deposition underneath appressorial germ tubes of attacking *Bgh* conidiospores (Kobayashi *et al.*, 1997b). Overexpression of *HvADF3* also resulted in considerably diminished amounts of callose at penetration sites corroborating the proposed F-actin

dependence of focal callose deposition. Callose accumulates in CWAs of both *Mlo* as well as *mlo* barley genotypes (Aist and Israel, 1986). Interestingly, both *HvADF3* overexpression and application of actin-disrupting drugs (see Chapters 4.2.6 and 4.2.12) frequently resulted in faint fluorescence at the infection sites of successfully penetrated *mlo* epidermal cells. This may indicate that at least some deposited callose might be required for successful cell wall penetration. Contrary to this assumption, residual callose accumulation beneath attempted fungal penetration sites in an *Arabidopsis* line defective in a callose synthase gene coincided with reduced susceptibility to a virulent powdery mildew pathogen (Jacobs *et al.*, 2003; Nishimura *et al.*, 2003). However, also wound-induced actin-independent deposition of callose at disrupted cell walls upon appressorial germ tube penetration might account for the observed fluorescence (Stone and Clarke, 1992). It is not likely that depositions of residual callose upon *HvADF3* overexpression or drug application is the simple consequence of incomplete disruption of the cytoskeleton, since faint aniline blue-derived fluorescence was only observed at successful penetration sites.

The finding that *forma specialis* and non-host resistance were compromised by *HvADF3* overexpression in a *Mlo*-dependent manner was unexpected, but is consistent with previous reports that MLO also functions in *forma specialis* resistance of barley against *Bgt* (Peterhänsel *et al.*, 1997; Elliott *et al.*, 2002).

The virulent powdery mildew fungus *Bgh* is assumed to modulate host-defence mechanisms via MLO to gain access to barley epidermal cells (see Chapter 1.2.1.2). According to the results of this work, MLO may negatively control actin-dependent and actin-independent defence mechanisms [Fig. 38A]. Due to an apparent incomplete suppression of the actin cytoskeleton-based defence mechanisms via MLO, disruption of filamentous actin in *Mlo* genotypes results in enhanced penetration [Fig. 38B]. It is conceivable that the virulent *Bgh* fungus has evolutionarily at least partially adapted to the subset of defence mechanisms that are controlled via MLO but do not require the actin cytoskeleton. This might explain why in the case of *Bgh* sole interference with actin-based defence processes is sufficient to allow enhanced penetration in *mlo* genotype cells [Fig. 38C].

Concerning the wheat powdery mildew fungus *Bgt*, it was previously demonstrated that *mlo*-mediated resistance is also effective against penetration by the

inappropriate pathogen (Peterhänsel *et al.*, 1997). Apparently *Bgt* also exploits regulatory functions of MLO to suppress defence mechanisms in order to try to gain access to cells of the non-host genus barley (Elliott *et al.*, 2002), but in contrast to *Bgh* appears to have evolutionary-conditioned deficiencies to modulate actin-based defence processes via the heterologous barley MLO protein [Fig. 38D].
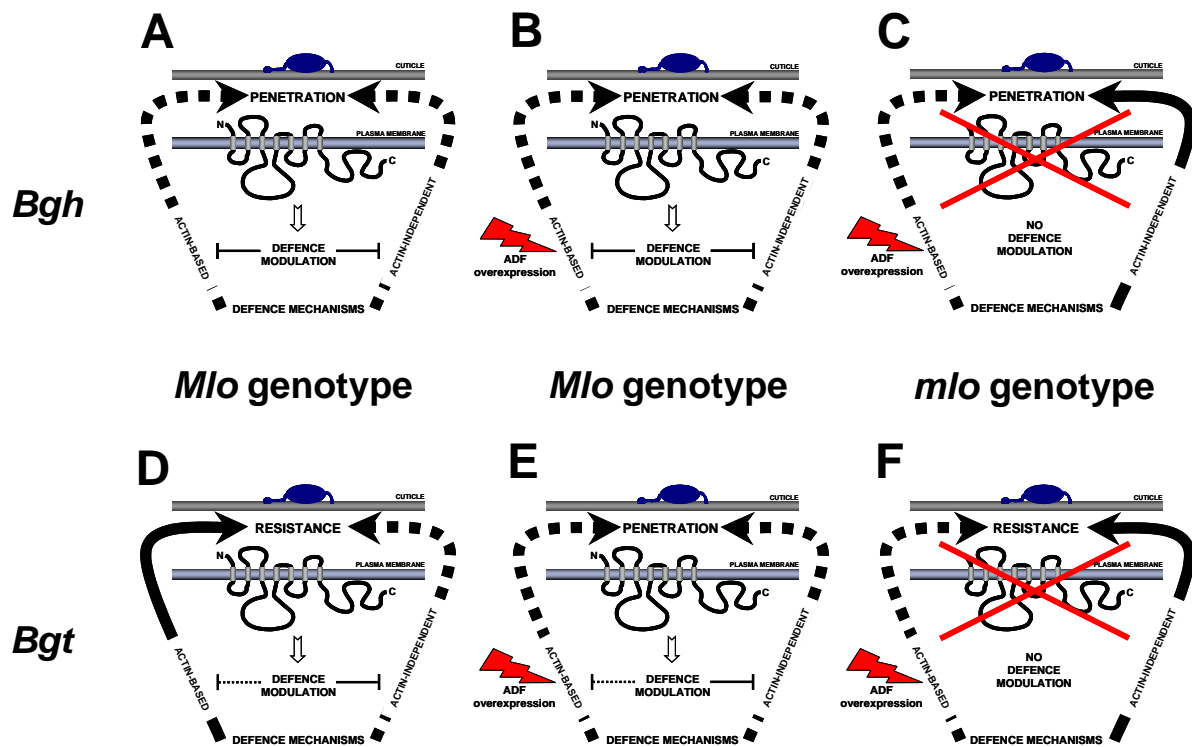
FIGURE 38. Model of the MLO-dependency of host and *forma specialis* defence mechanisms.
The 7-TM MLO protein (represented by the bended black line; light grey boxes symbolise transmembrane helices) is localized in the plasma membrane. A powdery mildew conidiospore is depicted as blue structure on the cuticle. The cell wall is depicted as green area. Red arrows indicate actin cytoskeleton interference upon ADF overexpression. Solid or dashed black arrows represent strong or weak efficiency of defence mechanisms, respectively. **A-C** illustrate the interaction between barley of a *Mlo* (A +B) or *mlo* (C) genotype and the virulent *Bgh* pathogen, **D-E** illustrate the interaction between a barley *Mlo* (A+B) or *mlo* (C) genotype and the inappropriate *Bgt* pathogen.

Hence, *Bgt* cannot acquire entrance to epidermal cells of barley *Mlo* genotypes. This may explain why F-actin disruption in combination with MLO-based manipulation of further defence mechanisms results in enhanced penetration efficiency of *Bgt* in barley non-host cells [Fig. 38E]. As mentioned above, for this model it has to be assumed that *Bgh* is evolutionarily adapted to a subset of MLO-suppressible defence mechanisms [Fig. 38C], whereas *Bgt* is strictly subjected to MLO-controlled defence

mechanisms [Fig. 38D and E]. This would mean that loss of MLO-dependent defence modulation (e.g. in *mlo* genotypes) is sufficient to terminate *Bgt* attacks despite successful interference with actin-based defence mechanisms [Fig. 38F].

The same model may also apply for *Erysiphe pisi*. Phylogenetic relationships of *Bgt* and *Erysiphe pisi* to *Bgh* (Wyand and Brown, 2003) might explain the significant difference in penetration rates between the two inappropriate pathogens upon disruption of the actin cytoskeleton (Fig. 29A and Fig. 30A). It is assumed that *Blumeria graminis* only recently separated into the *formae speciales hordei* and *tritici*. Thus, both *formae speciales* did not co-evolve with their respective cereal hosts (Wyand and Brown, 2003). Strict diversification of *Blumeria graminis* into *formae speciales* with extremely narrow host-ranges is rather unusual in an evolutionary context. The close phylogenetic relationship between *Blumeria graminis* f. sp. *hordei* and *tritici* possibly enables successful *Bgt* ingress into barley epidermal cells that are compromised in F-actin-dependent defence mechanisms and might also account for the higher penetration efficiency compared with the dicot pathogen *Erysiphe pisi*.

Even though rearrangement of actin filaments towards sites of pathogenic attack in race-specific resistance was observed in the interaction of *Arabidopsis* with the oomycete pathogen *Peronospora parasitica* (Takemoto *et al.*, 2003), no specific function for the actin cytoskeleton in *R* gene-mediated resistance has been reported so far. Pharmacological and genetic experiments testing the impact of impaired focal F-actin rearrangements on the efficiency of several barley race-specific resistances revealed that this kind of defence mechanism might generally act independently of the actin cytoskeleton (see Chapter 4.2.12). These experiments together with the finding that *Bgt* and *Erysiphe pisi* penetrate in barley non-host cells in a MLO-dependent manner demonstrate that absence of the actin cytoskeleton does not generally interfere with all defence mechanisms in barley.

Mlg-specified race-specific resistance, like *mlo* resistance, arrests fungal penetration attempts at sites of papilla formation (Görg *et al.*, 1993). However, unlike *mlo* resistance, MLG-controlled resistance proved functional upon interference with the actin cytoskeleton. This finding suggests distinct requirements of actin dynamics in broad-spectrum and race-specific *Mlg* resistance despite the temporal and spatial correlation of papilla formation in both types of resistance. Additionally, it could be

demonstrated that disruption of actin cytoskeleton architecture seemingly interferes with whole-cell callose accumulation (a likely indicator of cell death) in race-specific interactions in barley (see Chapter 4.2.12). Compromised HR-like cell death upon pharmacological disruption of the actin cytoskeleton was also reported in the interactions of barley coleoptiles with an avirulent *Bgh* isolate (Hazen and Bushnell, 1983) and cowpea (*Vigna unguiculata*) with the cowpea rust fungus *Uromyces vignae* (Skalamera and Heath, 1996; Skalamera and Heath, 1998).

The phenotype of *HvADF3* overexpression differs from those of the two *mlo ror* mutants since *mlo ror* genotypes are partially susceptible (Freialdenhoven *et al.*, 1996), whereas *HvADF3* overexpression enhanced *Bgh* penetration rates only. In phytopathology, the term "susceptibility" is used to indicate a completed asexual life-cycle of a pathogen on a host plant. Growth of *Bgh* on HvADF3-OE transfected leaf epidermal cells was delayed after haustorium differentiation and the formation of short secondary hyphae. Different factors might account for the observed retarded development of epiphytic fungal structures. Obligate biotrophic fungal pathogens likely redirect host cell physiology to their own benefit (Murphy *et al.*, 1997). *Bgh*, for example, is supposed to actively suppress senescence of colonised cells and subtending mesophyll tissue to maintain biotrophy (Schulze-Lefert and Vogel, 2000). Additionally, haustoria of *Erysiphe pisi* have been shown to be in close proximity to the host actin cytoskeleton (Green *et al.*, 2002). It is conceivable that actin cytoskeleton-based transport processes towards the fungal feeding organ are exploited to facilitate uptake of intracellular host metabolites. Impairment of the presumed actin transport tracks would consequently lead to an insufficient nutrient supply for the fungus, finally resulting in cessation of fungal growth. Alternatively, F-actin disruption may cause pleiotropic effects impairing intracellular metabolic processes to an extent that prevent a sufficient nutrient supply for the fungus.
Notably, it can be excluded that cell death causes retarded fungal growth. Successful host cell entry in *HvADF3* overexpression experiments in which cells were inoculated with *Bgh* as late as 96 h after bombardment (data not shown) indicates that actin cytoskeleton disruption does not cause plant cell lethality at late time points. It was shown that 48 h after *HvADF3* overexpression phalloidin-stainable actin filaments were undetectable in transfected cells (see Chapter 4.2.4). A prolonged incubation period (96 h) before inoculation might presumably result in the complete absence of

the actin cytoskeleton. Successful penetration at this late time point is indicative of cell viability since the obligate biotrophic powdery mildew fungus can only colonise living plant tissue. Moreover, GUS staining successfully performed after 48 h of fungal growth (144 h post transfection) further corroborates that transfected cells are still alive. Absence of cell death upon transient *ADF* overexpression is consistent with findings about *ADF* overexpression in transgenic *Arabidopsis* lines (Dong *et al.*, 2001a).

Interestingly, Yun and colleagues reported that *Bgt* occasionally sporulates on cytochalasin E-treated non-host *Arabidopsis* plants harbouring a mutation in the *EDS1* gene (Yun *et al.*, 2003). These findings appear contradictory to the results of this work, which suggest an essential role for the host-actin cytoskeleton for the maintenance of biotrophic fungal growth. However, it can be envisaged that fungal colonisation of non-host epidermal cells is initially promoted by the impaired actin microfilament polymerisation upon drug treatment, similarly as reported for successful non-host cell entry by *Erysiphe pisi* or *Bgt* upon *HvADF3* overexpression (see Chapter 4.2.11). However, in the experiments described by Yun *et al.* (2003), F-actin polymerisation was inhibited by a single pressure infiltration of cytochalasin E in rosette leaves of *Arabidopsis* plants. It has been previously shown that removal of actin polymerisation inhibitors results in recovery of actin dynamics (Mathur *et al.*, 2002). Reduction of cytochalasin E concentrations by plant metabolic processes while/after haustorial complex formation could have allowed recovery of actin dynamics causing progress of fungal growth.

It is conceivable that impaired fungal growth caused by actin cytoskeleton-disrupting ADF overexpression might be exploited for the biotechnological generation of powdery mildew resistant plant species. An approach to circumvent undesired side effects of F-actin interference, e.g. in plant development, would be the application of pathogen-responsible promoters (Rushton *et al.*, 2002) driving local *ADF* overexpression only when a fungal pathogen attempts to gain access to a plant cell.

How may absence of the actin cytoskeleton upon either pharmacological treatments or ADF overexpression mechanistically interfere with *mlo* resistance in barley? It is conceivable that *Bgh* is capable to impair defence-related actin remodelling in compatible interactions by means of MLO modulation. Investigation of actin

cytoskeleton architecture upon pathogen challenge in epidermal cells of barley *Mlo* and *mlo*-5 genotypes support this assumption. Recently it was reported that focal rearrangements of actin filaments in *Mlo* genotype cells towards sites of *Bgh* penetration attempts were less frequent and seemingly delayed (Opalski *et al.*, 2004; in press). Previous experiments by Kobayashi and co-workers demonstrated that papilla formation is dependent on the actin cytoskeleton (Kobayashi *et al.*, 1997b). The delayed actin polarisation in pathogen challenged *Mlo* epidermal cells and the actin dependence of papilla formation are consistent with findings that in resistant *mlo* genotypes papillae generally appear earlier and are larger in size compared to susceptible *Mlo* genotypes. Therefore, pathogenic modulation of MLO might interfere with actin polarisation leading to a delay in papilla formation in wild-type plants.

Polar translocations of organelles to infection sites, reported from various patho-systems, comprise the accumulation of Golgi stacks (dictyosomes), accumulation of endoplasmic reticulum (ER) membranes and movement of both the nucleus and vesicles in pathogen-challenged plant cells (see Chapter 1.4). These processes can all be attributed to the actin cytoskeleton.

For example, nuclear movements towards sites of pathogen penetration attempts are attributable to actin cytoskeleton function. In cowpea, actin filament depolymerisation triggered by pharmacological inhibitor treatment prevented nuclear movements upon challenge with the cowpea rust fungus *Uromyces vignae* (Skalamera and Heath, 1998).

Likewise, movement of plant peroxisomes requires the actin cytoskeleton (Jedd and Chua, 2002; Mathur *et al.*, 2002). Although there is no direct evidence for an involvement of peroxisome-derived ROS during plant defence processes, it is conceivable that enzymes residing in the peroxisomal matrix contribute to ROS production upon pathogen challenge (Bolwell and Wojtaszek, 1997).

Additionally, Golgi stack positioning and movement are dependent on F-actin (Nebenführ *et al.*, 1999; Hawes and Satiat-Jeunemaitre, 2001; Nebenführ and Staehelin, 2001). It is conceivable that plasma membrane-delivered Golgi products, like *de novo* synthesised hemicelluloses or pectins, are components used for the fortification of the host epidermal cell wall or act as initiators of plant defence processes upon pathogen challenge. For example, application of hemicellulose to sites of plant cell wall damage in the cowpea-*Uromyces* patho-system was reported to trigger nuclear movements (Heath *et al.*, 1997). Moreover, the Golgi apparatus

works in close spatial association with the cortical ER, for which the actin network also serves as a scaffold (Boevink *et al.*, 1998). Thus, a concurrent focal localisation of Golgi stacks and ER upon pathogen attack appears likely.

A major route for exocytotic vesicles from the Golgi to the plasma membrane is provided by the actin cytoskeleton (Mathur and Hülskamp, 2002). SNARE proteins are key players in targeted membrane fusion events during exocytosis (Guo *et al.*, 2000; Bonifacino and Glick, 2004; Pratelli *et al.*, 2004) and have been shown to be involved in defence processes in barley and *Arabidopsis* (Collins *et al.*, 2003). It is conceivable that shortened transport distances for Golgi- and also nucleus- and ER-derived products, achieved by the translocation of the respective "production sites" towards sites of pathogenic attack, might account for a temporal advantage to stop fungal ingress at early infection stages. Interestingly, it is proposed that F-actin in addition delimits the area where exocytosis occurs (Ketelaar *et al.*, 2003). This contributes to the assumption that an F-actin-guided polarised transport of antimicrobial compounds and/or defence-involved components are essential for disease resistance.

Since all above mentioned processes are interconnected to a polarised rearrangement of actin-filaments, which is presumably necessary for their proper function in plant defence, it is not fully unexpected that pharmacological or genetic disruption of the actin cytoskeleton impairs at least broad-spectrum and non-host resistance. Thus, the actin cytoskeleton provides a target for pathogens to interfere with a plethora of host defence mechanisms. A pathogen-triggered MLO-mediated modulation of actin dynamics therefore appears likely.

Whether ADFs play a direct role in these processes remains questionable but the likelihood that *HvADF3* is regulated by reversible phosphorylation of a specific amino acid residue renders *HvADF3* a possible target for post-translational modification by CDPKs (Allwood *et al.*, 2001). It is known that at least some CDPK isoforms contribute to plant defence responses (Xu *et al.*, 1997; Romeis *et al.*, 2001) Involvement of CDPKs in ADF regulation via phosphorylation would provide a link of HvADF3 to cytosolic calcium fluxes (Hussey *et al.*, 2002). An increase of $[Ca^{2+}]_{cyt}$ has been reported as one of the earliest cellular events upon various biotic and abiotic stress stimuli (Blume *et al.*, 2000; Grant *et al.*, 2000; Ludwig *et al.*, 2004). In a naive scenario, elevation of $[Ca^{2+}]_{cyt}$ upon pathogen challenge would result in activation of

CDPKs in turn leading to a higher phosphorylation rate of ADFs, thereby resulting in a counterintuitive de-activation of the actin-modulating enzymes. However, this interruption of ongoing actin filament turnover upon initial $[Ca^{2+}]_{cyt}$ spike might be necessary for the cell to initiate polarisation towards the stress site.

5 Investigation of the impact of cytoskeleton-modifying factors on barley defence mechanisms

5.1 Introduction

A plethora of proteins are associated with cell cytoskeleton dynamics. The regulation and maintenance of actin microfilament structure involves approximately 70 classes of actin-binding proteins in animals (Kreis and Vale, 1999). Based on functional characteristics, plant ABPs can be divided in five somewhat artificial categories (Staiger and Hussey, 2004). Given the importance of actin dynamising processes in plant defence (see Chapter 1.4), ABPs in general are likely candidates for key regulatory elements of plant defence responses.

Recent findings suggest that *mlo*-mediated disease resistance is associated with cell polarisation (Schulze-Lefert, 2004). The fact that focal rearrangement of the actin cytoskeleton is required for efficient plant defence (Schmelzer, 2002) suggests that genes involved in cell polarisation might also contribute to plant defence responses. The a̱ctin-r̲elated p̲rotein (ARP) complex 2/3 is essential for the formation of dynamic actin patches that are associated with sites of polar growth in yeast cells (Evangelista *et al.*, 2002). In *Arabidopsis* the ARP2/3 complex controls actin organisation that is required for the proper polar expansion of leaf trichomes, epidermal pavement cell lobes, organelle transport, and membrane fusion (Mathur *et al.*, 2003a; Mathur *et al.*, 2003b).

Enteroinvasive pathogens of vertebrates like *Salmonella* ssp., *Yersinia* ssp., *Litsteria* ssp., and *Shigella* ssp. actively modify actin dynamics by exploiting host-derived regulators of the cytoskeleton to induce their own uptake by phagocytosis in normally nonphagocytic cells (Cossart and Sansonetti, 2004). Furthermore, pathogenicity of invasive bacteria arises in part by inhibition of the host immune system. Macrophage-mediated phagocytosis, which is responsible for defence against bacterial pathogens, is based on the local rearrangement of the actin microfilament cytoskeleton (Chimini and Chavrier, 2000). Some pathogenic bacteria have evolved mechanisms to interfere with actin cytoskeleton architecture to evade phagocytosis (Würtele *et al.*, 2001; Grosdent *et al.*, 2002). It was suggested that bacterial effectors

might operate in a similar manner during pathogenesis in animal and plant cells since homology has been determined between an invasive bacteria-derived actin cytoskeleton-disrupting toxin (YopT) and an *Avr* gene (AVRPPHB) involved in pathogenesis on susceptible host plants (Shao *et al.*, 2002).

Therefore, depletion of host cytoskeleton dynamics-modulating proteins by means of PTGS or overexpression of toxin effector domains from invasive bacterial pathogens were investigated in respect to their impact on the barley defence response to *Bgh*. Moreover, several *Arabidopsis* mutant plants showing defects in cell polarisation were tested for their ability to defend themselves against challenge of appropriate and inappropriate powdery mildew pathogens.

5.2 Results

5.2.1 dsRNAi-mediated silencing of cell cytoskeleton-associated factors

The IPK barley EST database of sequenced clones of the epidermal cDNA library described in Chapter 2.2.2.6 was systematically searched for sequences with homology to genes implicated in cytoskeletal organisation (Table 2).

Table 2. Clones encoding putative cytoskeleton-associated proteins identified in the barley epidermal cDNA library.

Putative protein encoded by epidermal cDNA clone	HO library clone ID	EMBL accession number
Tubulin alpha-5 chain-like protein	01E15	CD054502
Tubulin alpha-6 chain-like protein	02A22	CD054263
Myosin	15L09	CD057630
Putative myosin heavy chain	02B24	CD054205
Putative fimbrin	03I12	CD053773
Kinesin-related protein	01F16	CD054464
Putative kinesin light chain	04J02	CD053436
Profilin3	09A03	CD055357

Actin-like protein	01P09	CD054279
GTP-binding protein	09E08	CD055449
GTP-binding protein	15I08	CD057568
GTP-binding protein	03M13	CD053690
GTP-binding protein	07G13	CD054810
GTP-binding protein	05C17	CD058303
GTP-binding nuclear protein (RAN-2)	06D22	CD057972
GTP-binding protein (LEPA)	14O21	CD057368
Ras-related small GTP-binding protein	06L21	CD057830
Ran-binding protein (ATRANBP1B)	05K15	CD058193
Ran-binding protein (ATRANBP1B)	03C02	CD053895
ADP ribosylation GTPase-like protein	09A12	CD055366
Calcium-dependent protein kinase	14H02	CD057192
Calcium-dependent protein kinase	09F20	CD055479
Calcium-dependent protein kinase	09C22	CD055420
Putative calcium-dependent ser/thr protein kinase	10N20	CD056000
Calmodulin-domain protein kinase	08J12	CD055122
Calmodulin-domain protein kinase	03G19	CD053807
Calmodulin-domain protein kinase	15J19	CD057597
Actin	09E15	CD055456

All identified cDNAs were inserted in the ihpRNA vector pUAMBN via GATEWAY®-based site-specific recombination. However, ballistic delivery of pools of five pUAMBN constructs into leaves of barley *Mlo* or *mlo* genotypes did not affect penetration rates upon inoculation with *Bgh* at 96 h after bombardment (data not shown).

5.2.2 Investigation of the defence efficiency of *Arabidopsis* leaf hair morphology mutants due to defects in actin cytoskeleton polarisation

Pharmacological and genetic experiments demonstrated that plant leaf hair (trichome) development requires a precise cell cytoskeleton function. While microtubule cytoskeleton-based functions are required for polarised stalk and branch initiation of trichomes, the actin cytoskeleton seems responsible for a coordinated expansion of these structures. It has been shown that interference with microtubule dynamics can inhibit establishment of polarity, whereas interference with F-actin

results in distorted but branched trichomes. These findings suggest a role for actin microfilaments in polarised extension growth (Mathur *et al.*, 1999). Moreover, a concerted function of F-actin and microtubules for proper cell expansion has been proposed (Schwab *et al.*, 2003).

Several *Arabidopsis* mutants were identified showing trichome morphologies resembling those of plants treated with drugs that interfere with cytoskeleton architecture (Hülskamp *et al.*, 1994). Since barley defence mechanisms against powdery mildews apparently act independently of microtubules (see Chapter 4.2.12) the investigations were focused on mutant plants which contained defects in actin organisation. All of these plants show the distorted trichome phenotype.

alien (*ali*s25) and *gnarled* (*grl*247) are *Arabidopsis* mutants in which more actin filaments can be observed in trichomes compared to those of wild-type plants. While actin filaments of wild-type trichomes are normally tip-oriented, stretched and organised in compact actin cables, spirals and loops of F-actin predominate in these two mutants (Mathur *et al.*, 1999). The mutation in the *alien* genome still needs to be elucidated, but *gnarled* has been identified to contain a mutation in a gene distantly related to human *NAP125* (El-Assal *et al.*, 2004a). AtNAP125 is part of the so-called WAVE regulatory protein complex, which is an activator of the actin-related protein (ARP) 2/3 complex (Eden *et al.*, 2002; Frank *et al.*, 2004). A further component of the WAVE complex in animals is the PIR121 protein (Smith and Li, 2004), for which also a homolog exists in *Arabidopsis* (Brembu *et al.*, 2004). *Klunker* (*klk*) is apparently allelic to *AtPir1* (Li *et al.*, 2004) and the mutant displays an increased number of randomly linked, sub-cortical actin filaments that vary in thickness (Mathur *et al.*, 1999). Interestingly, further tested plants of the "distorted group" harboured mutations in subunits of the ARP2/3 complex. *crooked* (*crk1*-1), the mutant with the most apparent aberration of the actin cytoskeleton, shows thick, randomly cross-linked F-actin (Mathur *et al.*, 1999) and harbours a mutation in ARPC5, the smallest subunit of the ARP2/3 complex (Mathur *et al.*, 2003b). In other organisms the ARP2/3 complex is known to be essential for creating dendritic arrays of fine F-actin (Machesky and Gould, 1999; Svitkina and Borisy, 1999). Although *Wurm* and *Distorted1* encode the distinct *Arabidopsis* ARP2 and ARP3 subunits, respectively (Mathur *et al.*, 2003a), the mutants *wurm* (*wrm1*-1) and *distorted1* (*dis1*-1) both show similar effects by exhibiting numerous actin bundles arranged in a random zigzag orientation (Mathur

et al., 1999). Both ARP2 and ARP3 are the only proteins of the seven subunits comprising the ARP2/3 complex (Higgs and Pollard, 2001) that are sequence-related to actin and are thought to mimic an actin dimer seed from which new actin filaments can be nucleated (Robinson *et al.*, 2001). Furthermore, the mutant of *Distorted2* (*dis2*-1) encoding a paralogue of the ARP2/3 complex subunit ARPC2 (El-Assal *et al.*, 2004b; Saedler *et al.*, 2004) was tested. In the *Distorted2* mutant the F-actin is organised in thick, short, and cross-linked bundles (Saedler *et al.*, 2004). The *spirrig* mutant (*spis12*) has not been extensively characterised yet. Thus, no publicly accessible data concerning the structure of the actin cytoskeleton are available and the identity of the affected gene is unknown.

In addition to alterations of actin microfilaments, trichomes of the "distorted group" were reported to show an aberrant organisation of the microtubule cytoskeleton. Detailed investigations suggested an involvement of actin filaments in the positioning of cortical microtubules and thereby in plant cell expansion (Schwab *et al.*, 2003).

The trichome mutant *angustifolia* (*an*), which does not belong to the "distorted group", was also tested. The mutant shows wild-type actin architecture but an aberrant distribution of microtubules The *Angustifolia* gene encodes a C-terminal binding proteins/brefeldin A ADP-ribosylated substrates (CtBP/BARS)-related protein that presumably is involved in the control of Golgi dynamics and vesicle trafficking (Folkers *et al.*, 2002).

Six week-old *Arabidopsis* plants of the above described genotypes were either inoculated with the virulent powdery mildew fungus, *Golovinomyces orontii* or with *Erysiphe pisi* and *Bgh* for which in both cases *Arabidopsis* is a non-host. Due to the small size of haustoria, *Erysiphe pisi*-inoculated leaves were evaluated for growth of fungal secondary hyphae, an indirect indicator of host cell entry. *Bgh*-inoculated leaves were stained for callose deposition by aniline blue and evaluated for callose encased haustorial complexes [Fig. 39A] or whole-cell callose accumulation [Fig. 39B].
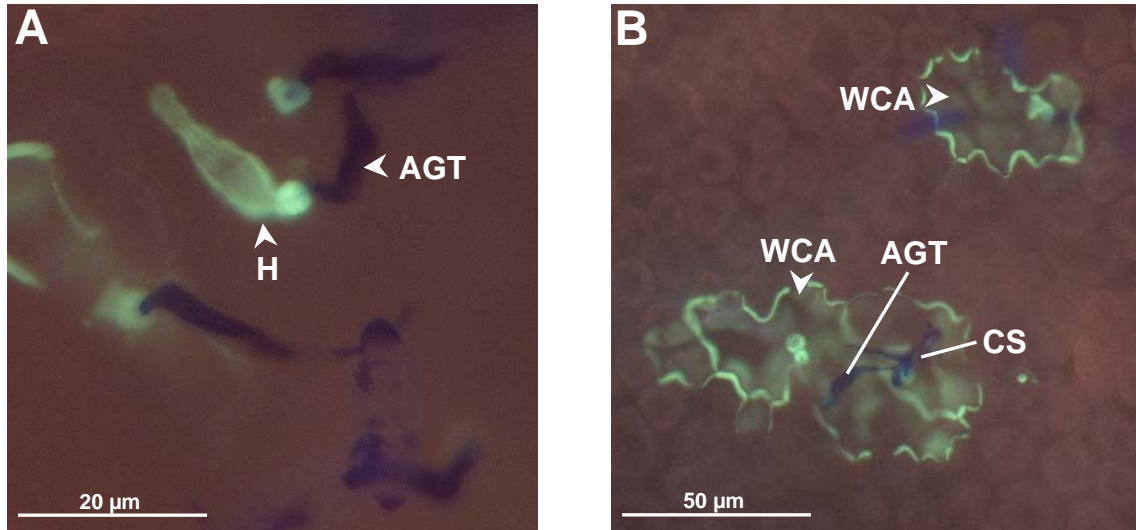
Figure 39. Callose accumulation patterns upon challenge with the powdery mildew fungus *Bgh*.
Arabidopsis leaves of the *crooked* mutant were inoculated with *Bgh* conidiospores and stained with the aniline blue fluorochrome.
    (C) Callose-encapsulated haustorial complex **(H)**.
    (D) Whole-cell callose accumulation in epidermal cells **(WCA)**.
Micrographs were taken 48 hpi using a Zeiss Axiophot microscope. They represent an overlay of UV-excited aniline blue-stained callose and bright-field microscopy of Coomassie brilliant blue-stained epiphytic fungal structures. **(AGT)**, appressorial germ tube of *Bgh* conidiospores **(CS)**. The scale bars in the bottom left corners represent the absolute sizes.

Some mutant plants inoculated with the virulent pathogen *Golovinomyces orontii* showed macroscopically absence of fungal growth. Unexpectedly, this was also the case for the control plant of the ecotype *Landsberg*, which is the genetic background for most of the "distorted mutants" and *angustifolia*. However, microscopic evaluation revealed that the fungus was able to sporulate to different extents on all tested plants, although hyphal growth and sporulation was extremely reduced on *angustifolia*. Since all data base on single experiments, repetitions are necessary to confirm the different phenotypes.

Most of the tested mutants, with the exception of *crooked* and *distorted1*, showed no dramatic alterations in their defence response when challenged with the respective inappropriate pathogens, since infection phenotypes were within the range of naturally occurring variations (Jan Dittgen, personal communication) [Fig. 40 and Fig. 41].

Microscopic evaluation of *Erysiphe pisi*-inoculated plants revealed that the powdery mildew fungus apparently shows a higher penetration frequency in epidermal cells of the *crooked* mutant [Fig. 40]. Additionally, in contrast to the other genotypes, cells that contain encapsulated haustoria were more frequent than cells showing whole-cell callose accumulation in *angustifolia* and *gnarled* [Fig. 41].
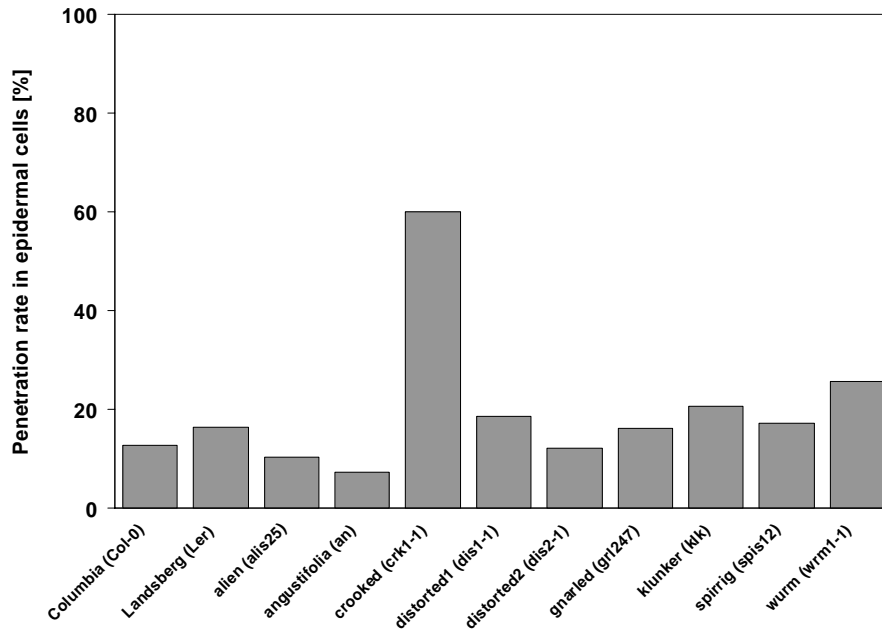
Figure 40. The *crooked* mutant is compromised in non-host resistance against *Erysiphe pisi*.
Rosette leaves of six-week old *Arabidopsis* mutant plants were densely inoculated with pea powdery mildew (*Erysiphe pisi*) conidiospores. Columns represent percentage of successful penetration attempts of *Erysiphe pisi* conidia 48 h after inoculation of *Arabidopsis* leaves, scored by absence or presence of elongating secondary hyphae [%]. Columns represent one experiment in which at least 300 interaction sites of single *Erysiphe pisi* sporelings attacking epidermal *Arabidopsis* cells were microscopically evaluated.

Interestingly, *crooked* mutant plants seemed also more accessible and/or sensitised to the inappropriate pathogen *Bgh*. It was observed that pathogen-challenged epidermal cells showed more whole-cell callose fluorescence [Fig. 41], which can be indicative of cell death subsequent to successful penetration (Jacobs *et al.*, 2003) but might also account for sensitive cells that died upon stress-inducing pathogenic penetration attempts. A closer inspection of fluorescing cells for presence of haustorial complexes may clarify which circumstance applies to the mutant.

Additionally, *distorted1* plants also showed higher amounts of whole-cell callose accumulation upon inoculation with *Bgh* but in contrast to *crooked* plants seemed not more accessible to *Erysiphe pisi* [Fig. 40 and Fig. 41].
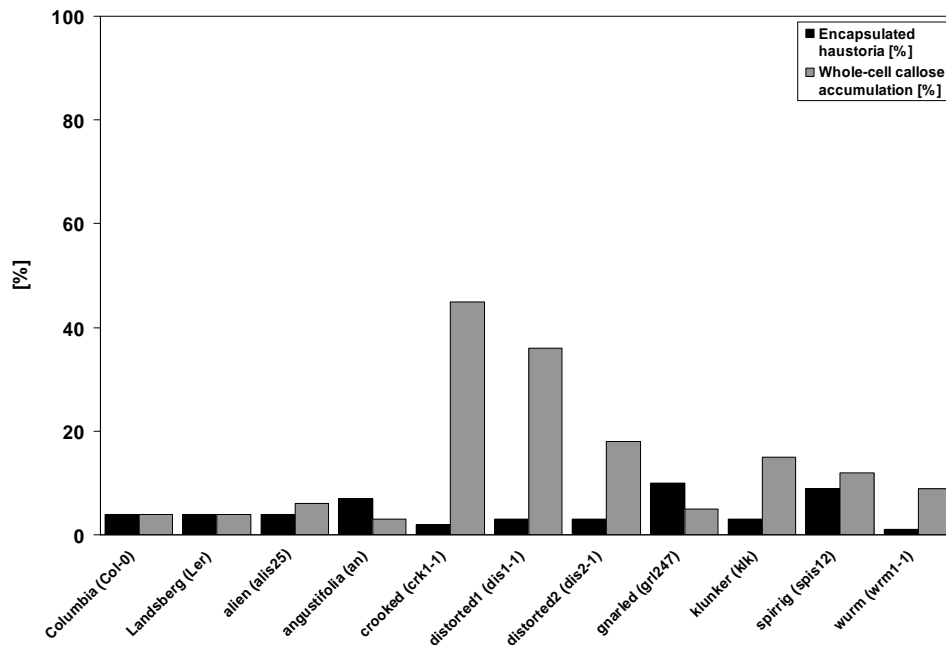
Figure 41. The *crooked* and *distorted1* mutants show enhanced whole-cell callose deposition in non-host epidermal cells upon *Bgh* attack.

Rosette leaves of six-week old *Arabidopsis* mutant plants were densely inoculated with barley powdery mildew (*Bgh*) conidiospores. Columns represent percentage of successful penetration attempts of *Bgh* conidia 48 h after inoculation of *Arabidopsis* leaves, scored by absence or presence of callose-encapsulated haustoria (black columns) and whole-cell callose accumulation (grey columns) [%]. Columns represent one experiment in which at least 300 interaction sites of single *Bgh* sporelings attacking epidermal *Arabidopsis* cells were microscopically evaluated.

5.2.3 Pathogenicity factors derived from enteroinvasive human pathogens do not affect barley defence mechanisms

Host defence suppression in vertebrate cells by invasive bacterial pathogens is frequently accomplished by interference with Rho GTPases known to regulate actin dynamising processes (Aktories *et al.*, 2000). Three major classes of Rho GTPases, namely Rho, Rac, and Cdc42 exist in metazoans. Each class acts in the control distinct cellular functions. In respect to the actin cytoskeleton, Rho GTPases adjust the organisation of stress fibers; Rac GTPases are involved in the organisation of lamellipodia, causing membrane ruffling and locomotion; and Cdc42 GTPases

regulate filopodia or microspikes and are important for defining the polarity of cellular organization (Nobes and Hall, 1995). In plants, the only existing Rho family subgroup of Rop GTPases are more similar to Rac than to Rho (Schultheiss *et al.*, 2003), but these small monomeric GTPases are also thought to function as molecular switches in plant defence signalling (Ono *et al.*, 2001; Agrawal *et al.*, 2003; Schultheiss *et al.*, 2003). Therefore, three bacterial effector proteins were chosen known to be involved in actin rearrangements during pathogenesis in animal cells by targeting Rho family GTPases. Additionally, a bacterial effector protein that competes with ADF/cofilin was selected. The rational of this set of experiments was to investigate whether targets of these effectors exist in plants and if they have an impact on the barley defence responses to *Bgh*.

The cysteine protease YopT of *Yersinia* ssp. mediates pathogenesis by cleaving a Rho GTP-binding protein (RhoA) which results in disruption of the actin cytoskeleton in the mammalian host cells. (Würtele *et al.*, 2001; Shao *et al.*, 2002; Shao *et al.*, 2003a). Interestingly, the plant pathogen *Pseudomonas syringae* contains a gene (*AvrPphB*) encoding a protein with high sequence homology to YopT. AVRPPHB was found to proteolytically cleave PBS1, which mediates perception of AVRPPHB by the R protein RPS5 (Swiderski and Innes, 2001; Shao *et al.*, 2003b).

Another cytotoxin modulating host actin filament dynamics is encoded by the gene *exoS* from *Pseudomonas aeruginosa*. ExoS is a member of the class of <u>G</u>TPase-<u>a</u>ctivating <u>p</u>roteins (GAP). GTPases of the Rho family are inactivated by binding of GDP and kept in this status by <u>g</u>uanine <u>n</u>ucleotide <u>d</u>issociation <u>i</u>nhibitors (GDI) [Fig. 42]. Upon exchange of GDP by GTP, which is mediated by <u>g</u>uanine nucleotide <u>e</u>xchange <u>f</u>actors (GEF), the GTPase remains active until the bound GTP is hydrolysed to GDP and Pi. GTP hydrolysis is catalyzed by GAPs. The GAP ExoS stimulates GTP hydrolysis catalysed by the Rho GTPases Rac and Cdc42 (Barbieri *et al.*, 2002).

The third bacterial toxin investigated in this study is encoded by *sopE* from *Salmonella typhimurium*. SopE induces membrane ruffling and cytoskeletal rearrangements in host cells. Recently, it was shown that SopE is a GEF protein activating Rac and Cdc42 (Hardt *et al.*, 1998; Buchwald *et al.*, 2002). Additionally,

SopE may contribute to ADF/cofilin regulation cycles by activation of Cdc42 which subsequently triggers phosphorylation of the two ABPs (Dai *et al.*, 2004).
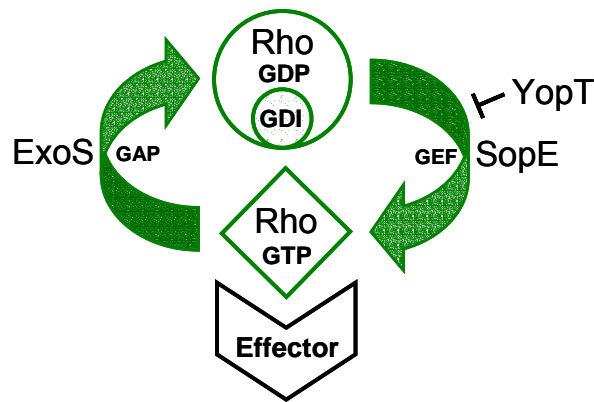
Regulation of actin cytoskeleton dynamics

Figure 42. Regulation cycle of Rho family-associated small GTP-binding proteins.
For details, see text. **(GAP)** GTPase-activating protein; **(GDI)** guanine nucleotide dissociation inhibitor; **(GEF)** guanine nucleotide exchange factor; **(GTP)** guanosine triphosphate; **(GDP)** guanosine diphosphate. (Modified from Aktories *et al.*, 2000)

Recently, an ADF/cofilin-competing protein (SipA) secreted by *Salmonella typhimurium* into host cells has been identified. SipA is involved in the initial steps of pathogen-host interactions in mammalian cells (Dai *et al.*, 2004; McGhie *et al.*, 2004) by promoting actin polymerisation.

cDNAs encoding YopT, SipA as well as catalytic domains of ExoS (Pederson *et al.*, 2002), and SopE (Buchwald *et al.*, 2002) were PCR-amplified from plasmids pIM157, pcDNA3.1-SipA, pGEX2T-Δ96ExoS, pGEX2T-Δ78SopE, respectively, using primer pairs that rendered PCR products suitable for GATEWAY®-cloning. Subsequently, amplicons were introduced into the overexpression vector pUbiGATE.

Ballistic delivery of individual toxin overexpression constructs to epidermal cells of detached barley leaves of either *Mlo* or *mlo* genotypes and subsequent inoculation with *Bgh* at 4 h after bombardment revealed no impact on powdery mildew penetration rates (data not shown).

5.3   Discussion

Silencing of a set of barley genes likely associated with the regulation of cytoskeleton dynamics did not induce any alteration of the penetration rate of *Bgh* in transfected barley epidermal cells. Several reasons may account for these negative results. First, only a small subset of known cytoskeleton-associated factors was represented in the epidermal cDNA library at the time when the experiments were carried out. For example, no homolog to the at least eight known members of the actin-related proteins from the crucifer *Arabidopsis* (Kandasamy *et al.*, 2004) was present in the set of silenced genes. Additionally, redundant functions of genes which were not co-silenced due to insufficient DNA sequence homology could also have masked putative effects. Finally, silencing of single genes may not necessarily result in drastic changes of *Bgh* penetration rates. Subtle effects mediated by depletion of individual genes might have been overlooked due to natural biological variation, especially in the *Mlo* genotypes.

Interestingly, impaired polar arrangement of the cytoskeleton due to mutations in the ARP2/3 complex has, with the exception of mutations in the *Crooked* and *Distorted1* genes, apparently no impact on the defence response of *Arabidopsis* against virulent and avirulent powdery mildew pathogens. Examination of actin architecture in the "distorted" mutants was mostly confined to trichomes; therefore, only limited data are currently available about actin microfilament organisation in rosette leaf epidermal cells. However, for the *crooked, wurm, distorted1,* and *distorted2* mutants an aberrant actin organisation has also been reported for cotyledon epidermal pavement cells leading to loss of the characteristic lobes of *Arabidopsis* wild-type epidermal cells (Mathur *et al.*, 2003a; Mathur *et al.*, 2003b; El-Assal *et al.*, 2004b). These randomly-shaped, less-lobed epidermal cells were also paving the rosette leaves investigated in the above reported pathogen assays. This excludes the possibility that lack of alterations in the disease response of the *wurm* and *distorted2* mutants was due to actin cytoskeleton abnormalities restricted to trichomes (note that *crooked* and *distorted1* showed altered disease responses; see below).

Interestingly, the *crooked* mutant, having an impact on the defence response against both pathogens, *Erysiphe pisi* and *Bgh*, shows the most apparent aberration of F-actin (Mathur *et al.*, 1999). The ARP2/3 complex subunit ARPC5, encoded by

Crooked, specifically contributes to the motility and distribution of mitochondria in yeast (Boldogh *et al.*, 2001). In *Arabidopsis*, unusually large Golgi stacks accumulate at sites of densely packed actin bundles in the *Crooked* mutant (Mathur *et al.*, 2003b). Therefore, it can be speculated that impaired vesicle and/or organelle motility due to disturbed actin polarisation might contribute to enhanced accessibility of epidermal cells to fungal pathogens. To what extent dictyosomes or organelles in general contribute to plant defence mechanisms is currently poorly understood, but a polarised translocation of organelles towards sites of pathogenic penetration attempts, most likely via the actin cytoskeleton, has been observed in several patho-systems (Heath and Heath, 1978; Kunoh *et al.*, 1985; Gross *et al.*, 1993; Freytag *et al.*, 1994; Kobayashi *et al.*, 1994; Xu *et al.*, 1998; McLusky *et al.*, 1999; Takemoto *et al.*, 2003).

From a single experiment it can not be concluded whether the *distorted1* mutant is really compromised in resistance against *Bgh* as the results in Figure 41 suggest. Since, unlike the *crooked* mutant the defence response was not impaired in the interaction of *distorted1* with *Erysiphe pisi* it is likely that observed effects are due to natural biological variation. This assumption is further supported by the fact that the *wurm* mutant shows a similar actin cytoskeleton architecture as *distrorted1* but no altered defence response [Fig. 40 and Fig. 41]. Moreover, *wurm* is defective in the counterpart of the two ARP2/3 subunits which are both presumably required for actin filament nucleation (Schwab *et al.*, 2003). Thus, it remains enigmatic why only a mutation in a certain subunit of the ARP2/3 complex, namely ARPC5 (*Crooked*), compromises resistance, although for all mutants concerning the complex aberrant actin meshwork phenotypes have been shown. Nevertheless, the phytopathological analysis of multiple independent *crooked* mutant alleles is required to unequivocally assign a role for *Crooked* in plant defence.

Several reasons are conceivable why overexpression of the toxin *yopT* and the effector domains of *exoS* and *sopE* had no impact on *Bgh* penetration rates in ballistically transfected epidermal leaf cells. First, overexpression of bacterial toxins or their catalytic domains may lead to proteins that are instable *in planta*. Secondly, provided that the proteins are stable, it is also possible that the proteins are functional in plants but do not interfere with barley defence mechanisms resulting in

altered *Bgh* penetration rates. However, since plants only possess a small subset of the Rho-type GTPases that exist in animals, the most likely explanation might be that barley does not contain putative targets for the toxic polypeptides.

Notably, SipA functions in a different manner independently of Rho GTPases. SipA promotes actin polymerisation by binding to F-actin and preventing filament depolymerisation by structural competition with ADF/cofilin and gelsolin *in vitro* (Zhou *et al.*, 1999a; McGhie *et al.*, 2001, 2004). In these processes SipA functions as a kind of staple in which a globular domain and two non-globular arms mechanically stabilise the filament by tethering actin subunits in opposing strands (Lilic *et al.*, 2003). SipA also promotes filament assembly by lowering the critical G-actin concentration required for polymerisation (Zhou *et al.*, 1999a; Galkin *et al.*, 2002) and enhances F-actin bundling by host fimbrin (Zhou *et al.*, 1999b). Thus, SipA might prevent a focal rearrangement of the actin cytoskeleton in *Bgh*-challenged barley cells by stabilising existing filaments and competing with ADF for binding sites required for severing F-actin. However, no altered *Bgh* penetration phenotypes were observed upon *sipA* overexpression. This may indicate that either SipA is not stable *in planta* or it does not bind to plant actin. Alternatively, SipA might function as expected but the resulting perturbation in F-actin dynamics do not interfere with *Bgh* defence processes. The identification and functional analysis of effector proteins described from plant pathogens will possibly more effectively contribute to dissect the actin-associated host defence mechanisms in the future.

6   Summary

Attempted host cell invasion by pathogenic fungi is known to trigger cell polarisation. Barley MLO is a member of a family of heptahelical membrane proteins unique to plants and is thought to regulate polarised SNARE protein-dependent secretory processes. Recessively inherited mutations in *Mlo* mediate resistance against all isolates (broad-spectrum resistance) of the biotrophic barley powdery mildew fungus, *Blumeria graminis* f. sp. *hordei* (*Bgh*). It is assumed that the fungus utilizes MLO to suppress defence-associated secretion for successful host cell entry.

In this study, a genetic screen was established based on gene silencing by <u>d</u>ouble-<u>s</u>tranded <u>RNA</u> <u>i</u>nterference (dsRNAi). This was accomplished by transient expression of inverted repeat DNAs in single epidermal barley cells. To identify novel components of MLO-modulated defence processes to *Bgh*, approximately 700 inverted repeat DNA constructs, derived from barley epidermal cDNAs, were generated and ballistically delivered into epidermal cells of both *Mlo* and *mlo* genotypes. Two dsRNAi constructs were identified permitting enhanced *Bgh* entry in a resistant *mlo* genotype. Both target the same isoform of an <u>a</u>ctin <u>d</u>epolymerising <u>f</u>actor, designated HvADF3. ADFs exist throughout all eukaryotic kingdoms and function in actin filament turnover (treadmilling), thereby contributing to actin cytoskeleton dynamics.

Transient ectopic expression of *HvADF3* in *mlo* epidermal cells also permitted enhanced *Bgh* invasion. Ectopic expression of *HvADF3* or dsRNAi-mediated gene silencing resulted in the disappearance of phalloidin-stainable actin filaments, consistent with actin serving as substrate of ADFs. Closer inspection of the topology of the *HvADF3* dsRNAi constructs revealed that the presumed silencing effect might be triggered by undesired overexpression. However, due to published pharmacological evidence implicating actin filament reorganisation in plant defence responses, the role of HvADF3 was further investigated. *HvADF3* overexpression greatly reduced callose accumulation at pathogen entry sites, a common local stress response at the plant cell wall known to be sensitive to actin-depolymerising drugs. Replacements of an N-terminal serine residue, previously shown to be a phosphorylation target of ADF activity, to Ala or Asp enhanced and reduced *Bgh* entry rates, respectively, upon transient expression. Ectopic expression of six out of nine tested Arabidopsis *ADF* genes in barley phenocopied the effect of *HvADF3*

overexpression, demonstrating that multiple heterologous ADF isoforms can enhance pathogen entry. Although ectopic ADF expression impaired broad-spectrum resistance to *Bgh*, race-specific resistance (*R*) triggered by *R* genes *Mlg*, *Mla1*, or *Mla6* was not affected. This is consistent with previous genetic data indicating separate pathways for broad-spectrum and *R* gene-mediated immune responses. Resistance to two tested inappropriate powdery mildews, *Bg* f sp *tritici* and *Erysiphe pisi*, that colonise in nature monocotyledonous wheat and dicotyledonous pea hosts respectively, was impaired upon *HvADF3* overexpression. Interestingly, this impairment required the presence of *Mlo*, suggesting that both inappropriate powdery mildews potentially modulate barley defence reactions *via* MLO.

To identify presumed common components of pathogen-triggered and developmentally controlled cell polarity, a range of *Arabidopsis* mutants with defects in leaf hair (trichome) development were tested for altered infection phenotypes to diverse powdery mildew fungi. Preliminary data indicate that the absence of an actin-related protein (ARP) 2/3 complex component, CROOKED, enhances pathogen entry of inappropriate powdery mildew species.

7   Zusammenfassung

Es ist bekannt, daß Penetrationsversuche von Pilzpathogenen eine Polarisation des Cytosols in den von ihnen angegriffenen Wirtszellen auslöst. Das MLO Protein der Gerste ist ein Mitglied einer auf das Pflanzenreich beschränkten Familie von heptahelikalen Membranproteinen, das vermutlich an der Regulation von SNARE-Protein-abhängigen Sekretionsvorgängen beteiligt ist. Rezessiv vererbte Mutationen in *Mlo* führen zur vollständigen Resistenz gegenüber Angriffen aller Isolate (Breitspektrum-Resistenz) des biotrophen Gerste-Mehltaupilzes *Blumeria graminis* f.sp. *hordei* (*Bgh*). Es wird angenommen, daß *Bgh* im Stande ist, mittels MLO pflanzliche Abwehrmechanismen, die auf Sekretionsereignissen basieren, zu unterdrücken um somit Zugang zu Wirtszellen zu erlangen.

In der vorliegenden Arbeit wurde ein dsRNAi-Screen etabliert, der auf Gensilencing mittels transienter Expression von gegenläufig komplementären DNA Strängen in einzelnen Gerste-Epidermiszellen basiert. Um weitere Komponenten MLO-kontrollierter Abwehrmechanismen gegen *Bgh* zu identifizieren, wurden ca. 700 der Gensilencing-vermittelnden DNA Konstrukte für die ballistische Transfektion von Gerste-Blattepidermiszellen beider Genotypen (*Mlo* und *mlo*) benutzt. Die dabei verwendeten DNAs entstammten einer epidermalen Gerste cDNA Bibliothek. Während des Screens konnten zwei Gensilencing-Konstrukte identifiziert werden, die zu einer erhöhten *Bgh* Penetrationsrate in resistenten Epidermiszellen des *mlo* Genotyp führten. Beide Gensilencing-Konstrukte enthielten cDNAs die zur Ausschaltung eines A̲ctin-d̲epolymerisierenden F̲aktors (ADF) aus Gerste (HvADF3) führen sollten. ADFs, die in allen Eukaryonten vorkommen, tragen zur Umgruppierung von Actinfilamenten bei und spielen somit eine wichtige Rolle in dem dynamischen Verhalten des Actincytoskeletts. Ebenso führte die transiente Überexpression von *HvADF3* zu einer erhöhten *Bgh*-Penetrationsrate im *mlo*-Genotyp. Cytologische Untersuchungen ergaben, das sowohl das Gensilencing von *HvADF3* als auch die Überexpression zum Verschwinden Phalloidin-färbbarer Actinfilamente führte, die das Substrat für ADFs darstellen. Nähere Untersuchungen der Gensilencing-Vektortopologie ergaben, daß die Möglichkeit bestand, daß potentielle *HvADF3*-Silencingeffekte eher auf unerwünschte Überexpressions-artefakte des Vektors zurückzuführen sind.

Aufgrund des vielfach beschriebenen Zusammenhangs zwischen Actinfilament-dynamik und pflanzlichen Abwehrreaktionen gegenüber Pathogenen, wurde die Rolle von HvADF3 in Actinfilament-basierenden pflanzlichen Abwehrmechanismen weitergehend untersucht. Die Überexpression von *HvADF3* führte unter Anderem zu einer reduzierten Calloseablagerung in Zellwandappositionen (Papillen), die an Stellen versuchter Pathogenpenetration entstehen. Calloseablagerungen können als eine generelle lokale Stressreaktion angesehen werden, die auch durch die pharmakologische Beeinträchtigung des Actincytoskeletts unterdrückt werden können. Zudem konnte gezeigt werden, daß der Austausch eines N-terminal lokalisiertem Serins, von dem bekannt ist, daß es eine regulatorische Komponente der ADF-Aktivität aufgrund von Phosphorylierung darstellt, gegen Alanin oder Aspartat, jeweils zu einer erhöhten oder reduzierten *Bgh* Penetrationsrate in transfizierten Zellen führte. Des Weiteren führte die Überexpression von sechs von neun getesteten *Arabidopsis ADFs* in Gerste zu erhöhten *Bgh*-Penetrationsraten und damit zu Phenokopien der *HvADF3*-Überexpression. Somit konnte gezeigt werden, daß multiple heterologe ADF-Isoformen im Stande sind, zu einer erhöhten Penetrationsrate beizutragen. Obwohl ektopische ADF-Expression die Effizienz der Breitspektrum-Resistenz beinträchtigte, wurde rassenspezifische Resistenz, vermittelt durch die Resistenzgene *Mlg*, *Mla1* oder *Mla6*, nicht beeinflusst. Dieses Ergebnis bekräftigt vorausgegangene genetische Befunde, die getrennte Mechanismen beider Abwehrreaktionen postulieren. Hingegen wurden auch die *forma specialis* und die Nicht-Wirts Resistenz durch das Actincytoskelett beeinflusst. Sowohl der Weizen-Mehltau *Blumeria graminis* f.sp. *tritici* (*Bgt*) als auch der Erbsen-Mehltau *Erysiphe pisi* konnten in erhöhtem Maße in *HvADF3*-überexprimierende Epidermiszellen eindringen. Interessanterweise war dies den Pilzisolaten nur möglich, sofern ein intaktes MLO Protein vorhanden war. Dieser Befund spricht dafür, daß scheinbar beide biotrophe Mehltauarten (*Bgt* und *Erysiphe pisi*) potentiell im Stande sind Resistenzmechanismen mit Hilfe von MLO zu beeinträchtigen. Um wahrscheinliche Überschneidungspunkte der pathogen-induzierten sowie der enwicklungsbiologisch-kontrollierten Zellpolarität aufzudecken, wurden das Resistenzverhalten von *Arabidopsis* Mutanten, die Defekte in der polaren Ausrichtung des Actincytoskeletts aufweisen, gegenüber verschiedenen Mehltauspezies untersucht. Vorläufige Daten deuten daraufhin, daß die Nicht-

Wirtspflanze *Arabidopsis*, die eine Mutation in einer Untereinheit (CROOKED) des ARP2/3 Komplexes besitzt, anfälliger gegenüber avirulenten Pathogen ist.

8 Literature cited

Agnew, B.J., Minamide, L.S., and Bamburg, J.R. (1995). Reactivation of phosphorylated actin depolymerizing factor and identification of the regulatory site. J. Biol. Chem. **270,** 17582-17587.

Agrawal, G.K., Iwahashi, I., and Rakwal, R. (2003). Small GTPase 'Rop': molecular switch for plant defense responses. FEBS Lett. **546,** 173-180.

Aist, J.R., and Israel, H.W. (1986). Autofluorescent and ultraviolet-Absorbing components in cell walls and papillae of barley coleoptiles and their relationship to disease resistance. Can. J. Bot.-Rev. Can. Bot. **64,** 266-272.

Aizawa, H., Sutoh, K., and Yahara, I. (1996). Overexpression of cofilin stimulates bundling of actin filaments, membrane ruffling, and cell movement in Dictyostelium. J. Cell Biol. **132,** 335-344.

Aizawa, H., Sutoh, K., Tsubuki, S., Kawashima, S., Ishii, A., and Yahara, I. (1995). Identification, characterization, and intracellular distribution of cofilin in *Dictyostelium discoideum*. J. Biol. Chem. **270,** 10923-10932.

Aktories, K., Schmidt, G., and Just, I. (2000). Rho GTPases as targets of bacterial protein toxins. Biol Chem **381,** 421-426.

Allwood, E.G., Smertenko, A.P., and Hussey, P.J. (2001). Phosphorylation of plant actin depolymerising factor by calmodulin-like domain protein kinase. FEBS Lett **499,** 97-100.

Allwood, E.G., Anthony, R.G., Smertenko, A.P., Reichelt, S., Drøbak, B.K., Doonan, J.H., Weeds, A.G., and Hussey, P.J. (2002). Regulation of the pollen-specific actin depolymerizing factor LlADF1. Plant Cell **14,** 2915-2927.

Arabidopsis Genome Initiative, (2000). Analysis of the genome sequence of the flowering plant *Arabidopsis thaliana*. Nature **408,** 796-815.

Arber, S., Barbayannis, F.A., Hanser, H., Schneider, C., Stanyon, C.A., Bernard, O., and Caroni, P. (1998). Regulation of actin dynamics through phosphorylation of cofilin by LIM-kinase. Nature **393,** 805-809.

Asai, T., Tena, G., Plotnikova, J., Willmann, M.R., Chiu, W.L., Gómez-Gómez, L., Boller, T., Ausubel, F.M., and Sheen, J. (2002). MAP kinase signalling cascade in *Arabidopsis* innate immunity. Nature **415,** 977-983.

Asano, T., Masumura, T., Kusano, H., Kikuchi, S., Kurita, A., Shimada, H., and Kadowaki, K. (2002). Construction of a specialized cDNA library from plant cells isolated by laser capture microdissection: toward comprehensive analysis of the genes expressed in the rice phloem. Plant J. **32,** 401-408.

Austin, M.J., Muskett, P., Kahn, K., Feys, B.J., Jones, J.D., and Parker, J.E. (2002). Regulatory role of *SGT1* in early *R* gene-mediated plant defenses. Science **295,** 2077-2080.

Azevedo, C., Sadanandom, A., Kitagawa, K., Freialdenhoven, A., Shirasu, K., and Schulze-Lefert, P. (2002). The RAR1 interactor SGT1, an essential component of R gene-triggered disease resistance. Science **295,** 2073-2076.

Bamburg, J.R. (1999). Proteins of the ADF/cofilin family: Essential regulators of actin dynamics. Annu. Rev. Cell Dev. Biol. **15,** 185-230.

Barbieri, J.T., Riese, M.J., and Aktories, K. (2002). Bacterial toxins that modify the actin cytoskeleton. Annu Rev Cell Dev Biol **18,** 315-344.

Bernard, P., and Couturier, M. (1992). Cell killing by the F-Plasmid Ccdb Protein involves poisoning of DNA-topoisomerase-Ii Complexes. J. Mol. Biol. **226,** 735-745.

Bernstein, B.W., Painter, W.B., Chen, H., Minamide, L.S., Abe, H., and Bamburg, J.R. (2000). Intracellular pH modulation of ADF/cofilin proteins. Cell Motil. Cytoskeleton **47,** 319-336.

Blume, B., Nürnberger, T., Nass, N., and Scheel, D. (2000). Receptor-mediated increase in cytoplasmic free calcium required for activation of pathogen defense in parsley. Plant Cell **12,** 1425-1440.

Boevink, P., Oparka, K., Cruz, S.S., Martin, B., Betteridge, A., and Hawes, C. (1998). Stacks on tracks: the plant Golgi apparatus traffics on an actin/ER network. Plant J. **15,** 441-447.

Boldogh, I.R., Yang, H.C., Nowakowski, W.D., Karmon, S.L., Hays, L.G., Yates, J.R., and Pon, L.A. (2001). Arp2/3 complex and actin dynamics are required for actin-based mitochondrial motility in yeast. Proc. Natl. Acad. Sci. U. S. A. **98,** 3162-3167.

Brembu, T., Winge, P., Seem, M., and Bones, A.M. (2004). NAPP and PIRP encode subunit of a putative wave regulatory protein complex involved in plant cell morphogenesis. Plant Cell **16,** 2335-2349.

Bolwell, G.P., and Wojtaszek, P. (1997). Mechanisms for the generation of reactive oxygen species in plant defence - a broad perspective. Physiol. Mol. Plant Pathol. **51,** 347-366.

Bonifacino, J.S., and Glick, B.S. (2004). The mechanisms of vesicle budding and fusion. Cell **116,** 153-166.

Bosher, J.M., and Labouesse, M. (2000). RNA interference: genetic wand and genetic watchdog. Nat. Cell Biol. **2,** E31-E36.

Bowman, G.D., Nodelman, I.M., Hong, Y., Chua, N.H., Lindberg, U., and Schutt, C.E. (2000). A comparative structural analysis of the ADF/cofilin family. Proteins **41,** 374-384.

Boyd, L.A., Smith, P.H., Foster, E.M., and Brown, J.K.M. (1995). The effects of allelic variation at the *Mla* resistance locus in barley on the early development of *Erysiphe graminis* f. sp. *hordei* and host responses. Plant J. **7,** 959-968.

Braun, M., Hauslage, J., Czogalla, A., and Limbach, C. (2004). Tip-localized actin polymerization and remodeling, reflected by the localization of ADF, profilin and villin, are fundamental for gravity-sensing and polar growth in characean rhizoids. Planta **219,** 379-388.

Brisson, L.F., Tenhaken, R., and Lamb, C. (1994). Function of oxidative cross-linking of cell wall structural proteins in plant disease resistance. Plant Cell **6,** 1703-1712.

Brown, I., Trethowan, J., Kerry, M., Mansfield, J., and Bolwell, G.P. (1998). Localization of components of the oxidative cross-linking of glycoproteins and of callose synthesis in papillae formed during the interaction between non-pathogenic strains of *Xanthomonas campestris* and French bean mesophyll cells. Plant J. **15,** 333-343.

Buchwald, G., Friebel, A., Galan, J.E., Hardt, W.D., Wittinghofer, A., and Scheffzek, K. (2002). Structural basis for the reversible activation of a Rho protein by the bacterial toxin SopE. Embo J **21,** 3286-3295.

Burridge, K., and Wennerberg, K. (2004). Rho and Rac take center stage. Cell **116,** 167-179.

Büschges, R., Hollricher, K., Panstruga, R., Simons, G., Wolter, M., Frijters, A., van Daelen, R., van der Lee, T., Diergaarde, P., Groenendijk, J., Töpsch, S., Vos, P., Salamini, F., and Schulze-Lefert, P. (1997). The barley *Mlo* gene: a novel control element of plant pathogen resistance. Cell **88,** 695-705.

Carlier, M.F. (1998). Control of actin dynamics. Curr. Opin. Cell Biol. **10,** 45-51.

Carlier, M.F., Laurent, V., Santolini, J., Melki, R., Didry, D., Xia, G.X., Hong, Y., Chua, N.H., and Pantaloni, D. (1997). Actin depolymerizing factor (ADF/cofilin) enhances the rate of filament turnover: implication in actin-based motility. J Cell Biol **136,** 1307-1322.

Chen, C.Y., Cheung, A.Y., and Wu, H.M. (2003). Actin-depolymerizing factor mediates Rac/Rop GTPase-regulated pollen tube growth. Plant Cell **15,** 237-249.

Chen, C.Y., Wong, E.I., Vidali, L., Estavillo, A., Hepler, P.K., Wu, H.M., and Cheung, A.Y. (2002). The regulation of actin organization by actin-depolymerizing factor in elongating pollen tubes. Plant Cell **14,** 2175-2190.

Chen, H., Bernstein, B.W., Sneider, J.M., Boyle, J.A., Minamide, L.S., and Bamburg, J.R. (2004a). In vitro activity differences between proteins of the ADF/cofilin family define two distinct subgroups. Biochemistry **43,** 7127-7142.

Chen, J.G., Pandey, S., Huang, J.R., Alonso, J.M., Ecker, J.R., Assmann, S.M., and Jones, A.M. (2004b). GCR1 can act independently of heterotrimeric G-protein in response to brassinosteroids and gibberellins in *Arabidopsis* seed germination. Plant Physiol. **135,** 907-915.

Chimini, G., and Chavrier, P. (2000). Function of Rho family proteins in actin dynamics during phagocytosis and engulfment. Nat. Cell Biol. **2,** E191-E196.

Chuang, C.F., and Meyerowitz, E.M. (2000). Specific and heritable genetic interference by double-stranded RNA in *Arabidopsis thaliana*. Proc Natl Acad Sci U S A **97,** 4985-4990.

Collinge, D.B., Gregersen, P.L., and Thordal-Christensen, H. The nature and role of defense response genes in cereals. In: Belanger R.R., Bushnell W.R., Dik A.J., Carver T.L.W., editors. The powdery mildews: A comprehensive treatise. St Paul: APS Press; 2002. p. 146-160.

Collins, N.C., Thordal-Christensen, H., Lipka, V., Bau, S., Kombrink, E., Qiu, J.L., Hückelhoven, R., Stein, M., Freialdenhoven, A., Somerville, S.C., and Schulze-Lefert, P. (2003). SNARE-protein-mediated disease resistance at the plant cell wall. Nature **425,** 973-977.

Cossart, P., and Sansonetti, P.J. (2004). Bacterial invasion: The paradigms of enteroinvasive pathogens. Science **304,** 242-248.

Dai, S.P., Sarmiere, P.D., Wiggan, O., Bamburg, J.R., and Zhou, D.G. (2004). Efficient *Salmonella* entry requires activity cycles of host ADF and cofilin. Cell Microbiol. **6,** 459-471.

Daly, C.J., and McGrath, J.C. (2003). Fluorescent ligands, antibodies, and proteins for the study of receptors. Pharmacol. Ther. **100,** 101-118.

Dangl, J.L., and Jones, J.D. (2001). Plant pathogens and integrated defence responses to infection. Nature **411,** 826-833.

Darvill, A.G., and Albersheim, P. (1984). Phytoalexins and their elicitors - a defense against microbial infection in plants. Annu. Rev. Plant Physiol. Plant Molec. Biol. **35,** 243-275.

Deslandes, L., Olivier, J., Peeters, N., Feng, D.X., Khounlotham, M., Boucher, C., Somssich, L., Genin, S., and Marco, Y. (2003). Physical interaction between RRS1-R, a protein conferring resistance to bacterial wilt, and PopP2, a type III effector targeted to the plant nucleus. Proc. Natl. Acad. Sci. U. S. A. **100,** 8024-8029.

Devoto, A., Piffanelli, P., Nilsson, I., Wallin, E., Panstruga, R., von Heijne, G., and Schulze-Lefert, P. (1999). Topology, subcellular localization, and sequence diversity of the *Mlo* family in plants. J Biol Chem **274,** 34993-35004.

Devoto, A., Hartmann, H.A., Piffanelli, P., Elliott, C., Simmons, C., Taramino, G., Goh, C.S., Cohen, F.E., Emerson, B.C., Schulze-Lefert, P., and Panstruga, R. (2003). Molecular phylogeny and evolution of the plant-specific seven-transmembrane MLO family. J Mol Evol **56,** 77-88.

Dong, C.H., Kost, B., Xia, G., and Chua, N.H. (2001a). Molecular identification and characterization of the *Arabidopsis AtADF1, AtADF5 and AtADF6* genes. Plant Mol Biol **45,** 517-527.

Dong, C.H., Xia, G.X., Hong, Y., Ramachandran, S., Kost, B., and Chua, N.H. (2001b). ADF proteins are involved in the control of flowering and regulate F-actin organization, cell expansion, and organ growth in *Arabidopsis*. Plant Cell **13,** 1333-1346.

Dos Remedios, C.G., Chhabra, D., Kekic, M., Dedova, I.V., Tsubakihara, M., Berry, D.A., and Nosworthy, N.J. (2003). Actin binding proteins: Regulation of cytoskeletal microfilaments. Physiological Reviews **83,** 433-473.

Drøbak, B.K., Franklin-Tong, V.E., and Staiger, C.J. (2004). The role of the actin cytoskeleton in plant cell signalling. New Phytol. **163,** 13-30.

Eden, S., Rohatgi, R., Podtelejnikov, A.V., Mann, M., and Kirschner, M.W. (2002). Mechanism of regulation of WAVE1-induced actin nucleation by Rac1 and Nck. Nature **418,** 790-793.

El-Assal, S.E., Le, J., Basu, D., Mallery, E.L., and Szymanski, D.B. (2004a). *Arabidopsis GNARLED* encodes a NAP125 homolog that positively regulates *ARP2/3*. Curr. Biol. **14,** 1405-1409.

El-Assal, S.E., Le, J., Basu, D., Mallery, E.L., and Szymanski, D.B. (2004b). *DISTORTED2* encodes an ARPC2 subunit of the putative *Arabidopsis* ARP2/3 complex. Plant J. **38,** 526-538.

Elliott, C., Zhou, F., Spielmeyer, W., Panstruga, R., and Schulze-Lefert, P. (2002). Functional conservation of wheat and rice *Mlo* orthologs in defense modulation to the powdery mildew fungus. Mol Plant Microbe Interact **15,** 1069-1077.

Eulgem, T., Rushton, P.J., Robatzek, S., and Somssich, I.E. (2000). The WRKY superfamily of plant transcription factors. Trends in Plant Science **5,** 199-206.

Evangelista, M., Pruyne, D., Amberg, D.C., Boone, C., and Bretscher, A. (2002). Formins direct Arp2/3-independent actin filament assembly to polarize cell growth in yeast. Nat. Cell Biol. **4,** 32-41.

Falk, A., Feys, B.J., Frost, L.N., Jones, J.D.G., Daniels, M.J., and Parker, J.E. (1999). *EDS1*, an essential component of *R* gene-mediated disease resistance in *Arabidopsis* has homology to eukaryotic lipases. Proc. Natl. Acad. Sci. U. S. A. **96,** 3292-3297.

Fire, A., Xu, S.Q., Montgomery, M.K., Kostas, S.A., Driver, S.E., and Mello, C.C. (1998). Potent and specific genetic interference by double-stranded RNA in *Caenorhabditis elegans*. Nature **391,** 806-811.

Flor, H.H. (1971). Current status of gene-for-gene concept. Annu. Rev. Phytopathol. **9,** 275-296.

Folkers, U., Kirik, V., Schöbinger, U., Falk, S., Krishnakumar, S., Pollock, M.A., Oppenheimer, D.G., Day, I., Reddy, A.R., Jürgens, G., and Hülskamp, M. (2002). The cell morphogenesis gene *ANGUSTIFOLIA* encodes a CtBP/BARS-like protein and is involved in the control of the microtubule cytoskeleton. Embo J. **21,** 1280-1288.

Frank, M., Egile, C., Dyachok, J., Djakovic, S., Nolasco, M., Li, R., and Smith, L.G. (2004). Activation of Arp2/3 complex-dependent actin polymerization by plant proteins distantly related to Scar/WAVE. PNAS **101,** 16379-16384.

Freialdenhoven, A., Peterhänsel, C., Kurth, J., Kreuzaler, F., and Schulze-Lefert, P. (1996). Identification of genes required for the function of non-race-specific *mlo* resistance to powdery mildew in barley. Plant Cell **8,** 5-14.

Freisleben, R., and Lein, A. (1942). Über die Auffindung einer mehltauresistenten Mutante nach Röntgenbestrahlung einer anfälligen reinen Linie von Sommergerste. Naturwiss. **30,** 608.

Freytag, S., Arabatzis, N., Hahlbrock, K., and Schmelzer, E. (1994). Reversible cytoplasmic rearrangements precede wall apposition, hypersensitive cell-death and defense-related gene activation in potato *Phytophthora infestans* interactions. Planta **194,** 123-135.

Frye, C.A., and Innes, R.W. (1998). An *Arabidopsis* mutant with enhanced resistance to powdery mildew. Plant Cell **10,** 947-956.

Fu, Y., and Yang, Z.B. (2001). Rop GTPase: a master switch of cell polarity development in plants. Trends in Plant Science **6,** 545-547.

Galkin, V.E., Orlova, A., VanLoock, M.S., Zhou, D.G., Galan, J.E., and Egelman, E.H. (2002). The bacterial protein SipA polymerizes G-actin and mimics muscle nebulin. Nat. Struct. Biol. **9,** 518-521.

Gjetting, T., Carver, T.L.W., Skot, L., and Lyngkjær, M.F. (2004). Differential gene expression in individual papilla-resistant and powdery mildew-infected barley epidermal cells. Mol. Plant-Microbe Interact. **17,** 729-738.

Glazebrook, J. (2001). Genes controlling expression of defense responses in *Arabidopsis* - 2001 status. Curr. Opin. Plant Biol **4,** 301-308.

Glazebrook, J., Rogers, E.E., and Ausubel, F.M. (1996). Isolation of *Arabidopsis* mutants with enhanced disease susceptibility by direct screening. Genetics **143,** 973-982.

Gómez-Gómez, L., and Boller, T. (2002). Flagellin perception: a paradigm for innate immunity. Trends in Plant Science **7,** 251-256.

Görg, R., Hollricher, K., and Schulze-Lefert, P. (1993). Functional analysis and RFLP-mediated mapping of the *Mlg* resistance locus in barley. Plant J. **3,** 857-866.

Grant, M., Brown, I., Adams, S., Knight, M., Ainslie, A., and Mansfield, J. (2000). The RPM1 plant disease resistance gene facilitates a rapid and sustained increase in cytosolic calcium that is necessary for the oxidative burst and hypersensitive cell death. Plant J. **23,** 441-450.

Gregersen, P.L., Thordal-Christensen, H., Forster, H., and Collinge, D.B. (1997). Differential gene transcript accumulation in barley leaf epidermis and mesophyll in response to attack by *Blumeria graminis* f.sp. *hordei* (syn. *Erysiphe graminis* f.sp. *hordei*). Physiol. Mol. Plant Pathol. **51,** 85-97.

Green J.R., Carver T.L.W., and Gurr S.J. The formation and function of infection and feeding structures. In: Belanger R.R., Bushnell W.R., Dik A.J., Carver T.L.W., editors. The powdery mildews: A comprehensive treatise. St Paul: APS Press; 2002. p. 66-82.

Grosdent, N., Maridonneau-Parini, I., Sory, M.P., and Cornelis, G.R. (2002). Role of YopS and adhesins in resistance of *Yersinia enterocolitica* to phagocytosis. Infect. Immun. **70,** 4165-4176.

Gross, P., Julius, C., Schmelzer, E., and Hahlbrock, K. (1993). Translocation of cytoplasm and nucleus to fungal penetration sites is associated with depolymerization of microtubules and defense gene activation in infected, Cultured Parsley Cells. Embo J. **12,** 1735-1744.

Gungabissoon, R.A., and Bamburg, J.R. (2003). Regulation of growth cone actin dynamics by ADF/cofilin. J. Histochem. Cytochem. **51,** 411-420.

Gungabissoon, R.A., Jiang, C.-J., Drøbak, B.K., Maciver, S.K., and Hussey, P.J. (1998). Interaction of maize actin-depolymerising factor with actin and phosphoinositides and its inhibition of plant phospholipase C. Plant J **16,** 689 - 696.

Guo, W., Sacher, M., Barrowman, J., Ferro-Novick, S., and Novick, P. (2000). Protein complexes in transport vesicle targeting. Trends Cell Biol. **10,** 251-255.

Halterman, D., Zhou, F.S., Wei, F.S., Wise, R.P., and Schulze-Lefert, P. (2001). The MLA6 coiled-coil, NBS-LRR protein confers *AvrMla6*-dependent resistance specificity to *Blumeria graminis* f. sp *hordei* in barley and wheat. Plant J. **25,** 335-348.

Halterman, D.A., and Wise, R.P. (2004). A single amino acid substitution in the sixth leucine-rich repeat of barley MLA6 and MLA13 alleviates dependence on RAR1 for disease resistance signaling. Plant J. **38,** 215-226.

Halterman, D.A., Wei, F., and Wise, R.P. (2003). Powdery mildew-induced *Mla* mRNAs are alternatively spliced and contain multiple upstream open reading frames. Plant Physiol **131,** 558-567.

Hammond-Kosack, K.E., and Jones, J.D.G. (1997). Plant disease resistance genes. Annu. Rev. Plant Physiol. Plant Molec. Biol. **48,** 575-607.

Hammond-Kosack, K.E., and Parker, J.E. (2003). Deciphering plant-pathogen communication: fresh perspectives for molecular resistance breeding. Curr Opin Biotechnol **14,** 177-193.

Hardt, W.D., Chen, L.M., Schuebel, K.E., Bustelo, X.R., and Galan, J.E. (1998). *S. typhimurium* encodes an activator of Rho GTPases that induces membrane ruffling and nuclear responses in host cells. Cell **93,** 815-826.

Hawes, C.R., and Satiat-Jeunemaitre, B. (2001). Trekking along the cytoskeleton. Plant Physiol. **125,** 119-122.

Hazen, B.E., and Bushnell, W.R. (1983). Inhibition of the hypersensitive reaction in barley to powdery mildew by heat-shock and cytochalasin B. Physiological Plant Pathology **23,** 421-438.

Heath, I.B., and Heath, M.C. (1978). Microtubules and organelle movements in rust fungus *Uromyces phaseoli* var. *vignae*. Cytobiologie **16,** 393-411.

Heath, M.C. (1981). A generalized concept of host-parasite specificity. Phytopathology **71,** 1121-1123.

Heath, M.C. (2000). Non-host resistance and non-specific plant defenses. Curr Opin Plant Biol **3,** 315-319.

Heath, M.C., Nimchuk, Z.L., and Xu, H.X. (1997). Plant nuclear migrations as indicators of critical interactions between resistant or susceptible cowpea epidermal cells and invasion hyphae of the cowpea rust fungus. New Phytol. **135,** 689-700.

Heyworth, P.G., Robinson, J.M., Ding, J.B., Ellis, B.A., and Badwey, J.A. (1997). Cofilin undergoes rapid dephosphorylation in stimulated neutrophils and translocates to ruffled membranes enriched in products of the NADPH oxidase complex. Evidence for a novel cycle of phosphorylation and dephosphorylation. Histochem. Cell Biol. **108,** 221-233.

Higgs, H.N., and Pollard, T.D. (2001). Regulation of actin filament network formation through Arp2/3 complex: Activation by a diverse array of proteins. Annu. Rev. Biochem. **70,** 649-676.

Holmes, D.S., and Quigley, M. (1981). A Rapid Boiling Method for the Preparation of Bacterial Plasmids. Anal. Biochem. **114,** 193-197.

Hückelhoven, R., and Kogel, K.H. (2003). Reactive oxygen intermediates in plant-microbe interactions: who is who in powdery mildew resistance? Planta **216,** 891-902.

Hückelhoven, R., Trujillo, M., and Kogel, K.H. (2000). Mutations in *Ror1* and *Ror2* genes cause modification of hydrogen peroxide accumulation in mlo-barley under attack from the powdery mildew fungus. Mol Plant Pathol **1,** 287-292.

Hückelhoven, R., Dechert, C., and Kogel, K.H. (2001). Non-host resistance of barley is associated with a hydrogen peroxide burst at sites of attempted penetration by wheat powdery mildew fungus. Mol Plant Pathol **2,** 199-205.

Hückelhoven, R., Fodor, J., Preis, C., and Kogel, K.H. (1999). Hypersensitive cell death and papilla formation in barley attacked by the powdery mildew fungus are associated with hydrogen peroxide but not with salicylic acid accumulation. Plant Physiol **119,** 1251-1260.

Huitema, E., Vleeshouwers, V., Francis, D.M., and Kamoun, S. (2003). Active defence responses associated with non-host resistance of *Arabidopsis thaliana* to the oomycete pathogen *Phytophthora infestans*. Molecular Plant Pathology **4,** 487-500.

Hülskamp, M., Misera, S., and Jürgens, G. (1994). Genetic dissection of trichome cell-development in *Arabidopsis*. Cell **76,** 555-566.

Hussey, P.J., Allwood, E.G., and Smertenko, A.P. (2002). Actin-binding proteins in the *Arabidopsis* genome database: properties of functionally distinct plant actin-depolymerizing factors/cofilins. Philosophical Transactions of the Royal Society of London - Series B: Biological Sciences **357,** 791-798.

Hussey, P.J., Yuan, M., Calder, G., Khan, S., and Lloyd, C.W. (1998). Microinjection of pollen-specific actin-depolymerizing factor, ZmADF1, reorientates F-actin strands in *Tradescantia* stamen hair cells. Plant J. **14,** 353-357.

Iida, K., and Yahara, I. (1999). Cooperation of two actin-binding proteins, cofilin and Aip1, in Saccharomyces cerevisiae. Genes Cells **4,** 21-32.

Jacobs, A.K., Lipka, V., Burton, R.A., Panstruga, R., Strizhov, N., Schulze-Lefert, P., and Fincher, G.B. (2003). An *Arabidopsis* callose synthase, GSL5, is required for wound and papillary callose formation. Plant Cell **15,** 2503-2513.

Janßen, M., Hunte, C., Schulz, M., and Schnabl, H. (1996). Tissue specification and intracellular distribution of actin isoforms in *Vicia faba* L. Protoplasma **191,** 158-163.

Jares-Erijman, E.A., and Jovin, T.M. (2003). FRET imaging. Nat. Biotechnol. **21,** 1387-1395.

Jarosch, B., Kogel, K.H., and Schaffrath, U. (1999). The ambivalence of the barley *Mlo* locus: Mutations conferring resistance against powdery mildew (*Blumeria graminis* f. sp. *hordei*) enhance susceptibility to the rice blast fungus *Magnaporthe grisea*. Mol. Plant-Microbe Interact. **12,** 508-514.

Jarosch, B., Jansen, M., and Schaffrath, U. (2003). Acquired resistance functions in mlo barley, which is hypersusceptible to *Magnaporthe grisea*. Mol Plant Microbe Interact **16,** 107-114.

Jedd, G., and Chua, N.H. (2002). Visualization of peroxisomes in living plant cells reveals acto-myosin-dependent cytoplasmic streaming and peroxisome budding. Plant Cell Physiol **43,** 384-392.

Jia, Y., McAdams, S.A., Bryan, G.T., Hershey, H.P., and Valent, B. (2000). Direct interaction of resistance gene and avirulence gene products confers rice blast resistance. Embo J. **19,** 4004-4014.

Jiang, C.J., Weeds, A.G., Khan, S., and Hussey, P.J. (1997). F-actin and G-actin binding are uncoupled by mutation of conserved tyrosine residues in maize actin depolymerizing factor (ZmADF). Proc. Natl. Acad. Sci. U. S. A. **94,** 9973-9978.

Jones, D.A., and Takemoto, D. (2004). Plant innate immunity - direct and indirect recognition of general and specific pathogen-associated molecules. Curr. Opin. Immunol. **16,** 48-62.

Jørgensen, J.H. (1976) Identification of powdery mildew resistant barley mutants and their allelic relationship. In: Barley Genetics III, Karl Thiemig, München pp. 446–455.

Jørgensen, J.H. (1992). Discovery, characterization and exploitation of *Mlo* powdery mildew resistance in barley. Euphytica **63,** 141-152.

Jørgensen, J.H. (1994). Genetics of Powdery Mildew Resistance in Barley. Crit. Rev. Plant Sci. **13,** 97-119.

Kandasamy, M.K., Deal, R.B., McKinney, E.C., and Meagher, R.B. (2004). Plant actin-related proteins. Trends in Plant Science **9,** 196-202.

Kang, L., Li, J., Zhao, T., Xiao, F., Tang, X., Thilmony, R., He, S., and Zhou, J.M. (2003). Interplay of the *Arabidopsis* non-host resistance gene *NHO1* with bacterial virulence. Proc Natl Acad Sci U S A **100,** 3519-3524.

Kanzaki, H., Saitoh, H., Ito, A., Fujisawa, S., Kamoun, S., Katou, S., Yoshioka, H., and Terauchi, R. (2003). Cytosolic HSP90 and HSP70 are essential components of INF1-mediated hypersensitive response and non-host resistance to Pseudomonas cichorii in Nicotiana benthamiana. Molecular Plant Pathology **4,** 383-391.

Kasschau, K.D., and Carrington, J.C. (1998). A counterdefensive strategy of plant viruses: Suppression of posttranscriptional gene silencing. Cell **95,** 461-470.

Kenrick, P., and Crane, P.R. (1997). The origin and early evolution of plants on land. Nature **389,** 33-39.

Ketelaar, T., de Ruijter, N.C.A., and Emons, A.M.C. (2003). Unstable F-actin specifies the area and microtubule direction of cell expansion in *Arabidopsis* root hairs. Plant Cell **15,** 285-292.

Ketelaar, T., Allwood, E.G., Anthony, R., Voigt, B., Menzel, D., and Hussey, P.J. (2004). The actin-interacting protein AIP1 is essential for actin organization and plant development. Curr. Biol. **14,** 145-149.

Khaitlina, S.Y., Efremova, T.N., and Komissarchik, Y.Y. (2003). Actin dynamics during bacterial invasion of eukaryotic cells. Biol. Membr. **20,** 33-39.

Kim, M.C., Panstruga, R., Elliott, C., Müller, J., Devoto, A., Yoon, H.W., Park, H.C., Cho, M.J., and Schulze-Lefert, P. (2002a). Calmodulin interacts with MLO protein to regulate defence against mildew in barley. Nature **416,** 447-451.

Kim, M.C., Lee, S.H., Kim, J.K., Chun, H.J., Choi, M.S., Chung, W.S., Moon, B.C., Kang, C.H., Park, C.Y., Yoo, J.H., Kang, Y.H., Koo, S.C., Koo, Y.D., Jung, J.C., Kim, S.T., Schulze-Lefert, P., Lee, S.Y., and Cho, M.J. (2002b). *Mlo*, a modulator of plant defense and cell death, is a novel calmodulin-binding protein - Isolation and characterization of a rice *Mlo* homologue. J. Biol. Chem. **277,** 19304-19314.

Kobayashi, I., Kobayashi, Y., and Hardham, A.R. (1994). Dynamic reorganization of microtubules and microfilaments in flax cells during the resistance response to flax rust infection. Planta **195,** 237-247.

Kobayashi, Y., Yamada, M., Kobayashi, I., and Kunoh, H. (1997a). Actin microfilaments are required for the expression of non-host resistance in higher plants. Plant & Cell Physiology **38,** 725-733.

Kobayashi, Y., Kobayashi, I., Funaki, Y., Fujimoto, S., Takemoto, T., and Kunoh, H. (1997b). Dynamic reorganization of microfilaments and microtubules is necessary for the expression of non-host resistance in barley coleoptile cells. Plant J **11,** 525-537.

Koprek, T., McElroy, D., Louwerse, J., Williams-Carrier, R., and Lemaux, P.G. (2000). An efficient method for dispersing Ds elements in the barley genome as a tool for determining gene function. Plant J. **24,** 253-263.

Kovar, D.R., Gibbon, B.C., McCurdy, D.W., and Staiger, C.J. (2001). Fluorescently-labeled fimbrin decorates a dynamic actin filament network in live plant cells. Planta **213,** 390-395.

Kreis, T., and Vale, R. Guidebook to the cytoskeletal and motor proteins, 2nd edition. (New York, U.S.A.: Oxford University Press, 1999)

Kumar, J., Hückelhoven, R., Beckhove, U., Nagarajan, S., and Kogel, K.H. (2001). A compromised *Mlo* pathway affects the response of barley to the necrotrophic fungus *Bipolaris sorokiniana* (Teleomorph : *Cochliobolus sativus*) and its toxins. Phytopathology **91,** 127-133.

Kunoh, H., Aist, J.R., and Hayashimoto, A. (1985). The occurrence of cytoplasmic aggregates induced by *Erysiphe pisi* in barley coleoptile cells before the host-cell walls are penetrated. Physiological Plant Pathology **26,** 199-207.

Lauber, M.H., Waizenegger, I., Steinmann, T., Schwarz, H., Mayer, U., Hwang, I., Lukowitz, W., and Jurgens, G. (1997). The *Arabidopsis* KNOLLE protein is a cytokinesis-specific syntaxin. J. Cell Biol. **139,** 1485-1493.

Levine, A., Tenhaken, R., Dixon, R., and Lamb, C. (1994). H_2O_2 from the Oxidative Burst Orchestrates the Plant Hypersensitive Disease Resistance Response. Cell **79,** 583-593.

Li, Y., Sorefan, K., Hemmann, G., and Bevan, M.W. (2004). Arabidopsis NAP and PIR Regulate Actin-Based Cell Morphogenesis and Multiple Developmental Processes. Plant Physiol. **136,** 3616-3627.

Lilic, M., Galkin, V.E., Orlova, A., VanLoock, M.S., Egelman, E.H., and Stebbins, C.E. (2003). *Salmonella* SipA polymerizes actin by stapling filaments with nonglobular protein arms. Science **301,** 1918-1921.

Lin, M.R., and Edwards, H.H. (1974). Primary penetration process in powdery mildewed barley related to host-cell age, cell type, and occurrence of basic staining material. New Phytol. **73,** 131-137.

Lopez, I., Anthony, R.G., Maciver, S.K., Jiang, C.J., Khan, S., Weeds, A.G., and Hussey, P.J. (1996). Pollen specific expression of maize genes encoding actin depolymerizing factor-like proteins. Proc Natl Acad Sci U S A **93,** 7415-7420.

Lu, M., Tang, X.Y., and Zhou, J.M. (2001). *Arabidopsis* NHO1 is required for general resistance against Pseudomonas bacteria. Plant Cell **13,** 437-447.

Lu, R., Martin-Hernandez, A.M., Peart, J.R., Malcuit, I., and Baulcombe, D.C. (2003a). Virus-induced gene silencing in plants. Methods **30,** 296-303.

Lu, R., Malcuit, I., Moffett, P., Ruiz, M.T., Peart, J., Wu, A.J., Rathjen, J.P., Bendahmane, A., Day, L., and Baulcombe, D.C. (2003b). High throughput virus-induced gene silencing implicates heat shock protein 90 in plant disease resistance. Embo J. **22,** 5690-5699.

Ludwig, A.A., Romeis, T., and Jones, J.D.G. (2004). CDPK-mediated signalling pathways: specificity and cross-talk. J. Exp. Bot. **55,** 181-188.

Mabuchi, I. (1983). An actin-depolymerizing protein (Depactin) from starfish oocytes - properties and interaction with actin. J. Cell Biol. **97,** 1612-1621.

Machesky, L.M., and Gould, K.L. (1999). The Arp2/3 complex: a multifunctional actin organizer. Curr. Opin. Cell Biol. **11,** 117-121.

Maciver, S.K., and Hussey, P.J. (2002). The ADF/cofilin family: actin-remodeling proteins. Genome Biol **3,** reviews3007.

Maciver, S.K., Pope, B.J., Whytock, S., and Weeds, A.G. (1998). The effect of two actin depolymerizing factors (ADF/cofilins) on actin filament turnover: pH sensitivity of F-actin binding by human ADF, but not of Acanthamoeba actophorin. Eur. J. Biochem. **256,** 388-397.

Martin, C., Bhatt, K., and Baumann, K. (2001). Shaping in plant cells. Curr. Opin. Plant Biol **4,** 540-549.

Mathur, J., and Hülskamp, M. (2002). Microtubules and microfilaments in cell morphogenesis in higher plants. Curr. Biol. **12,** R669-R676.

Mathur, J., Mathur, N., and Hülskamp, M. (2002). Simultaneous visualization of peroxisomes and cytoskeletal elements reveals actin and not microtubule-based peroxisome motility in plants. Plant Physiol **128,** 1031-1045.

Mathur, J., Spielhofer, P., Kost, B., and Chua, N.H. (1999). The actin cytoskeleton is required to elaborate and maintain spatial patterning during trichome cell morphogenesis in *Arabidopsis thaliana*. Development **126,** 5559-5568.

Mathur, J., Mathur, N., Kernebeck, B., and Hülskamp, M. (2003a). Mutations in actin-related proteins 2 and 3 affect cell shape development in *Arabidopsis*. Plant Cell **15,** 1632-1645.

Mathur, J., Mathur, N., Kirik, V., Kernebeck, B., Srinivas, B.P., and Hülskamp, M. (2003b). *Arabidopsis* CROOKED encodes for the smallest subunit of the ARP2/3 complex and controls cell shape by region specific fine F-actin formation. Development **130,** 3137-3146.

McCann, R.O., and Craig, S.W. (1997). The I/LWEQ module: a conserved sequence that signifies F-actin binding in functionally diverse proteins from yeast to mammals. Proc Natl Acad Sci U S A **94,** 5679-5684.

McGhie, E.J., Hayward, R.D., and Koronakis, V. (2001). Cooperation between actin-binding proteins of invasive Salmonella: SipA potentiates SipC nucleation and bundling of actin. Embo J. **20,** 2131-2139.

McGhie, E.J., Hayward, R.D., and Koronakis, V. (2004). Control of actin turnover by a Salmonella invasion protein. Mol. Cell **13,** 497-510.

McLusky, S.R., Bennett, M.H., Beale, M.H., Lewis, M.J., Gaskin, P., and Mansfield, J.W. (1999). Cell wall alterations and localized accumulation of feruloyl-3 '-methoxytyramine in onion epidermis at sites of attempted penetration by Botrytis allii are associated with actin polarisation, peroxidase activity and suppression of flavonoid biosynthesis. Plant J. **17,** 523-534.

Mellersh, D.G., Foulds, I.V., Higgins, V.J., and Heath, M.C. (2002). H_2O_2 plays different roles in determining penetration failure in three diverse plant-fungal interactions. Plant J **29,** 257-268.

Moriyama, K., Iida, K., and Yahara, I. (1996). Phosphorylation of Ser-3 of cofilin regulates its essential function on actin. Genes Cells **1,** 73-86.

Mullen, R.T., and Trelease, R.N. (2000). The sorting signals for peroxisomal membrane-bound ascorbate peroxidase are within its C-terminal tail. J. Biol. Chem. **275,** 16337-16344.

Murphy, A.M., PryceJones, E., Johnstone, K., and Ashby, A.M. (1997). Comparison of cytokinin production in vitro by Pyrenopeziza brassicae with other plant pathogens. Physiol. Mol. Plant Pathol. **50,** 53-65.

Mysore, K.S., and Ryu, C.M. (2004). Nonhost resistance: how much do we know? Trends in Plant Science **9,** 97-104.

Nebenführ, A., and Staehelin, L.A. (2001). Mobile factories: Golgi dynamics in plant cells. Trends in Plant Science **6,** 160-167.

Nebenführ, A., Gallagher, L.A., Dunahay, T.G., Frohlick, J.A., Mazurkiewicz, A.M., Meehl, J.B., and Staehelin, L.A. (1999). Stop-and-go movements of plant Golgi stacks are mediated by the acto-myosin system. Plant Physiol **121,** 1127-1142.

Nelson, A.J., and Bushnell, W.R. (1997). Transient expression of anthocyanin genes in barley epidermal cells: Potential for use in evaluation of disease response genes. Transgenic Res. **6,** 233-244.

Nhieu, G.T., Clair, C., Grompone, G., and Sansonetti, P. (2004). Calcium signalling during cell interactions with bacterial pathogens. Biol. Cell **96,** 93-101.

Nielsen, K., Olsen, O., and Oliver, R. (1999). A transient expression system to assay putative antifungal genes on powdery mildew infected barley leaves. Physiol. Mol. Plant Pathol. **54,** 1-12.

Nishimura, M.T., Stein, M., Hou, B.H., Vogel, J.P., Edwards, H., and Somerville, S.C. (2003). Loss of a callose synthase results in salicylic acid-dependent disease resistance. Science **301,** 969-972.

Niwa, R., Nagata-Ohashi, K., Takeichi, M., Mizuno, K., and Uemura, T. (2002). Control of actin reorganization by Slingshot, a family of phosphatases that dephosphorylate ADF/cofilin. Cell **108,** 233-246.

Nobes, C.D., and Hall, A. (1995). Rho, Rac, and Cdc42 GTPases regulate the assembly of multimolecular focal complexes associated with actin stress fibers, lamellipodia, and filopodia. Cell **81,** 53-62.

Nover, I., and Schwarzbach, E. (1971) Inheritance studies with a mildew resistant barley mutant. Barley Genet. Newsl. **1,** 36-37

Nürnberger, T., Brunner, F., Kemmerling, B., and Piater, L. (2004). Innate immunity in plants and animals: striking similarities and obvious differences. Immunol. Rev. **198,** 249-266.

Okada, K., Obinata, T., and Abe, H. (1999). XAIP1: a Xenopus homologue of yeast actin interacting protein 1 (AIP1), which induces disassembly of actin filaments cooperatively with ADF cofilin family proteins. J. Cell Sci. **112,** 1553-1565.

Ono, E., Wong, H.L., Kawasaki, T., Hasegawa, M., Kodama, O., and Shimamoto, K. (2001). Essential role of the small GTPase Rac in disease resistance of rice. Proc. Natl. Acad. Sci. U. S. A. **98,** 759-764.

Ono, K., Parast, M., Alberico, C., Benian, G.M., and Ono, S. (2003). Specific requirement for two ADF/cofilin isoforms in distinct actin-dependent processes in *Caenorhabditis elegans*. J. Cell Sci. **116,** 2073-2085.

Opalski, K.S., Schultheiss, H., Kogel, K.H., and Hückelhoven, R. (2004) The receptor-like MLO protein and the RAC/ROP family G-protein RACB modulate actin reorganization in barley attacked by the biotrophic powdery mildew fungus *Blumeria graminis* f.sp. *hordei*. Plant Journal, in press.

Ouellet, F., Carpentier, E., Cope, M., Monroy, A.F., and Sarhan, F. (2001). Regulation of a wheat actin-depolymerizing factor during cold acclimation. Plant Physiol. **125,** 360-368.

Panchuk-Voloshina, N., Haugland, R.P., Bishop-Stewart, J., Bhalgat, M.K., Millard, P.J., Mao, F., and Leung, W.Y. (1999). Alexa dyes, a series of new fluorescent dyes that yield exceptionally bright, photostable conjugates. J Histochem Cytochem **47,** 1179-1188.

Pandey, S., and Assmann, S.M. (2004). The *Arabidopsis* putative G protein-coupled receptor GCR1 interacts with the G protein alpha subunit GPA1 and regulates abscisic acid signaling. Plant Cell **16,** 1616-1632.

Panstruga, R. (2003). Establishing compatibility between plants and obligate biotrophic pathogens. Curr. Opin. Plant Biol **6,** 320-326.

Panstruga, R. (2004). A golden shot: how ballistic single cell transformation boosts the molecular analysis of cereal-mildew interactions. Molecular Plant Pathology **5,** 141-148.

Panstruga, R., and Schulze-Lefert, P. (2003). Corruption of host seven-transmembrane proteins by pathogenic microbes: a common theme in animals and plants? Microbes Infect **5,** 429-437.

Panstruga, R., Kim, M.C., Cho, M.J., and Schulze-Lefert, P. (2003). Testing the efficiency of dsRNAi constructs in vivo: a transient expression assay based on two fluorescent proteins. Mol Biol Rep **30,** 135-140.

Parker, J.E., Holub, E.B., Frost, L.N., Falk, A., Gunn, N.D., and Daniels, M.J. (1996). Characterization of *eds1*, a mutation in *Arabidopsis* suppressing resistance to *Peronospora parasitica* specified by several different RPP genes. Plant Cell **8,** 2033-2046.

Peart, J.R., Lu, R., Sadanandom, A., Malcuit, I., Moffett, P., Brice, D.C., Schauser, L., Jaggard, D.A.W., Xiao, S.Y., Coleman, M.J., Dow, M., Jones, J.D.G., Shirasu, K., and Baulcombe, D.C. (2002). Ubiquitin ligase-associated protein SGT1 is required for host and nonhost disease resistance in plants. Proc. Natl. Acad. Sci. U. S. A. **99,** 10865-10869.

Pederson, K.J., Krall, R., Riese, M.J., and Barbieri, J.T. (2002). Intracellular localization modulates targeting of ExoS, a type III cytotoxin, to eukaryotic signalling proteins. Mol Microbiol **46,** 1381-1390.

Penninckx, I., Eggermont, K., Terras, F.R.G., Thomma, B., DeSamblanx, G.W., Buchala, A., Metraux, J.P., Manners, J.M., and Broekaert, W.F. (1996). Pathogen-induced systemic activation of a plant defensin gene in *Arabidopsis* follows a salicylic acid-independent pathway. Plant Cell **8,** 2309-2323.

Peterhänsel, C., Freialdenhoven, A., Kurth, J., Kolsch, R., and Schulze-Lefert, P. (1997). Interaction analyses of genes required for resistance responses to powdery mildew in barley reveal distinct pathways leading to leaf cell death. Plant Cell **9,** 1397-1409.

Pierce, K.L., Premont, R.T., and Lefkowitz, R.J. (2002). Seven-transmembrane receptors. Nat Rev Mol Cell Biol **3,** 639-650.

Piffanelli, P., Zhou, F., Casais, C., Orme, J., Jarosch, B., Schaffrath, U., Collins, N.C., Panstruga, R., and Schulze-Lefert, P. (2002). The barley MLO modulator of defense and cell death is responsive to biotic and abiotic stress stimuli. Plant Physiol **129,** 1076-1085.

Plakidou-Dymock, S., Dymock, D., and Hooley, R. (1998). A higher plant seven-transmembrane receptor that influences sensitivity to cytokinins. Curr. Biol. **8,** 315-324.

Pratelli, J., Sutter, J.U., and Blatt, M.R. (2004). A new catch in the SNARE. Trends in Plant Science **9,** 187-195.

Reddy, V.S., Ali, G.S., and Reddy, A.S.N. (2003). Characterization of a pathogen-induced calmodulin-binding protein: mapping of four Ca^{2+}-dependent calmodulin-binding domains. Plant Mol.Biol. **52,** 143-159.

Reumann, S. (2004). Specification of the peroxisome targeting signals type 1 and type 2 of plant peroxisomes by bioinformatics analyses. Plant Physiol. **135,** 783-800.

Robinson, R.C., Turbedsky, K., Kaiser, D.A., Marchand, J.B., Higgs, H.N., Choe, S., and Pollard, T.D. (2001). Crystal structure of Arp2/3 complex. Science **294,** 1679-1684.

Rogers, S.L., and Gelfand, V.I. (2000). Membrane trafficking, organelle transport, and the cytoskeleton. Curr. Opin. Cell Biol. **12,** 57-62.

Romeis, T., Ludwig, A.A., Martin, R., and Jones, J.D.G. (2001). Calcium-dependent protein kinases play an essential role in a plant defence response. Embo J. **20,** 5556-5567.

Rushton, P.J., Reinstadler, A., Lipka, V., Lippok, B., and Somssich, I.E. (2002). Synthetic plant promoters containing defined regulatory elements provide novel insights into pathogen- and wound-induced signaling. Plant Cell **14,** 749-762.

Saedler, R., Mathur, N., Srinivas, B.P., Kernebeck, B., Hülskamp, M., and Mathur, J. (2004). Actin control over microtubules suggested by *DISTORTED2* encoding the *Arabidopsis* ARPC2 subunit homolog. Plant Cell Physiol. **45,** 813-822.

Sanger, F., Nickle, S., and Coulsen, A.R., (1977). DNA sequencing with chain terminating inhibitors. Proc. Natl. Acad. Sci. U. S. A. **71,** 5463-5467.

Schenk, P.M., Kazan, K., Wilson, I., Anderson, J.P., Richmond, T., Somerville, S.C., and Manners, J.M. (2000). Coordinated plant defense responses in *Arabidopsis* revealed by microarray analysis. Proc. Natl. Acad. Sci. U. S. A. **97,** 11655-11660.

Schmelzer, E. (2002). Cell polarization, a crucial process in fungal defence. Trends Plant Sci **7,** 411-415.

Schultheiss, H., Dechert, C., Kogel, K.H., and Hückelhoven, R. (2002). A small GTP-binding host protein is required for entry of powdery mildew fungus into epidermal cells of barley. Plant Physiol **128,** 1447-1454.

Schultheiss, H., Dechert, C., Kogel, K.H., and Hückelhoven, R. (2003). Functional analysis of barley RAC/ROP G-protein family members in susceptibility to the powdery mildew fungus. Plant J **36,** 589-601.

Schulze-Lefert, P. (2004). Plant immunity: The origami of receptor activation. Curr. Biol. **14,** R22-R24.

Schulze-Lefert, P., and Vogel, J. (2000). Closing the ranks to attack by powdery mildew. Trends Plant Sci **5,** 343-348.

Schwab, B., Mathur, J., Saedler, R.R., Schwarz, H., Frey, B., Scheidegger, C., and Hülskamp, M. (2003). Regulation of cell expansion by the DISTORTED genes in *Arabidopsis thaliana*: actin controls the spatial organization of microtubules. Mol. Genet. Genomics **269,** 350-360.

Schweizer, P., Pokorny, J., Abderhalden, O., and Dudler, R. (1999). A transient assay system for the functional assessment of defense-related genes in wheat. Mol. Plant-Microbe Interact. **12,** 647-654.

Schweizer, P., Pokorny, J., Schulze-Lefert, P., and Dudler, R. (2000). Technical advance. Double-stranded RNA interferes with gene function at the single-cell level in cereals. Plant J **24,** 895-903.

Shao, F., Merritt, P.M., Bao, Z., Innes, R.W., and Dixon, J.E. (2002). A *Yersinia* effector and a *Pseudomonas* avirulence protein define a family of cysteine proteases functioning in bacterial pathogenesis. Cell **109,** 575-588.

Shao, F., Vacratsis, P.O., Bao, Z., Bowers, K.E., Fierke, C.A., and Dixon, J.E. (2003a). Biochemical characterization of the *Yersinia* YopT protease: cleavage site and recognition elements in Rho GTPases. Proc Natl Acad Sci U S A **100,** 904-909.

Shao, F., Golstein, C., Ade, J., Stoutemyer, M., Dixon, J.E., and Innes, R.W. (2003b). Cleavage of *Arabidopsis* PBS1 by a bacterial type III effector. Science **301,** 1230-1233.

Shen, Q.H., Zhou, F., Bieri, S., Haizel, T., Shirasu, K., and Schulze-Lefert, P. (2003). Recognition specificity and RAR1/SGT1 dependence in barley *Mla* disease resistance genes to the powdery mildew fungus. Plant Cell **15,** 732-744.

Shirasu, K., Nielsen, K., Piffanelli, P., Oliver, R., and Schulze-Lefert, P. (1999a). Cell-autonomous complementation of *mlo* resistance using a biolistic transient expression system. Plant J **17,** 293-299.

Shirasu, K., Lahaye, T., Tan, M.W., Zhou, F., Azevedo, C., and Schulze-Lefert, P. (1999b). A novel class of eukaryotic zinc-binding proteins is required for disease resistance signaling in barley and development in *C. elegans.* Cell **99,** 355-366.

Sijen, T., Fleenor, J., Simmer, F., Thijssen, K.L., Parrish, S., Timmons, L., Plasterk, R.H., and Fire, A. (2001). On the role of RNA amplification in dsRNA-triggered gene silencing. Cell **107,** 465-476.

Skalamera, D., and Heath, M.C. (1996). Cellular mechanisms of callose deposition in response to fungal infection or chemical damage. Can. J. Bot.-Rev. Can. Bot. **74,** 1236-1242.

Skalamera, D., and Heath, M.C. (1998). Changes in the cytoskeleton accompanying infection-induced nuclear movements and the hypersensitive response in plant cells invaded by rust fungi. Plant J **16,** 191-200.

Skou, J.P. (1982). Callose formation responsible for the powdery mildew resistance in barley with genes in the Ml-o locus. Phytopathologische Zeitschrift-Journal of Phytopathology **104,** 90-95.

Skou, J.P., Jorgensen, J.H., and Lilholt, U. (1984). Comparative studies on callose formation in powdery mildew compatible and incompatible barley. Phytopathologische Zeitschrift-Journal of Phytopathology **109,** 147-168.

Smertenko, A.P., Jiang, C.J., Simmons, N.J., Weeds, A.G., Davies, D.R., and Hussey, P.J. (1998). Ser6 in the maize actin-depolymerizing factor, ZmADF3, is phosphorylated by a calcium-stimulated protein kinase and is essential for the control of functional activity. Plant J **14,** 187-193.

Smertenko, A.P., Allwood, E.G., Khan, S., Jiang, C.J., Maciver, S.K., Weeds, A.G., and Hussey, P.J. (2001). Interaction of pollen-specific actin-depolymerizing factor with actin. Plant J. **25,** 203-212.

Smith, L.G., and Li, R. (2004). Actin polymerization: Riding the wave. Curr. Biol. **14,** R109-R111.

Smith, N.A., Singh, S.P., Wang, M.B., Stoutjesdijk, P.A., Green, A.G., and Waterhouse, P.M. (2000). Total silencing by intron-spliced hairpin RNAs. Nature **407,** 319-320.

Song, W.Y., Wang, G.L., Chen, L.L., Kim, H.S., Pi, L.Y., Holsten, T., Gardner, J., Wang, B., Zhai, W.X., Zhu, L.H., Fauquet, C., and Ronald, P. (1995). A receptor kinase-like protein encoded by the rice disease resistance gene, *Xa21.* Science **270,** 1804-1806.

Stagljar, I., Korostensky, C., Johnsson, N., and te Heesen, S. (1998). A genetic system based on split-ubiquitin for the analysis of interactions between membrane proteins in vivo. Proc. Natl. Acad. Sci. U. S. A. **95,** 5187-5192.

Staiger, C.J. (2000). Signaling to the actin cytoskeleton in plants. Annu. Rev. Plant Physiol. Plant Molec. Biol **51,** 257-288.

Staiger, C.J., and Hussey, P.J. 2004. Actin and actin-modulating proteins. In: Hussey PJ, ed. The plant cytoskeleton in cell differentiation and development. Oxford, UK: Blackwell, 32-80.

Stolzenburg, M.C., Aist, J.R., and Israel, H.W. (1984). The role of papillae in resistance to powdery mildew conditioned by the *Ml-o* gene in barley .1. Correlative Evidence. Physiological Plant Pathology **25,** 337-346.

Stone, B.A., and Clarke, A.E.. Chemistry and biology of (1→3)-D-glucans. (Victoria, Australia: La Trobe University Press; 1992.

Svitkina, T.M., and Borisy, G.G. (1999). Arp2/3 complex and actin depolymerizing factor cofilin in dendritic organization and treadmilling of actin filament array in lamellipodia. J. Cell Biol. **145,** 1009-1026.

Swiderski, M.R., and Innes, R.W. (2001). The *Arabidopsis* PBS1 resistance gene encodes a member of a novel protein kinase subfamily. Plant J. **26,** 101-112.

Takemoto, D., Jones, D.A., and Hardham, A.R. (2003). GFP-tagging of cell components reveals the dynamics of subcellular re-organization in response to infection of *Arabidopsis* by oomycete pathogens. Plant J **33,** 775-792.

Takemoto, D., Maeda, H., Yoshioka, H., Doke, N., and Kawakita, K. (1999). Effect of cytochalasin D on defense responses of potato tuber discs treated with hyphal wall components of *Phytophthora infestans*. Plant Sci. **141,** 219-226.

Takenawa, T., and Itoh, T. (2001). Phosphoinositides, key molecules for regulation of actin cytoskeletal organization and membrane traffic from the plasma membrane. Biochim. Biophys. Acta Mol. Cell Biol. Lipids **1533,** 190-206.

Tavernarakis, N., Wang, S.L., Dorovkov, M., Ryazanov, A., and Driscoll, M. (2000). Heritable and inducible genetic interference by double-stranded RNA encoded by transgenes. Nat Genet **24,** 180-183.

Thomma, B., Cammue, B.P.A., and Thevissen, K. (2002). Plant defensins. Planta **216,** 193-202.

Thordal-Christensen, H. (2003). Fresh insights into processes of nonhost resistance. Curr Opin Plant Biol **6,** 351-357.

Thordal-Christensen, H., Zhang, Z.G., Wei, Y.D., and Collinge, D.B. (1997). Subcellular localization of H_2O_2 in plants. H_2O_2 accumulation in papillae and hypersensitive response during the barley-powdery mildew interaction. Plant J. **11,** 1187-1194.

Tijsterman, M., Ketting, R.F., and Plasterk, R.H.A. (2002). The genetics of RNA silencing. Annu. Rev. Genet. **36,** 489-519.

Torres, M.A., Dangl, J.L., and Jones, J.D.G. (2002). *Arabidopsis* gp91(phox) homologues *AtrbohD* and *AtrbohF* are required for accumulation of reactive oxygen intermediates in the plant defense response. Proc. Natl. Acad. Sci. U. S. A. **99,** 517-522.

Toshima, J., Toshima, J.Y., Takeuchi, K., Mori, R., and Mizuno, K. (2001a). Cofilin phosphorylation and actin reorganization activities of testicular protein kinase 2 and its predominant expression in testicular Sertoli cells. J. Biol. Chem. **276,** 31449-31458.

Toshima, J., Toshima, J.Y., Amano, T., Yang, N., Narumiya, S., and Mizuno, K. (2001b). Cofilin phosphorylation by protein kinase testicular protein kinase 1 and its role in integrin-mediated actin reorganization and focal adhesion formation. Mol. Biol. Cell **12,** 1131-1145.

Turner, M., and Schuch, W. (2000). Post-transcriptional gene-silencing and RNA interference: genetic immunity, mechanisms and applications. J. Chem. Technol. Biotechnol. **75,** 869-882.

Underhill, D.M., and Ozinsky, A. (2002). Toll-like receptors: key mediators of microbe detection. Curr. Opin. Immunol. **14,** 103-110.

Van Breusegem, F., Vranova, E., Dat, J.F., and Inze, D. (2001). The role of active oxygen species in plant signal transduction. Plant Sci. **161,** 405-414.

van der Biezen, E.A., and Jones, J.D.G. (1998). Plant disease-resistance proteins and the gene-for-gene concept. Trends Biochem.Sci. **23,** 454-456.

van Wees, S.C.M., Chang, H.S., Zhu, T., and Glazebrook, J. (2003). Characterization of the early response of *Arabidopsis* to *Alternaria brassicicola* infection using expression profiling. Plant Physiol. **132,** 606-617.

Vaucheret, H., Beclin, C., and Fagard, M. (2001). Post-transcriptional gene silencing in plants. J Cell Sci **114,** 3083-3091.

Vogel, J.P., Raab, T.K., Schiff, C., and Somerville, S.C. (2002). *PMR6*, a pectate lyase-like gene required for powdery mildew susceptibility in *Arabidopsis*. Plant Cell **14,** 2095-2106.

Voinnet, O. (2002). RNA silencing: small RNAs as ubiquitous regulators of gene expression. Curr Opin Plant Biol **5,** 444-451.

von Röpenack, E., Parr, A., and Schulze-Lefert, P. (1998). Structural analyses and dynamics of soluble and cell wall-bound phenolics in a broad spectrum resistance to the powdery mildew fungus in barley. J. Biol. Chem. **273,** 9013-9022.

Vorwerk, S., Somerville, S., and Somerville, C. (2004). The role of plant cell wall polysaccharide composition in disease resistance. Trends in Plant Science **9,** 203-209.

Walhout, A.J.M., Temple, G.F., Brasch, M.A., Hartley, J.L., Lorson, M.A., van den Heuvel, S., and Vidal, M. (2000). GATEWAY recombinational cloning: Application to the cloning of large numbers of open reading frames or ORFeomes. In Applications of Chimeric Genes and Hybrid Proteins, Pt C (San Diego: ACADEMIC PRESS INC), pp. 575-592.

Waterhouse, P.M., Wang, M.B., and Lough, T. (2001). Gene silencing as an adaptive defence against viruses. Nature **411,** 834-842.

Wei, F.S., Gobelman-Werner, K., Morroll, S.M., Kurth, J., Mao, L., Wing, R., Leister, D., Schulze-Lefert, P., and Wise, R.P. (1999). The *Mla* (powdery mildew) resistance cluster is associated with three NBS-LRR gene families and suppressed recombination within a 240-kb DNA interval on chromosome 5S (1HS) of barley. Genetics **153,** 1929-1948.

Wesley, S.V., Helliwell, C.A., Smith, N.A., Wang, M., Rouse, D.T., Liu, Q., Gooding, P.S., Singh, S.P., Abbott, D., Stoutjesdijk, P.A., Robinson, S.P., Gleave, A.P., Green, A.G., and Waterhouse, P.M. (2001). Construct design for efficient, effective and high-throughput gene silencing in plants. Plant J **27,** 581-590.

Williams, J.S., and Cooper, R.M. (2004). The oldest fungicide and newest phytoalexin - a reappraisal of the fungitoxicity of elemental sulphur. Plant Pathol. **53,** 263-279.

Wolter, M., Hollricher, K., Salamini, F., and Schulze-Lefert, P. (1993). The *Mlo* resistance alleles to powdery mildew infection in barley trigger a developmentally controlled defense mimic phenotype. Mol. Gen. Genet. **239,** 122-128.

Wulf, E., Deboben, A., Bautz, F.A., Faulstich, H., and Wieland, T. (1979). Fluorescent phallotoxin, a tool for the visualization of cellular actin. Proc. Natl. Acad. Sci. U. S. A. **76,** 4498-4502.

Würtele, M., Wolf, E., Pederson, K.J., Buchwald, G., Ahmadian, M.R., Barbieri, J.T., and Wittinghofer, A. (2001). How the *Pseudomonas aeruginosa* ExoS toxin downregulates Rac. Nat. Struct. Biol. **8,** 23-26.

Wyand, R.A., and Brown, J.K.M. (2003). Genetic and forma specialis diversity in *Blumeria graminis* of cereals and its implications for host-pathogen co-evolution. Molecular Plant Pathology **4,** 187-198.

Xiao, S.Y., Ellwood, S., Calis, O., Patrick, E., Li, T.X., Coleman, M., and Turner, J.G. (2001). Broad-spectrum mildew resistance in *Arabidopsis thaliana* mediated by RPW8. Science **291,** 118-120.

Xing, T., Higgins, V.J., and Blumwald, E. (1997). Race-specific elicitors of *Cladosporium fulvum* promote translocation of cytosolic components of NADPH oxidase to the plasma membrane of tomato cells. Plant Cell **9,** 249-259.

Xu, J.R., Staiger, C.J., and Hamer, J.E. (1998). Inactivation of the mitogen-activated protein kinase Mps1 from the rice blast fungus prevents penetration of host cells but allows activation of plant defense responses. Proc. Natl. Acad. Sci. U. S. A. **95,** 12713-12718.

Xu, J.R., Urban, M., Sweigard, J.A., and Hamer, J.E. (1997). The *CPKA* gene of *Magnaporthe grisea* is essential for appressorial penetration. Mol. Plant-Microbe Interact. **10,** 187-194.

Yang, N., Higuchi, O., Ohashi, K., Nagata, K., Wada, A., Kangawa, K., Nishida, E., and Mizuno, K. (1998). Cofilin phosphorylation by LIM-kinase 1 and its role in Rac-mediated actin reorganization. Nature **393,** 809-812.

Yonezawa, N., Nishida, E., Iida, K., Yahara, I., and Sakai, H. (1990). Inhibition of the interactions of cofilin, destrin, and deoxyribonuclease-I with actin by phosphoinositides. J. Biol. Chem. **265,** 8382-8386.

Yonezawa, N., Nishida, E., Koyasu, S., Maekawa, S., Ohta, Y., Yahara, I., and Sakai, H. (1987). Distribution among tissues and intracellular-localization of cofilin, a 21kda actin-binding protein. Cell Struct. Funct. **12,** 443-452.

Yu, H., and Kumar, P.P. (2003). Post-transcriptional gene silencing in plants by RNA. Plant Cell Reports **22,** 167-174.

Yu, I.C., Parker, J., and Bent, A.F. (1998). Gene-for-gene disease resistance without the hypersensitive response in *Arabidopsis dnd1* mutant. Proc. Natl. Acad. Sci. U. S. A. **95,** 7819-7824.

Yun, B.W., Atkinson, H.A., Gaborit, C., Greenland, A., Read, N.D., Pallas, J.A., and Loake, G.J. (2003). Loss of actin cytoskeletal function and EDS1 activity, in combination, severely compromises non-host resistance in *Arabidopsis* against wheat powdery mildew. Plant J **34,** 768-777.

Zhou, D., Mooseker, M.S., and Galan, J.E. (1999a). Role of the *S. typhimurium* actin-binding protein SipA in bacterial internalization. Science **283,** 2092-2095.

Zhou, D.G., Mooseker, M.S., and Galan, J.E. (1999b). An invasion-associated *Salmonella* protein modulates the actin-bundling activity of plastin. Proc. Natl. Acad. Sci. U. S. A. **96,** 10176-10181.

Zhou, F.S., Kurth, J.C., Wei, F.S., Elliott, C., Vale, G., Yahiaoui, N., Keller, B., Somerville, S., Wise, R., and Schulze-Lefert, P. (2001). Cell-autonomous expression of barley *Mla1* confers race-specific resistance to the powdery mildew fungus via a *Rar1*-independent signalling pathway. Plant Cell **13,** 337-350.

9 Danksagung

Ein **herzliches Dankeschön** allen Menschen, die zum Gelingen dieser Arbeit maßgeblich beigetragen haben:

Herrn Prof. Dr. P. Schulze-Lefert danke ich für die Möglichkeit zur Erstellung dieser Dissertation am Max-Planck-Institut für Züchtungsforschung in Köln.

Herrn Prof. Dr. M. Hülskamp danke ich für die freundliche Übernahme des Korreferats.

Besonderer Dank gilt meinem Betreuer Ralph, der mir bei der Erstellung dieser Dissertation seine hundertprozentige Unterstützung zukommen ließ und nie die Geduld verloren hat – auch nicht im Bezug auf unterrepräsentierte Stop-Codons oder wilde Formulierungen – Ralph, einen besseren Betreuer kann ich mir nicht vorstellen, bleib wie Du bist!

Meinen ehemaligen Laborkollegen Stefan, genannt Dr. Bau, Andreas, genannt Aldi[®], Judith, genannt Tante Ju und last but not least Volker, meinem alten Ruhrpottkollegen danke ich für manch weisen Ratschlag, zahlreiche Tipps und Hilfestellung sowie für die tatkräftige Unterstützung.

Anja sei für ihre selbstlose Art und Hilfsbereitschaft gedankt, die mir geholfen haben, einige Engpässe zu überwinden – hast Du noch 'ne Benzplatte?

Many thanks belong to Riyaz for the help with the production of the CLSM pictures as well as for the introduction to the Kashmiri music-culture.

Den wissenschaftlichen Hilfskräften Jochen und Holger sowie der Praktikantin Anne schulde ich viele Stunden Mikroskopierarbeit, die mir so zur anderweitigen Verfügung standen. Vielen Dank dafür.

Der Parker-Bande, als da wären Marcel, Steffen (aka Franti), Shige, Michael und Pino, danke ich für viel Spaß und so manche Aufmunterung – Jungs, ohne Euch wäre es nur halb so lustig gewesen.

Für das Korrekturlesen dieser Arbeit sei nochmals Ralph und Judith gedankt.

Der allergrößte Dank gilt jedoch meiner Freundin Steffi, die mich durch ihre liebevolle Art während der ganzen Zeit, die zur Erstellung dieser Dissertation nötig war, besonders unterstützt hat. Steffi, ich liebe Dich!

"Ich versichere, daß ich die von mir vorgelegte Dissertation selbständig angefertigt, die benutzten Quellen und Hilfsmittel vollständig angegeben und die Stellen der Arbeit - einschließlich Tabellen, Karten und Abbildungen -, die anderen Werken im Wortlaut oder dem Sinn nach entnommen sind, in jedem Einzelfall als Entlehnung kenntlich gemacht habe; daß diese Dissertation noch keiner anderen Fakultät oder Universität zur Prüfung vorgelegen hat; daß sie - abgesehen von unten angegebenen Teilpublikationen - noch nicht veröffentlicht worden ist sowie, daß ich eine solche Veröffentlichung vor Abschluß des Promotionsverfahrens nicht vornehmen werde. Die Bestimmungen dieser Promotionsordnung sind mir bekannt. Die von mir vorgelegte Dissertation ist von Prof. Dr. Paul Schulze-Lefert betreut worden."

Köln, im Dezember 2004

(Marco Miklis)